REFERENCE

ProQuest Number: 10697098

ProQuest 10697098

The Development of Multisensor Arrays utilising Conducting Polymers

Andrew Hinton BSc (Hons) CChem MRSC

A thesis submitted in partial fulfilment of the requirements of Sheffield Hallam University for the degree of Doctor of Philosophy
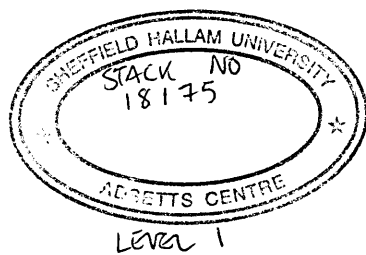
January 1997

This thesis is concerned with the continued development of multisensor array sensing technology for the detection and classification of aromas. The technology applies the use of conducting polymers grown across a gap between metallic conductors. The electrochemically deposited films complete a circuit and providing electrical resistance. In this format the films act as chemical resistors (chemiresistors) the current flow being influenced by the polymers' molecular electronics. Devices of this nature are potentially useful as sensors for analytes which cause the reversible modulation of the films' molecular electronics, leading to a detectable resistance change. Variation in the chemical and physical properties of the conducting polymer films has led to the generation of sensing devices capable of providing rapid, meaningful sensory information. The development of multisensor arrays containing a series of sensing devices having broad ranging sensitivities, has enabled effective discrimination of sample analytes. The information generated from such an array provides a 'fingerprint' or patterned response relating directly to the sample analyte. Complex statistical processing techniques have been coupled with the sensor technology to categorise and differentiate between the 'fingerprints' obtained.

Instrumentation based on multisensor array technology has been developed by Neotronics Scientific Ltd., who currently market the NOSE (Neotronics Olfactory Sensing Equipment) based upon conducting polymer sensors. The research project resulting in this thesis was intended to develop and examine conducting polymer chemiresistor technology and explore the parameters that contribute to the production of effective discriminating sensors for use in array devices.

The study involved an investigation of the variables involved in the electropolymerisation protocols, and expansion of the sensing chemiresistors available. This was achieved by analysis of polymer fabrication methods, and the variation in monomer and electrolyte feedstocks used during polymerisation. Polymer film stability was a major feature of the work performed as the long-term effectiveness of a sensing device is governed by environmental stability allowing reproducible analysis. Sensor optimisation was investigated using an individual system to determine the effect of the electrodeposition protocols, surface morphology, baseline resistance and film thickness. Polymer composition and stability were studied using a series of electrochemical, spectroscopic and surface analysis techniques. The data obtained resulted in the fabrication of chemiresistors not previously tested in electronic nose technology. Experimental optimisation studies also allowed variation in the nature of the responses obtained. A final area of investigation was the analysis of chemiresistors within a multisensor array environment using the NOSE technology. A series of arrays were prepared and the sensors exposed to a number of single, pure, organic analytes. From this data information was obtained on sensor response relating to molecular size, shape, position and nature of functional groups. The multifaceted nature of these experiments increased the number and response characteristics accessible to Neotronics, and provided a contribution to the knowledge surrounding the interactions between conducting polymer films and volatile organic analytes.

Contents

Chapter 3 Experimental

Chapter 4 Development of conducting polymer chemiresistors

Chapter 5 The modification of conducting polymer films and the optimisation of chemiresistor response

Chapter 1 Introduction

1.0 General Introduction

This thesis concerns the application of conducting polymers grown across a gap between metallic conductors such that the polymers complete a circuit but promise electrical resistance. In this arrangement the polymers act as electrical resistors (chemiresistors) whose influence on the current that can flow depends upon the molecular electronics of the particular polymer system. Devices based on chemiresistors of this type can be useful sensors for analytes that cause reversible modulation of the molecular electronics leading to changes in the resistance of sensor circuits that can be detected and displayed using appropriate instrumentation.

One application of this type of technology is in the characterisation of organic vapours of the sort encountered in the food/beverage, perfumery or tobacco industries. The investigations described in this thesis were funded by an EPSRC CASE award involving sponsorship by Neotronics Scientific Ltd (Essex, UK.) who market an electronic nose (Neotronics Olfactory Sensing Equipment) based upon conducting polymer sensors. The thesis begins with an introduction into the detection and recognition of odours both by the biological nose and by electronic noses, including the historical development and the various technologies incorporated into multisensor array based sensing devices (Chapter 1). Laboratory work is described in Chapters 2 and, especially, Chapter 3 and the results of that work are discussed in the rest of the thesis (Chapters 4 to 7). A more detailed description of the organisation of the Chapters 3 to 7 appears in Section 1.91 at the end of this chapter.

The development of an electronic analogue capable of mimicking the biological nose has begun to emerge as a result of studies completed during the past two decades. This is due to complex studies surrounding the mechanism by which the sense of smell operates and the furthering of material and integrated sensor based technology. Within

the area of gas sensing the aim has previously been to detect individual gases (usually of a toxic nature) which have exceeded a predetermined threshold level. The human olfactory system is a more comprehensive analytical tool for classifying and grading aromas, which also encompasses the detection of noxious substances. Nature has a system which is both sensitive and reliable at detecting and evaluating odours[1]. To develop an instrument which is in any way capable of reproducing these properties it is important to have an understanding of the mechanism of smell so that these principles can be incorporated into the design of an electronic analogue.

Commercially(via human panels) the human nose is still the 'primary instrument' used for the broad evaluation of flavour. This encompasses many industrial products, predominantly perfumes, foodstuffs and beverages. The physicochemical properties of the finished products are measured using conventional instrumental analytical techniques (e.g. GC and GC-MS) that are both time consuming and often inadequate[2]. Instrumental methods are often unable to detect the key flavour constituents of some products as the levels present are often below instrumental detection limits. As the relationship between the physicochemical properties of the odorant molecules and their impact on the odour of a product is still unclear there is a demand for an electronic instrument that can reproduce the information obtained from the human olfactory system. The provision of rapid, meaningful sensory information has led to the use of sensory arrays which have both broad ranging sensitivities and effective discriminatory abilities, coupled with enhanced data processing techniques

The sensory information obtained from multisensor arrays allows the generation of a unique 'fingerprint' or patterned response which is directly related to the sample aroma. Using data processing techniques such as pattern recognition, it is possible to categorise and differentiate between fingerprints obtained during sample analysis[3]. At present the commercial instruments capable of performing this type of analysis are based around conducting polymer chemiresistors and tin oxide sensors. The majority of the applications for electronic nose technology are in the areas of quality control and

quality assurance within processing industries. In the future it has been envisaged that technological advancements will allow more diverse uses of artificial noses, examples being the fields of clinical diagnostics for the detection of diseases such as schizophrenia, lung cancer, diabetes and duodenal ulcers, and also forensic science using human odour to determine an individual's identity in a similar manner to DNA testing and fingerprinting[4].

1.1 The Human olfactory system

The sensation of flavour within humans has contributions from three chemoreceptor systems. These are gestation, or the sense of taste, olfaction, or the sense of smell and lastly the trigeminal sense[5]. The sense of taste is predominately responsible for the detection of non-volatile components in an aroma, while the sense of smell is concerned with the more volatile components of an aroma. The receptors for the trigeminal sense are located in the mucous membranes and in the skin and these respond to irritants or chemically reactive species. All three of these chemoreceptor systems participate in flavour perception, the most significant contribution being from the sense of smell.

To design an electronic analogue of the biological nose it is important to have a general understanding of the latter's biochemical[6-7] and physiological properties[8-9]. The olfactory epithelium, which presents an odour sensitive surface to the external environment, is positioned high up within the nose at the front of the brain cavity (Fig 1.1)[10]. The structure of the epithelium consists of three layers (cell types), the supporting cells, the olfactory receptor cells and the basal cells. The supporting cellular structure secretes a mucous layer and after this initial mucous layer there is the layer containing the olfactory receptor cells. There are typically 100 million receptor cells (50 million per nostril) contained in a human epithelium[11]. The cells have a dendrite structure and extend into the mucus layer in a terminal swelling. From these structures a number of cilia (10-20) protrude out into the mucous layer. G-receptor proteins are located on the surface of the cilia that act as chemosensory receptors and interact with

the odorant molecules present[12]. There is believed to be around one hundred receptor protein types which have partially overlapping sensitivities and determine the specificity of the nose. The basal cells are precursors for new olfactory receptor cells, which are replaced on average every month, and are the only neurones which undergo cell division. The interaction of an odiferous molecule with a receptor site causes a change in the ionic permeability and a resultant change in membrane conductance. The olfactory receptor cells amplify this signal, which is transmitted to the olfactory bulb via the synapses of the olfactory nerve. Within the olfactory bulb there is a high degree of convergence; the generated signals from olfactory receptor cells(primary cells) are fed to mitral cells(secondary cells) in the bulb, where the 1-20 thousand primary cells are connected to a single secondary olfactory cell (Fig. 1.2). It is from the grandular layer that the signals are then sent to the brain, to be combined with other sensory information to generate a sensory response[13-16].

Fig 1.1 Location of the olfactory system in the human nose
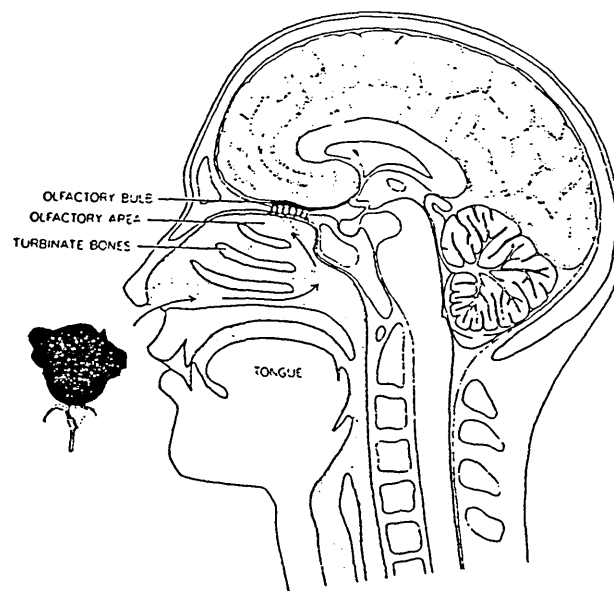
Fig 1.2 Schematic diagram of the olfactory pathway from the epithelium to the brain
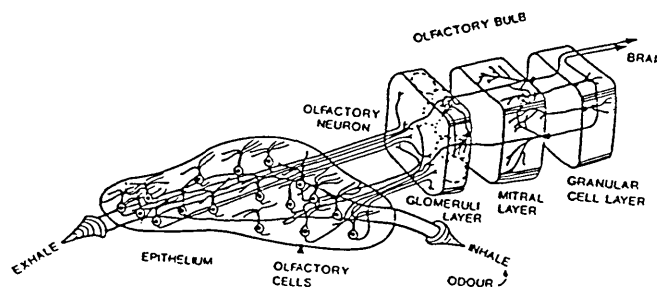
From the information obtained about the biological nose it seems that the receptor proteins have a low sensitivity (-100ppm), a low specificity, and require replacement an a regular basis[11]. These receptors have their signals enhanced by a series of neural processing techniques increasing their sensitivity and reducing drift. The combination of the G-receptor proteins and neural processing occurring in the olfactory bulb enables the discrimination of several thousand odours.

1.2 Odorants

Odorant molecules which interact with the olfactory receptor proteins cause the sensation of smell These molecules are generally hydrophobic, polar with molecular masses ranging up to ca. 300 Da, and have to be sufficiently volatile to reach the olfactory epithelium. It is noted that molecules with molecular masses much over 300 Da tend to be odourless[17]. The common odorants contain normally one functional group, with the majority containing oxygen in some form, predominantly in the polar group. The presence of nitrogen and sulphur containing odorants is infrequent, although they do arise, nitrogen in pyrazines(roasted products) and sulphur in animal odours[1].

Odours are generally described by direct comparison with a similar odour, and unlike sound and light there is no method of characterising odour intensity. A simple odour is one which consists of a single odorant molecule type, whereas a complex odour

consists of a variety of odorant molecules. Complex odours are generally natural smells, flavours and perfumes which may contain many thousands of constituents[18]. Odours are often given descriptive names i.e. musky, fruity, flowery and many odours have many descriptors attached to their aroma. However, this is very subjective way of categorising an aroma and the description obtained by an individual is of limited value, hence the use of trained panels to give a consensus of opinion.

The most important properties of odorant molecules are the odour type, the threshold value and the intensity curve. The present understanding of what controls an odour can be summarised by the following four categories, molecular size, molecular shape, polar properties, position of functional features. There has been a considerable number of studies[19] completed on rationalising these properties and the corresponding odour descriptor given to an odorant molecule. *Amoore*[20] proposed a classification of odours based upon their size/shape, but this scheme has been shown to oversimplify the complex nature of categorising an odour. Although it has been shown that the stereochemical parameters are particularly important, i.e. size and shape, with the position of the functional group perhaps being of more significance than the type of functionality present. The use of threshold values (Table 1.1)[5] underlines some of the problems in the detection and classification of odours. If an odorant with a low threshold value appears as a trace impurity in a complex odour with a high overall threshold value, the trace odorant can dominate the odour profile. The presence of odorants with low threshold values can generally mask the other constituents in an aroma, but their presence may also be vital in providing an aroma with its characteristic smell.

Table 1.1 Threshold values for some common simple odours

Odorant	Odour Type	Threshold value (ppb in water)
Diacetyl	off flavour of beer	500
Geraniol	rose	290
5-Isopropyl-methylphenol	thyme	86
Limonene	lemons	10
Triethylamine	fishy	0.47
Octa-1,5-diene-3-one	off flavour of butter	0.01
2-Isobutyl-3-methyoxpyrazine	green peppers	0.002

The intensity[5] of a particular odorant molecule is determined by its corresponding vapour pressure; a molecule such as diethyl ether has a low intensity as it has a high vapour pressure and can therefore reach high concentrations in the atmosphere. This provides a strong odour sensation but only at high concentrations. The reverse is true for high intensity odorants such as cyclopentadecanone, which has a lower vapour pressure, so that the concentration of molecules present in the atmosphere is lower. Despite this fact it is often the case that molecules with higher intensities can be smelt as they have low threshold values. These factors obviously require consideration when deciding upon sampling strategies when using an electronic nose, as low intensity odorants may breach sub-threshold levels whereas high intensity odorants may remain even when only a fraction of the original sample is present. It is also important to note that biological receptors can discriminate on the basis of stereochemical recognition rather than functional groups. Ideally the development of a multisensor array should operate on similar principles using the common principle of discrimination based on stereochemical parameters.

1.3 The Historical development of the electronic nose

Introduction

The earliest studies into the detection of odours date back to pioneering work by *Moncrieff*[21] in the early 1960's, where the absorption of odorants onto intact olfactory epitheliums and coated surfaces was studied. The first real mechanical form of an electronic nose was reported by *Wilkins et al*[22] in 1964; they studied the complex adsorption of odorants at an electrode involving redox reactions. The monitoring of conductivity changes of materials due to the interaction of odorants was studied by *Buck et al*[23] and further extensive studies by *Dravieks and Trotter*[24] established changes in the contact potentials of coated materials due to the interaction of odorants. The development of data processing technology to support the initial development of the early transducers was slow, the earliest work in this area being by *Deutsch* in 1967[25].

The first true experimental version of an electronic nose was developed by *Dodd and Persaud*[26] in 1982. This early device could solve elementary discrimination problems in the fragrance and food industries and highlighted the significant fact that it was not necessary to replicate the olfactory receptor proteins found in the olfactory epithelium. The system was based on commercially available doped tin-oxide gas sensors and highlighted their ability to discriminate between a wide range of odorants. The initial success of this system provided considerable interest in the field, and further devices were developed by *Ikegami et al*[27-28] in Japan. The nature of the electronic nose meant that it was potentially feasible to use a variety of sensor technologies. As the field became more established it expanded leading to the first conference dedicated to the topic in 1990[1]. The term "electronic noses" was qualified in the following statement, 'An electronic nose is an instrument, which comprises an array of electronic chemical sensors with partial specificity and an appropriate pattern recognition system, capable of recognising simple or complex odours[11]' .The definition of this term encompassed the types of chemical sensor array devices (ChemSADs) which are used

specifically for the monitoring of odorant based molecules, and data processing techniques used to enhance the sensory information obtained[29-31].

The initial studies[26] at Warwick University centred on the use of three commercial tin-oxide gas sensors. Using a static test rig, sensors were exposed to vapour samples at constant temperature. The change in resistance of the devices due to their exposure to analytes was monitored using a potential divider based circuit. The array was later upgraded from three to twelve sensing devices and conducting polymer sensors were also investigated[32-36] along with pattern recognition techniques[37-42]. The sensitivity of the instrument was enhanced by progressing from a potential divider circuit to an a.c bridge design[43]. The group also investigated the feasibility of reducing the power consumption of the Taguchi gas sensors[44].

Studies into the use of conducting polymers began with the devices being fabricated electrochemically across two parallel gold substrates[45], and it was found that rapid and reversible responses to methanol vapour could be obtained. A series of polypyrrole based sensors of similar design were manufactured and further reproducible results obtained, but it was found that the sensors were unstable during storage, their baseline resistances increasing rapidly[46]. Alternative monomers were studied[47], combined with the use of L-B technology[48]; mono-layers of L-B films were deposited onto the surface of polymer films to act as molecular sieves in an attempt to modify the sensor response.

The development of a commercial instrument was a result of a DTI LINK project involving Warwick University, Neotronics Ltd. and Bass Brewery[49]. The instrument was developed using the monomers of pyrrole, 3-methylthiophene, and aniline which were electrochemically deposited with a variety of counter-ion species. The data processing hardware used in conjunction with the sensor technology improved with the use of neural network pattern recognition techniques. The combination of these

different technologies enabled the electronic nose to distinguish between taints in beer samples[50]. As a result of this work a series of patents was filed[51,52].

As a result of the initial DTI project Neotronics Ltd launched the first commercially available electronic nose, the 'NOSE' (Neotronics Olfactory Sensing Equipment)[53,54], and further work on the development of sensor technology at Sheffield Hallam University led to the formation of a daughter company Neotronics Scientific Ltd[55] to concentrate directly on the electronic nose market. The instrument contains twelve individual conducting polymer based sensing chips and on exposure to analytes the instrument measures the conductivity change across the devices using a standard d.c technique

Other Universities have also exploited the technology. The Department of Instrumentation and Analytical Science at the University of Manchester Institute of Science and Technology (UMIST) have completed research into olfaction and sensor technology leading to the formation of Aromascan plc. Their instrument the 'Aromascanner' consists of a sensor chip containing thirty-two conducting polymer based devices[56-58]. Aromascan have investigated the feasibility of using high frequency a.c. measurement of their devices as an alternative to d.c measurement of sensor response[59-60].

Other systems are also commercially available Alpha MOS (France) produce the Fox 2000 electronic nose which was produced in conjunction with the universities of Warwick and Southampton. The instrument is designed around a series of eighteen devices (with a series of six devices located in three consecutive chambers), the devices being based on various conducting polymer and undoped oxide (SnO_2, ZnO, or WO_3) sensor types[61]. Leeds University in conjunction with Mastiff Security Systems are set to launch an odour evaluating device called 'Sentinel' in early 1997[62]. The instrument is designed to provide odour maps of human palms as a security device. It is speculated that this device is based on conducting polymers incorporating a form of biological

olfactory cells. At present Glasgow University under the direction of Dr. G. Dodd, are developing a 21st century electronic nose based on molecular electronics, bio-electronics and nanotechnology[63]. The group has a particular interest in the use of the technology for clinical diagnostics, in particular schizophrenia.

Further areas of both sensor technology and neural processing techniques have been investigated by many groups throughout the world. Particular interest has been shown in the use of surface acoustic wave devices, metal oxide field effect transistors (MOSFET's) and the use of Langmuir-Blodgett films, but as of yet these studies have not led to the realisation of commercial devices.

1.4 The development electronic nose sensor based technology

1.41 Inorganic semiconducting devices

The area of inorganic semiconducting devices includes a wide variety of sensor technologies. Variations of the following types have been investigated for use within electronic nose technology: metal oxide resistors[64-66], quartz crystal microbalances[67], surface acoustic wave (SAW) devices [68], metal oxide field effect transistors (MOSFET)[69] and metal insulating semiconductor (MIS) resistors[70]. The initial studies at Warwick University used a commercial form of the latter for use within the first electronic nose. The tin oxide Taguchi[71] gas sensor, commercially available from Figaro Inc. Japan has the general construction indicated (Fig. 1.3)[39]. The device contains a Taguchi gas sensor (TGS) sensor with a ceramic former and on the outer surface a sintered layer of gas sensitive material between an interdigitated metalised pattern. The gas sensitive material is predominatly tin-oxide, with catalytic additives (e.g. palladium) to favour the detection of particular gases. The device may be explained in terms of an n-type semiconducting device[72-74]. Oxygen absorbed at the gas-solid interface leads to the abstraction of electrons from the bulk of the tin-oxide. This leads to a decrease in the n-type character observed and the formation of surface oxygen ions (O^-, O^{2-} and O_2^-), the nature of which is temperature dependent. Changes

in the concentration of surface absorbed oxygen ions will affect device conductivity, so that in the presence of a reactive gas a surface-catalysed combustion may occur. A reducing gas will lead to the depletion of surface absorbed oxygen ions. The reduction in surface oxygen allows electrons to return to the bulk of the solid increasing device conductivity (for an n-type solid). The conductivity change can also be related to gas concentration. The devices operate at elevated temperatures 150-600°C, and have shown sensitivity to combustible gases in the ppm region although they are poor detectors of nitrogen and sulphur containing odorants. Response times to gases are typically ten seconds with a recovery period of one minute. The devices consume high quantities of power (1W per device in thick film devices), while sensors made with thinner films consume less power but have shown instability. The Taguchi devices are sensitive to both temperature and humidity with the best detection occurring at higher temperatures. Despite these disadvantages they have found applications in array devices.[75,76]

Fig 1.3 The construction of a Taguchi tin-oxide gas sensor
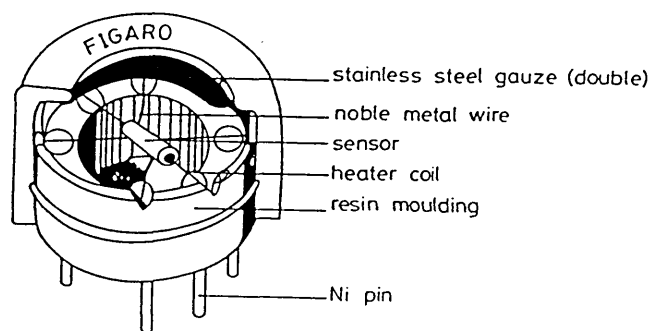
Quartz Crystal Microbalances (QCM's) are sensitive mass measuring devices, based upon quartz crystals with a characteristic resonance frequency which is dependent upon their mass[77]. The piezoelectric crystals used are predominantly AT-cut quartz which are then coated with a sensing membrane. On exposure to odorant molecules a certain level of absorption may take place causing the device to increase its mass, resulting in a decrease in the resonant frequency of the device. The frequency of the device recovers after desorption of the odorant[78]. With a range of selective membranes in a multisensor array the response of each device will be slightly different; hence a

12

characteristic output pattern is provided which can be used to identify odours. Each device is normally connected to an oscillation circuit with the frequency monitored via a frequency counter. The sampling period is nominally thirty seconds[79]. The phenomenon is termed a mass-loading effect with the effective frequency shift being proportional to the mass of absorbed molecules. It is summarised in the Sauerbury equation[80].

$$\Delta F = -2.3 \times 10^6 F_o^2 \, \Delta m / A$$

where Δm is the mass change of the crystal (grms), ΔF the related frequency change (Hz), A the gas sensitive area (cm^2) and F_o the initial frequency of the quartz crystal (MHz). The sensing membranes are varied[81-83] (polymers, lipids, etc.) but it is important to minimise film coatings to a thickness below $1\mu m$ as thick films give unstable oscillations due to acoustic loss. Errors can also be limited by ensuring that the sensing membrane is less than 2% of the crystal mass. Similar to most piezoelectric measurement sensors, moisture is a problem during sampling[80].

Surface Acoustic Wave (SAW) devices have many electrical applications but during the past decade their potential as gas sensing devices has been realised[84]. Surface acoustic waves are elastic waves propagating along the surface of an elastic (solid) surface, the amplitudes of which decay exponentially with substrate depth. If the material in question is a piezoelectric crystal the waves can be induced electrically. The most common media used as substrates in SAW devices are mono-crystalline substances such as quartz and lithium niobate. High performance devices rely upon the use of pure mode Rayleigh waves, which have electrical and mechanical properties in one plane, normal to the substrate surface. The phase velocity and amplitude of the SAW are determined by the piezoelectric, dielectric, conductive properties and substrate mass. If one of these properties can be modified by the odorant the effect of sensing can be created. Devices are normally prepared on an individual piezoelectric substrate, and normally contain two electrodes (interdigitated transducers, IDT's), a reference and working electrode (Fig. 1.4). The introduction of a reference electrode is primarily to monitor the effect that temperature and humidity have on the device. The

13

working electrode is normally coated with some form of selective gas sensing material. Each interdigitated transducer array contains transmitter and receiver IDT's, and a radio frequency voltage is applied to the transmitter inducing a Rayleigh surface wave. The surface wave introduces deformations in the piezoelectric crystal and when the mechanical wave reaches the receiver it is converted back to an output RF signal. The device has a characteristic frequency, any mass change occurring at the sensing surface will cause the frequency to change. The effect of gas adsorption will lead to an increase in mass of the sensing surface. This effect can be measured as a frequency shift which is proportional to the mass added[85-87].

Fig. 1.4 A common design of a surface acoustic wave device
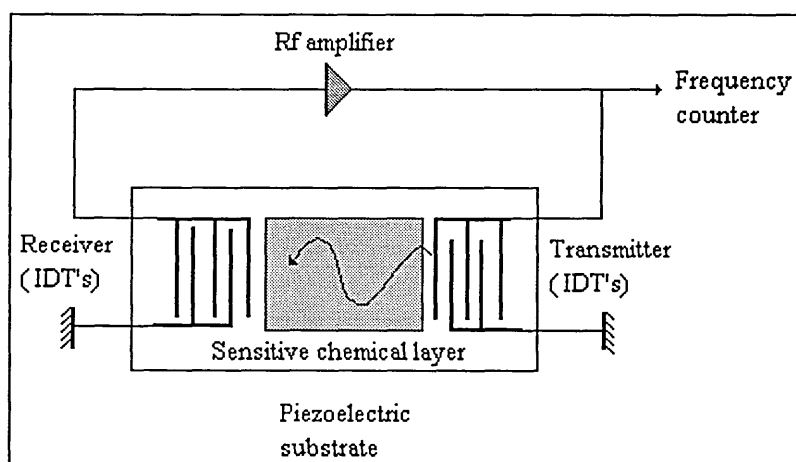
A variety of coatings offer a certain degree of selectivity to analyte gases. The literature shows that the following areas have been investigated for use with mass sensitive devices: thermotropic nematic liquid crystals[88], polymeric coatings[89], cyclodextrins[90], conducting polymers[91], olfactory cell proteins[92], Langmuir-Blodgett films[93], lipids[94] and molecular sieves[95].

The use of MOSFET's (metal-oxide semiconducting field effect transistors)[96,97] has been widespread in the composition of array based sensing systems[98]. They consist of a source and drain which are separated by a gate bridge (Fig. 1.5). The source and drain both comprise of n-type semiconducting material and the surrounding region is of p-type material. The gate consists of an channel on top of which a catalytic active metal is deposited (Pd, Pt or Ir). The device is a basic capacitor, the gate and channel acting as

14

two electrodes. The current flow between the source and the drain is dependent on the voltage applied across the gate. An applied voltage on the gate induces a charge which is reflected in the channel, thereby modifying the conduction of the channel. At a certain gate voltage, termed the threshold voltage, significant conduction occurs through the channel. The gate creates a field which enables the inversion of a layer of p-type material to n-type material, therefore allowing current to flow between the source and the drain. A change in the potential or the charge on the gate will alter the conductance of the channel; this change can be detected as an electrical signal which can be processed. Gases adsorbed or absorbed onto the gate will effect changes of this nature. A variety of gases have been detected including saturated and unsaturated hydrocarbons, carbon monoxide, ammonia and hydrogen sulphide. Different gate types of varied thickness, operated at temperatures between 150-200°C provide the selectivity required and the threshold voltage can be made dependent upon gas concentration.

Fig. 1.5 A graphical representation of a MOSFET device

V_g= gate voltage, V_d= applied junction bias
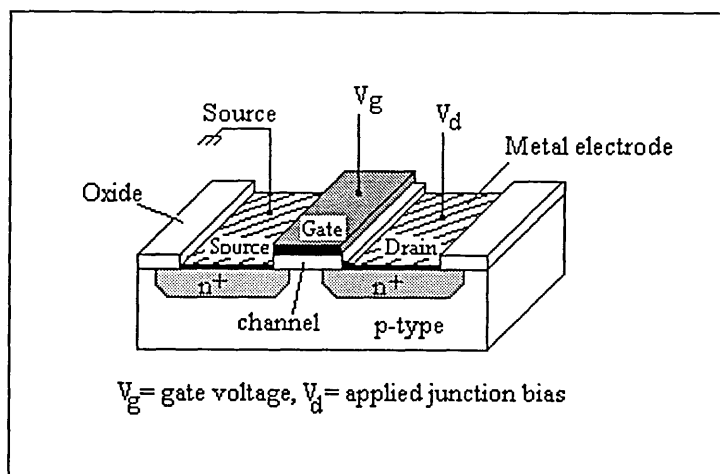
1.42 Langmuir-Blodgett films

The preparation of molecular electronic devices using L-B technology has been widely exploited in the area of gas sensing[39,66,99,100]. The process of controlling and monitoring the deposition of mono-layers is named after Irving Langmuir and Katherine Blodgett who devised the technique. It involves the deposition of molecules containing both hydrophobic and hydrophilic groups, the hydrophobic group typically being a hydrocarbon chain. The technology used involves the positioning of a small

15

quantity of a suitable material onto a liquid (normally water) after which the solvent is allowed to evaporate and the layer compressed to one monolayer. A quasi-solid is formed one molecule thick, in which there is molecular alignment, the hydrophobic groups protruding from the liquid sub-phase. The films are prepared in a Langmuir trough, where the surface tension is maintained by a compression system coupled to a microbalance (Fig. 1.6)[99]. This provides a monolayer even during the dipping procedure which normally uses an indium tin oxide (ITO) glass substrate. Film thickness can be controlled via the number of layers deposited. A variety of films have been produced which are responsive to gases stearic acid films have shown sensitivity to acetone, ethanol, menthol, methylamine, and ammonia[101]. The interaction of volatile molecules with LB-films changes either their conductance or capacitance which can be monitored. Substituted phthalocyanine (Pc)[102] and porphyrin[103] L-B films have been found to be highly sensitive to nitrogen dioxide, whereas copper tetracumylphenoxy-Pc plus stearyl alcohol films[104] have shown sensitivity to ammonia.

Fig. 1.6 Schematic diagram of a monolayer contained in a Langmuir trough
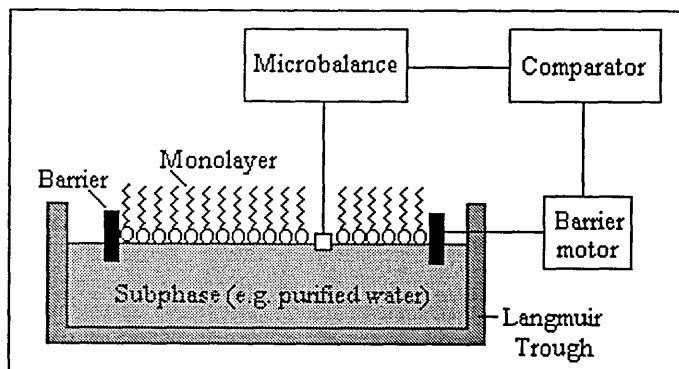
1.43 Conducting Polymers

Conducting electroactive polymers are generally derived from aromatic and heteroaromatic compounds. A common feature of these molecules is the alternate single and double bonds that give rise to a high degree of conjugation. This leads to a highly delocalised π-electron system and provides properties such as electrical conduction, giving rise to a wide range of applications, including gas sensing[105-107]. Polypyrrole

is one of the most widely studied conducting polymers. It was first prepared as a powder in 1916 [108], but Diaz *et al*[109] electrochemically produced the first free standing polypyrrole film in 1979. The anodic oxidation potential of polypyrrole is lower than the corresponding monomer, therefore the polymer is simultaneously oxidised during polymerisation[110]. Counter-ions from the electrolyte solution are incorporated during the process to maintain electroneutrality. The positive charges on the pyrrole rings are delocalised over a series of monomeric units when the polymer is in the oxidised (conducting) state. The number of pyrrole units in the charged state is inferred by the amount of incorporated anion. The standard representation of this implies that the positive charge is delocalised over about four monomer units[111].
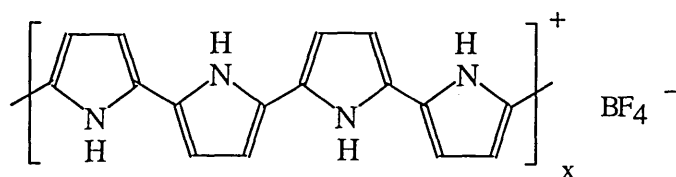
Variations in electrochemical film preparation can affect structural details such as the chain length, extent of oxidation, conductivity, porosity, film thickness and morphology. Therefore the way in which the sensing films are deposited requires tight control. Conducting polymer chemiresistor sensors are generally formed by electrochemical deposition of a polymeric film between two contacts separated by an insulating gap. When exposed to a volatile sample(aroma) the change in either, resistivity or conductivity is measured. The monomers of greatest interest in the development of the artificial nose have been pyrrole, 3-methylthiophene and aniline; their polymeric structures are shown here,
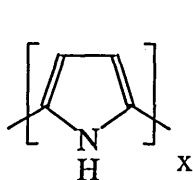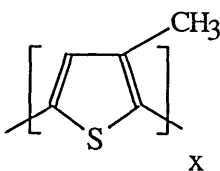
Polypyrrole   Poly (3-methylthiophene)   Polyaniline
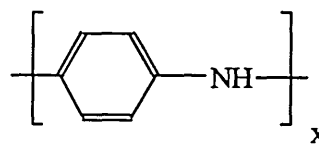
The properties of conducting polymers are well suited to array sensing devices. They can be chemically modified to produce sensors with overlapping sensitivities and when optimised show reversible conductivity changes at room temperature on a rapid time scale. Variations in polymer films are obtained by doping the films with different inorganic/organic counter-ions or by the functionalisation of monomers used in the polymerisation process. These modifications of the film architecture allow selective resistance changes when the films are exposed to volatile components in the vapour phase. The change in film resistance is related to the adsorption and desorption of volatiles on to the sensor.

1.5 Pattern recognition and Neural processing techniques

Pattern recognition is regarded as a branch of artificial intelligence that involves the reproduction and modelling of human intelligence. It is used predominantly as a method of solving classification related problems, normally involving statistical data analysis, to study relationships and trends within that particular data set. This form of analysis has been found to be especially useful in the analysis of sensory information obtained from sensory arrays. The use of pattern recognition can involve one of two techniques, either parametric or non-parametric. The first requires the estimation or analysis of a large data set to obtain the probability density function of the parameters used to characterise the system. The use of non-parametric based systems does not require knowledge of the fundamental distribution patterns of the data. Pre-processing techniques, such as auto scaling and feature weighting, are at the heart of this process to show underlying patterns within the data. Non-parametric learning processes can be further categorised into the subgroups of supervised and unsupervised. Cluster analysis is an example of an unsupervised method where no assumption is made of sample classes within the data set. Supervised methods require the classification of subgroups within the database so that the system can learn. Types of supervised methods are principal component analysis (PCA), multiple discriminate analysis (MDA), and artificial neural networks (ANN) (i.e. the form of ANN used in gas sensing uses the Rumelhart back-propagation learning method)[30].

The use of PCA as an advanced learning pattern recognition technique is widely employed in the physical and engineering sciences[31,40]. The principle involved is to take the n variables g which defines the rows in the response matrix (G) (i.e. response of a sensor to a given series of gases or responses of different sensors to a given gas) and to find the combinations which produce n indices X_r (the principal components). The indices which are obtained are ordered in such a way that the first component X_1 displays the greatest variance with X_2 displaying the next and so on. The theory relies on the fact that most of the variances for the components will be small so that the data

set can be adequately described by the first couple of X_r components (e.g. X_1 and X_2) which contain the largest amount of information on the variance in the data set. In a poor data set less information is contained within the initial principal components so that as a consequence of this, more information is obtained from the other components. Within this statistical model all samples are treated in a comparable manner to maximise the sample variance from which information can be gained on sample differences and similarities The use of MDA adds a further factor which defines the nature of the sub-set within the data sample, thus allowing the addition of unknown samples which can be categorised on the basis of the known data set.

The initial artificial neural network design by *Gardner*[112] relies on defining the processing layers into three categories which generally mimics the olfactory system. The system acts to converge the information obtained from the sensory array. The input layer consists of 12 inputs representing the individual sensors (i.e. the olfactory neurones). The hidden layer then produces a degree of convergence, so that there is a reduction in the processing units present. The final layer requires a number of processing units directly related to the number of samples requiring discrimination. Each processing unit is connected to each individual unit in the next layer (Fig. 1.7).[54]

The ANN is initially trained using a series of standards which the multisensor array is exposed to. The system works on the basis of monitoring the conductance change of each sensor. A back propagation technique is used such that the input layer information needs to be set between the values of zero and one; this requires pre-processing of the sensor outputs. The conductance change of each sensor on exposure to a gas is normalised and this procedure reduces the effect of gas concentration. The input values are fed forward to the next layer to calculate the output values for each process element in the next layer: this is termed the learning process. The procedure involves the iterative process of feeding forward the signals and back propagating the errors for each data set. A series of random weightings is used during the initial process and when

this has reached the outerlayer a comparison is made with a target value (expected output value). Then a difference parameter is calculated and used to modify the weightings. Thus the output values are weighted factors of their input values. When the output values converge near zero or one, the data sets have been learnt i.e. the network output is comparable to the target value. New data from the sensory arrays can now be analysed by the network and these unknowns classified, based upon the knowledge the network has gained. This is part of a continual learning process.

Fig. 1.7 A schematic diagram of an Artificial Neural Network
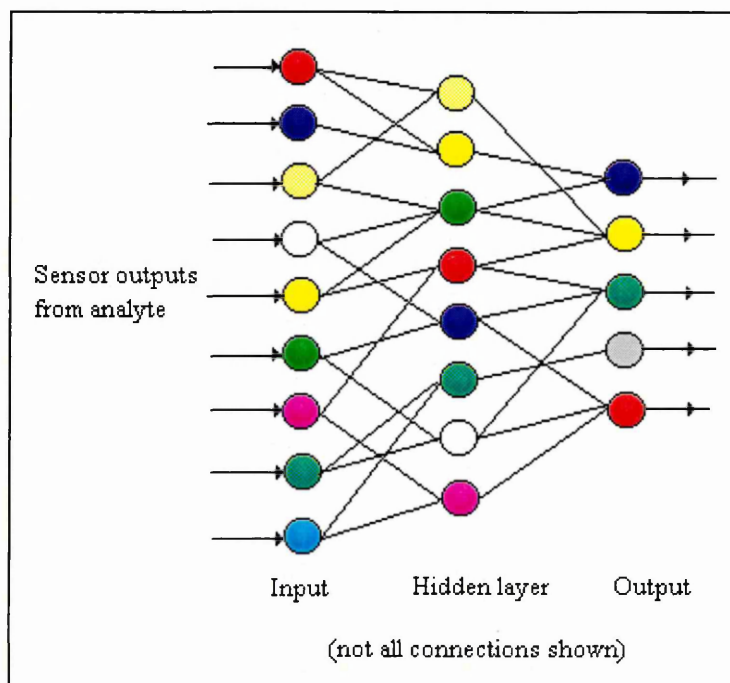
The use of pattern recognition techniques and neural network based software has been applied to a variety of multisensor array based technologies[40,49,]. The literature shows that the use of this type of technology, coupled with these data processing techniques, has found application in many commercial areas[113-115].

1.6 The requirements of an electronic chemoreception system

The development of an artificial system which replicates the characteristics of the human nose could in theory involve an array of chemical sensors each designed to match or mimic a receptor found in the biological nose. However, with an electronic system the reproduction of every receptor found in the biological nose is not necessary as long as the multisensor array contains sufficient sensors to provide discriminatory information about the odour, such that the patterns obtained can be translated in a similar manner to those of the human nose. The design and simulation of an electronic chemoreceptor system must be developed around a series of basic requirements[1,33,58,116] as follows:-

(a) The sensors used within the array must be individual non-specific gas sensing devices which exhibit broad overlapping sensitivities and the discriminatory ability to recognise odorants based on e.g. stereochemical or polarity parameters, rather than merely functional groups present in the odorant. Conducting polymer gas sensing devices have shown that they are satisfactory in the development of gas sensing devices of this nature.

(b) The information obtained from a multisensor array must be translatable into patterns which act as odour descriptors for an individual aroma. Once again this information must be based on the odour of the sample, not merely the structures of the molecules contributing to the odour.

(c) The software used in conjunction with the multisensor array must be able to analyse the data obtained into meaningful sensory information on a real-time basis. The analysis techniques must also allow for the recognition of unknowns within a data set and the ability to train the system to recognise individual aromas and classify them accordingly.

22

1.7 The Neotronics Olfactory Sensing Equipment ('NOSE')

The current e-NOSE™ 4000 (Figs. 1.8 and 1.9)[117] is an electronic nose which is fully computerised, incorporating the latest pattern recognition and neural processing technology. The software operates in Microsoft Windows™, and is multi-tasking, allowing comprehensive data manipulation. Conducting polymer sensors are used in the analysis of complex vapours and odours. The design allows for up to twelve individual conducting polymer devices to be incorporated into the multisensor array. The system uses a static head space system to allow reproducible presentation of the sample to the sensory array. The sample vessel and the sensor head are maintained at a constant temperature and humidity, removing further variables from sample analysis. The presence of temperature control also allows elevated temperature analysis, increasing the volatile components reaching the sensors. Combined with the sensor technology and sample analysis systems is the advanced data analysis system including a UNISTAT statistical analysis package and a neural network .

Fig. 1.8 Schematic representation of the Neotronics Olfactory Sensing Equipment.
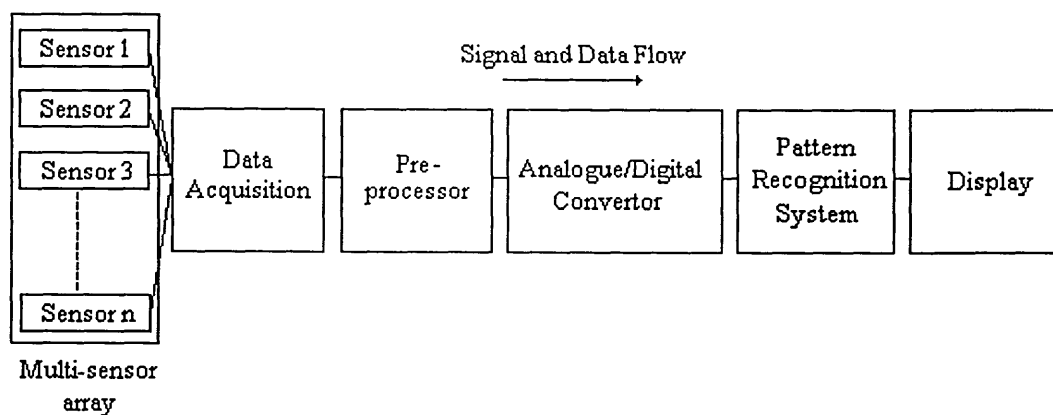
The data acquisition requirements for an electronic nose based upon a resistive multisensor array are show in the schematic diagram (Fig 9). Using this equipment an analogue signal obtained from the array is amplified, linearised and digitised before

entering a pattern recognition or neural processing system. The results are displayed on the operating computer terminal. The data acquisition process is one of multi-channel resistance measurement.

The system contains an array of twelve different conducting polymer sensors which have broad overlapping sensitivities, that provide sensory information when exposed to a sample. The interaction of the vapour with the sensor causes a change in the conductivity of the individual sensors. The conducting polymer films are chemically modified by the variation of the inorganic/organic counter ion or the monomer used during the electrochemical deposition process. The properties of these films are further enhanced by strict control of the growth parameters used, thus allowing the formation of films with comparable structural morphologies. This leads to the production of sensors which can give reproducible results between sensor batches and allows the operator to replace a sensor without compromising previous results obtained. Depending on the components present in the vapour each sensor responds uniquely, hence providing a patterned response to the aroma in question.

Fig. 1.9 e-NOSE 4000 Aroma Analysis System
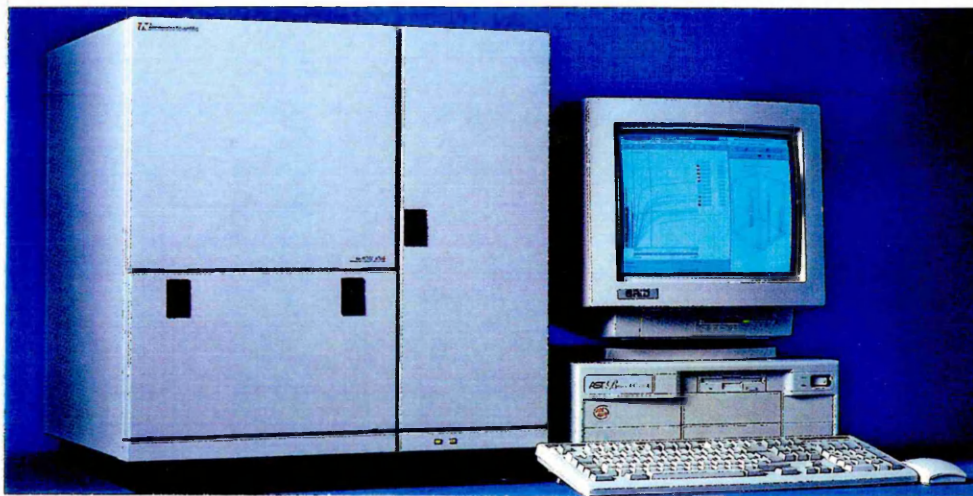
24

Electropolymerisation reactions are carried out at low anodic potentials to produce films that are both electroactive and electro-conductive. The films produced have many useful properties including stability (both electrical and mechanical), stability with respect to the electrolyte solution, high doping per unit mass and reversibility of doping[118].

The production, by polymerisation, of a polymeric film[119] involves a substitution reaction that proceeds via a radical cation The mechanism involves oxidation when the pyrrole monomer is converted to its radical cation in which the highest spin density is at the α-position.
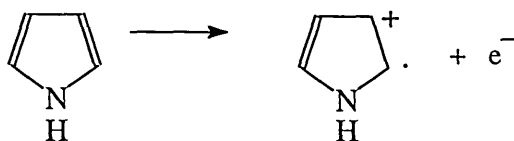
There follows a radical cation-radical cation coupling reaction at the α position to give a dimer.
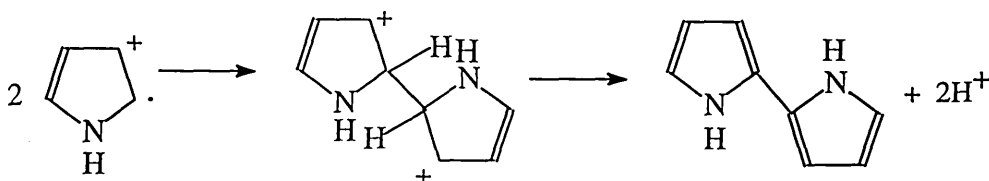
The chain propagation will proceed via the oxidation of the extending polymer and the $\alpha - \alpha'$ coupling with monomer radical cations.
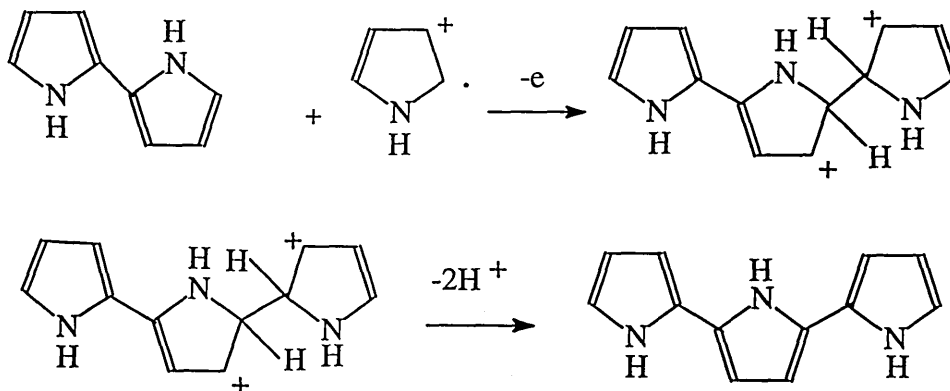
As oligomer chain length increases the molecules' solubility in solution decreases. This continues until nucleation sites are formed on the electrode surface from which film growth occurs.

Propagation

$-ne, -2nH^+$

Termination

Termination

H_2O

Termination
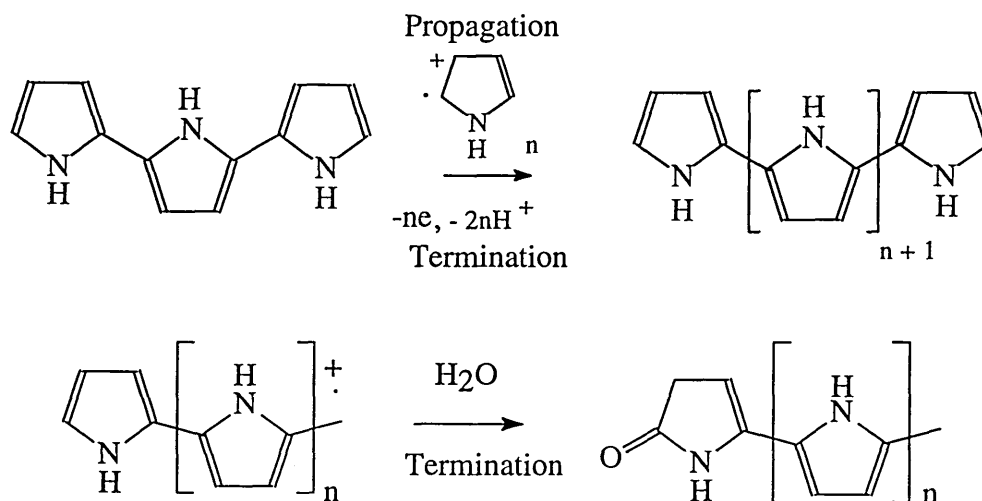
Growth rapidly occurs to form a continuous film that uniformly covers the surface of the electrode. Dimers and high oligomers are formed in the reactions between radical cations. The energetically favoured growth position is the α–position but coupling to other ring positions may also occur. As the polymeric chain length increases the selectivity of the α and β–positions becomes more equivalent resulting in the production of a more random chain. The termination step is as yet unknown but either of steps outlined above could take place, the latter involving the nucleophilic attack of water on the growing polymer chain. This step is obviously more likely to occur when films are deposited in aqueous media.

As a result of the monomer having a higher oxidation potential than the polymer, overoxidation of a polymeric film is a consequence of its formation[111]. This results in the majority of the structural defects which have been observed to occur in polypyrrole films (Fig. 1.10). These defects commonly involve oxygen, especially if the system is electrochemically deposited in water, when both carbonyl and hydroxy groups are produced[120]. The deprotonation during the polymerisation process leads to an acidic environment at the electrode interface and surrounding environment[121]. This

26

environment is thought to lead to the presence of aliphatic hydrocarbon groups on polymeric chains. The introduction of α–β coupling and the occasional presence of non-alternating rings (adjacent unrotated pyrrole units) can affect the chain linearity and the overall charge transport properties of the films formed[122].

Fig. 1.10 Diagram of possible structural defects occurring in polypyrrole[123]
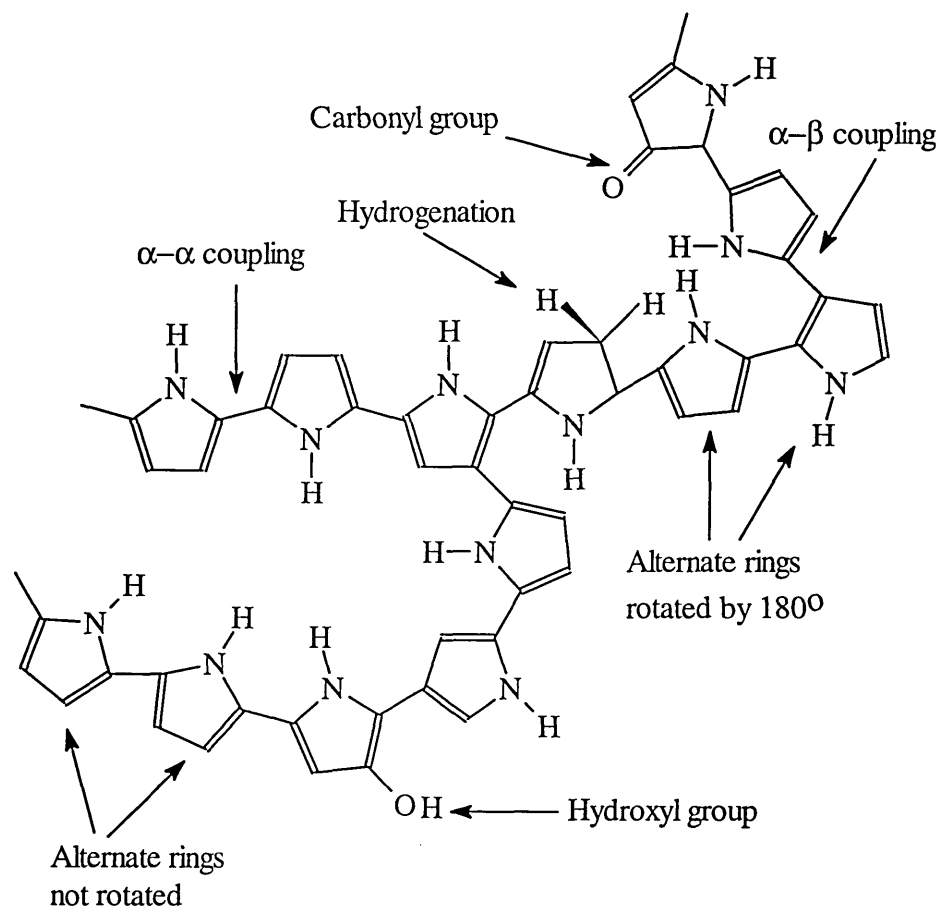
1.81 The conduction mechanism of polypyrrole

The electrical conductivity of materials depends on the energetics of their most mobile electrons so that the electronic structures of materials around the highest occupied and lowest unoccupied orbitals are significant. In solid lattices the discrete electron orbitals of the contributing lattice points (atoms in metals and simple elemental semi-conductors) must be combined in order to model the lattice electronic structure. This approach generates 'bands' of energy levels, which may be more or less continuous or may have sizeable 'band gaps' between clusters of allowed energy levels

The banding of orbitals (illustrated in Figure 1.11[124]) in the solid state is a consequence of the Pauli Principle since a lattice contains very many lattice points in the same 'system' where no two electrons may be in the same quantum state. The discrete energy levels of the contributing lattice points must, accordingly, spread somewhat producing bands of energy levels centred around the mean energy value of the contributing orbitals (e.g. the atomic orbitals of metal atoms contributing to a metallic lattice). The degree of spread of the energy levels is greatest for orbitals in the outer shells of the lattice points, since their outer surfaces are interacting most with their neighbours. Therefore the degree of spread is found to depend on the proximity in space of the contributing lattice points. In Figure 1.11 the spread on the energy scale is shown to vary with the interatomic spacing in an atomic lattice, but a similar diagram would result if energy were plotted against atomic size for lattices with the same internuclear distances. The spread is also affected by the co-ordination number in the lattice since the more atoms there are in the same region of space the more electrons having similar quantum states there will be.

Band theory can be applied to both atomic and molecular lattices (such as polypyrrole). Amongst atomic systems, metals have the most densely packed lattices. Here the spread is so great that the most significant outer band generally contains energy levels from two or more discrete orbitals of the contributing atoms (including vacant orbitals). In the lattice, therefore, there will be vacant orbitals in the same band as the highest occupied orbitals (in the ground state Aufbun electron structure). Promotion into these higher orbitals is facile above absolute zero (Fermi-Dirac theory) but, once promoted, an electron has a potential energy greater than the Fermi energy (which is approximately, the energy of the highest occupied orbital in the ground state) and corresponds to a 'free' (mobile) electron.

Covalent lattices have lower co-ordination and may have greater spacing than metal lattices. Silicon and germainium are semicondutors because the filled molecular orbitals and vacant molecular orbitals generate separate bands (called the 'valence band' and

'conduction band' respectively) with a band gap between them. The Fermi energy of such lattices is within the band gap which must therefore be bridged if an electron is to become mobile. Accordingly semicondutors become conductive either if energy is supplied (thermal or photo) to promote electrons (intrinsic conduction) or if dopants are added to alter the energetics and / or electron occupation of the lattice (extrinsic conduction). If the band gap is too great (e.g. diamond) then these strategies are ineffective and insulating behaviour results.

Molecular lattices are amenable to band theory analysis although most organic molecules form widely spaced, low co-ordination lattices with very large band gaps. Molecules containing fairly extensive π-systems do, however, provide some conductors and semiconductors. Whereas σ-molecular orbitals (MO) are confined close to the molecular core, π-MOs are directed outwards and combine (depending on the crystal structure) with similar π-MOs, reminiscent of semiconductor materials, i.e. there are significant band gaps

The 'organic metals' are a class of materials based on molecular lattices having structures with reduced band gaps usually due to doping. Conduction by molecules is achieved using planar structures which are highly conjugated, giving lattices which contain extensive molecular orbital overlap due to their molecular packing. The presence of orbital overlaps in the structure leads to a highly delocalised electron system. The conductivity of such 'organic metals' (e.g. polypyrrole) is proportional to the presence of charge carriers, (whether they be electrons, holes or ions), and their relative mobilities. This explains why reduced polypyrrole is a poor conductor since a lower number of charge carriers (holes) is present. As the extent of oxidation increases the number of charge carriers increases, and therefore so does the overall conductivity of an electropolymerised conducting polymer film[120].
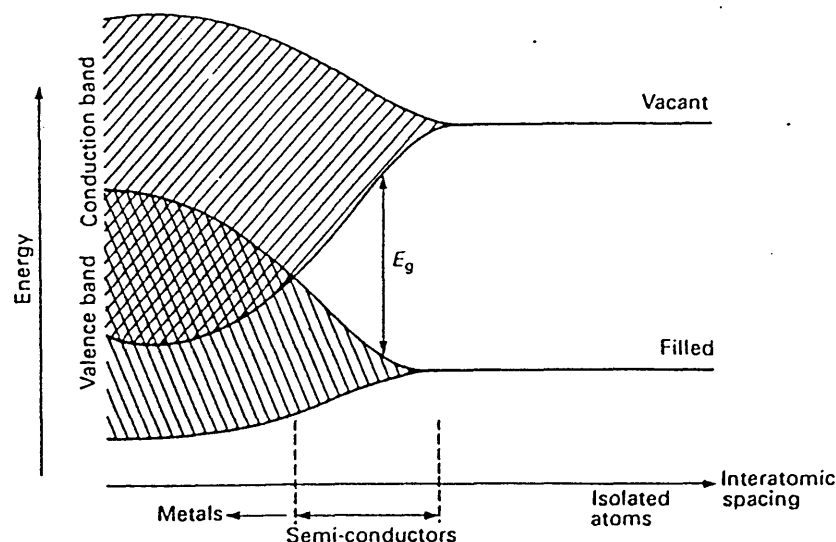
The mobility of charge carriers can be related to the ease with which charge moves through a system. Mobility is hindered if there is considerable structural disorder present in the system, e.g. a sample of polypyrrole. The way in which charge moves in a conducting polymer like polypyrrole can be separated into two possible components, intrachain charge transport occurring within a polymer chain and interchain charge transport involving the movement of charge between neighbouring chains ('hopping'). The latter process requires more energy, therefore the resistance of a polymer film is primarily due to the interchain charge transport component[125].

The type of charge carrying species present in polypyrrole has been the source of considerable research. The majority of conducting polymers have the common feature of a non-degenerate ground state[126,127], that is when the positions of the single and double bonds are reversed an equivalent structure results (quinoid structure in the case of PPy) but with a different energy. It has been determined that, as a result of oxidation an electron is removed from the valence band of polypyrrole creating a hole (in fact a radical cation is created). The radical cation which is created in combination with the adopted quinoid structure is not completely delocalised, and the charge is partially delocalised over a few monomer units (Fig 1.12)[128]. This partially delocalised radical cation is termed a polaron and has a spin contribution of 1/2. *Bredas et al*[129]

described the change from the stable ground state (aromatic form) of the polymer to the equivalent quinoid structure (containing the reversed single and double bonds) as a lowering of the ionisation energy (or the electron affinity) which is energetically favoured. The radical cation has a higher energy level associated with it compared with the valence band. Polaron formation leads to the production of two states within the band gap a bonding and an anti-bonding contribution, where the unpaired electron occupies the lower bonding state (Fig 1.13(b))[123]. On further oxidation of a polymer chain already containing a polaron, a further electron is removed. This induces the formation of a dication which is termed a bipolaron. The bipolaron species has a spin of zero.

Fig. 1.12 Polaron and Bipolaron states of polypyrrole

Polaron (spin = $\frac{1}{2}$)

Bipolaron (spin = 0)
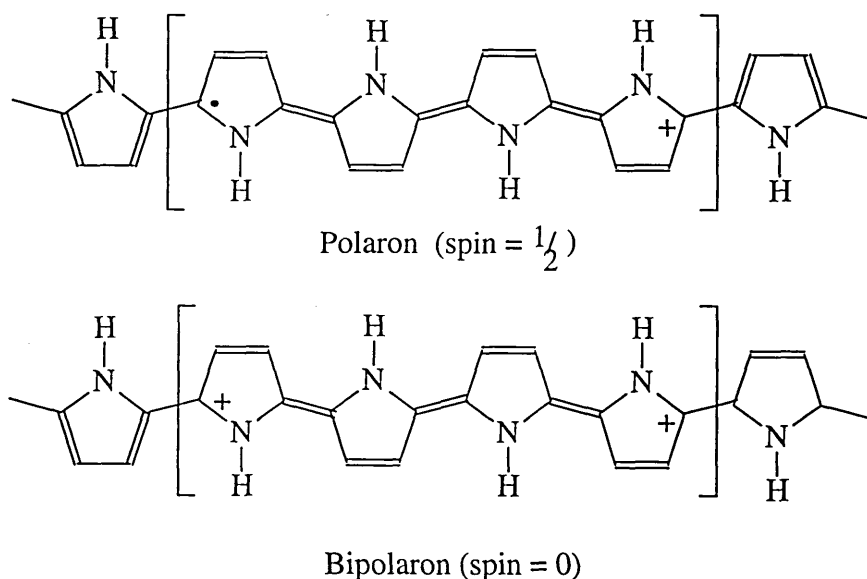
As the extent of the oxidised polymer increases, relative energies appear to overlap and the formation of bipolaron bands[130] appears within the bandgap. The electronic energy diagram displays the electronic states of the polypyrrole system from low levels of oxidation with the formation of polarons (Fig 1.13(b)) through to the bipolaron (Fig. 1.13(c)) and finally a structure which compares to the higher levels of doping (33%) found in electrochemically deposited films. The movement of charge carriers through a film is a matter of uncertainty although it is likely that the bipolaron dissociates into two polarons prior to movement[126].

Fig. 1.13 Electronic energy level diagrams of polypyrrole at various levels of oxidation
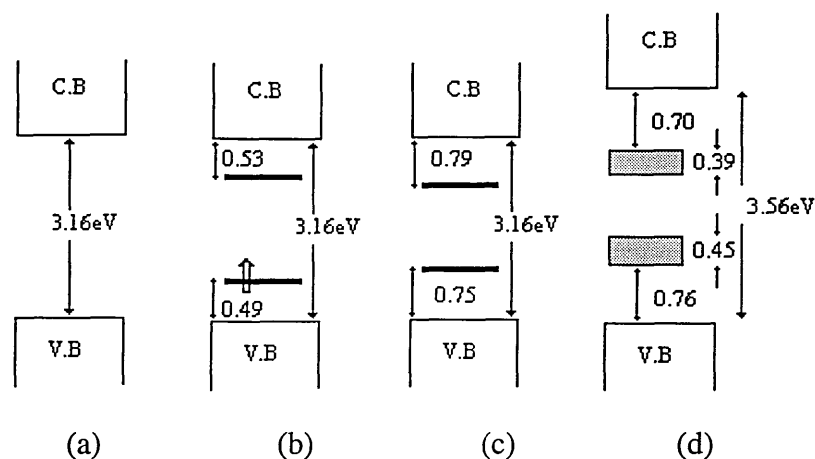
It is was intended that the films produced under the electrochemical conditions used in this thesis would adopt the configuration of the final energy diagram, with conduction primarily due to bipolarons as a result of high levels of doping and oxidation. Theoretical calculations have suggested that it is not feasible for PPy to display metallic type conduction i.e. the band gap would not close even on 100% doping were this possible.

1.9 Aims of the research project.

The development of conducting polymer chemiresistors for use within multisensor arrays is still, in some ways, in its infancy. The incorporation of such arrays into electronic nose technology allows the analysis of outputs from individual sensors and the whole array, using dedicated statistical analysis software for data processing. A primary, general aim of the work described here, was the exploration of all those parameters that contribute to the production of sensors that are effective discriminators when part of a multisensor array.

Three main approaches were used. Detailed electrochemical studies were used to prepare and examine those sensors with proven efficacy and investigate variants of the electropolymerisation protocols. Secondly new sensors were prepared mainly by variation of the electropolymerisation systems (especially the electrolytes that provide

primary dopant counterions), in order to assess their ability to extend the discriminatory power of multisensor arrays. Thirdly the sensor films were subjected to a range of characterisation techniques (especially electrochemical analysis and surface analysis) in order to attempt (in the long term) to draw correlations between polymer fabrication, film structures and surface textures, and electrochemical behaviour as conductors/chemiresistors. The new sensors might usefully enhance discrimination by the electronic nose via different pattern recognition characteristics while the correlation studies could eventually lead to rational design of sensor arrays for different, specific analytical application based tasks.

There were several strands to the laboratory work carried out, each involving one or more of the foregoing approaches. The most significant strands of the work were as follows:-

1. Initial studies by *Bartlett et al*[49] had highlighted the effectiveness of polypyrrole based films as chemiresistors within multisensor arrays. A major task in the current work was a comprehensive study of chemiresistors available using polypyrrole (starting with *Bartlett's* systems but extending into new territory). The nature of the counterions incorporated into films during the deposition from aqueous media was examined. A wide variety of electrolytes (the sources of counterions) was used including univalent inorganic anions, alkyl and arylsulphonates, metal complexes and ionic polymers. As a result several new film fabrications were achieved that had not previously been tested in electronic nose technology.

2. Linked to (1) a selection of the polypyrrole chemiresistors was prepared in non-aqueous media, to highlight any differences and to address a key variable in sensor fabrication - the effect of the deposition solvent on sensing characteristics.

3. Other monomers for electropolymerisation to give potential chemiresistor sensors were investigated. They included heterocyclic, cyclic and functionalised monomers, many selected from the literature as bearing some resemblance to

polypyrrole conductors (i.e. primary doped conductors having band gaps of different sizes but vulnerable to secondary doping effects). This aspect of the work was necessarily limited since it had been decided to restrict studies to those systems that were compatible with the Neotronics NOSE instrumentation, that fell within the narrow range of resistances acceptable to the instrumentation, and that were economically viable

4. A selection of the sensors produced in (1), (2) and (3) that seemed of interest were investigated by electrochemical and surface analysis techniques

5. A study was carried out to investigate sensor optimisation. One generally useful system was examined to determine the effects of the electrodeposition protocol, film thickness surface morphology and baseline resistance on its sensory responses.

6. A selection of the sensors was used in studies of the responses of polypyrrole chemiresistors to a range of pure, single organic vapours. These studies utilised both commercial Neotronics NOSE instrumentation and in-house test-rigs (essentially sealed flasks incorporating test sensors and allowing the introduction and pumping away of organic volatiles). As a result, semi-quantitiative information was gleaned relating sensor response to the effects of e.g. shape, size and the position and nature (e.g. polarity) of functional groups in analyte molecules.

The multifaceted series of experiments was intended both as an aid (soundly based academically) to the enhancement of sensor elements available for Neotronics, and as a contribution to the (surprisingly small) knowledge base concerning the interaction between differing conducting polymer films and volatile organic molecules.

1.91 Layout of the thesis

The remainder of the thesis describes the experimental work performed, presents the results obtained, and discusses the outcomes with particular reference to multisensor arrays related to the electronic nose technology.

A key aspect of the fabrication of electropolymerised chemiresistor sensors is the substrate and electrode onto which the conducting polymer film is deposited. While this was not a part of the main body of the work performed, studies into the fabrication of gold electrodes onto suitable substrates featured in the preliminaries to the main work. This aspect of the project is described in Chapter 2.

In Chapter 3 descriptions are given of the various experimental techniques deployed to accomplish the aims and objectives discussed in Section 1.9 (but c.f. Section 1.7 for an additional description of the Neotronics NOSE) As implied above, a variety of methodologies was required encompassing electropolymerisation, chemical synthesis (monomers and novel electrolytes), cyclic voltammetry, scanning electron microscopy, spectroscopy (X-ray and reflection-absorption infra red for surface analysis) and the use of the electronic nose itself. Instrumentation and the theoretical background is addressed in Chapter 3 together with descriptions of procedures used for the formation and electrochemical characterisation of conducting films. Finally, full details are presented of chemical synthesis of those monomers and electrolytes which are not available commercially.

The outcomes and implications of the experimental work are described in Chapters 4, 5 and 6. Chapter 4 addresses the impact of electropolymerisation on key sensor characteristics, via the use of different monomers, electrolytes and solvents, and the films which result. Chapter 5 builds towards an optimisation of the fabrication procedure (i.e. the electropolymerisation conditions rather than chemical variables). The studies consider the impact of both potentiostatic and galvanostatic deposition, and the

relationships between baseline resistance, film thickness and morphology with respect to the sensing responses obtained.

In Chapter 6 the focus is narrowed in order to consider the efficacy of the more promising new polymer systems when incorporated into sensor heads for electronic nose applications. Criteria are identified for effective sensor arrays, and results are discussed of a detailed study of a polypyrrole/arylsulphonate system comparing analyte responses for films deposited in aqueous and non-aqueous media

The thesis closes (Chapter 7) with a description of the major conclusions to be drawn from the original work performed (in the context of previous knowledge), and an assessment of some future work resulting from ideas generated in this thesis. All references cited in the thesis are assembled in their order of citation at the end of the main work (Chapter 7).

Chapter 2 Substrate design and development

2.0 Introduction

The fabrication of substrates was based on initial studies carried out by *Bartlett et al*[49] who had physically evaporated pure gold onto alumina tiles. Using conventional photolithographic techniques the gold surface had been patterned, and a passivation layer spin coated onto the gold surface. An area was etched through the passivation layer for the electrochemical deposition of the desired polymeric film. The active area for film growth was $1mm^2$ with a 15μm insulating gap vertically down the centre of each device. The films were deposited across the gap, hence completing the electrical circuit. Due to the increasing use of semiconductor technology and its availability, designs were completed with a view to producing substrates on silicon wafers.

2.1 Fabrication procedures

The experimental fabrication of the new substrate devices was performed in a class 100 semiconductor clean room operating to standard industrial conditions. The silicon wafers used in the manufacturing process have a 100-type crystal structure, and during their manufacture they have been n-doped with phosphorus $(\rho = 2.8\Omega cm)$. The silicon wafers act purely as a supporting medium to the substrate design. A masking layer is required to block any diffusion processes between the substrate and the wafer; this should be robust, uniform, and adhere strongly to the surface of the wafer. For this purpose an insulating silicon dioxide layer was used. All the wafers used underwent a pre-treatment process which involved the generation of a silicon dioxide layer, achieved by placing the wafers in an oven at 1000°C where nitrogen, bubbled through water at 95°C, was blown over the wafer's surface. The oxide layer produced from this was in the region of 0.8 - 1.0 μm thick, as measured using elipsometry (this technique determines the thickness by measuring the rotation of plane polarised light due to the quartz layer).

The generation of an integrated circuit required the use of optical techniques to project the image of the design onto the wafer. The use of visible light is not feasible as the component geometries are of similar size to the wave length of visible light. A high resolution image can be obtained by using radiation with a wave length smaller than the item to be imaged, either x-rays or ultra-violet. Standard photolithographic techniques were used to project the image of the substrate design onto the wafer using ultra-violet light; the design information is held on previously prepared photolithographic plates. The dioxide coated wafer is coated with a photosensitive material called a photoresist. The image held on the photolithographic plate is exposed onto the wafer and then developed. Areas of the wafer remain covered in the resist material while others are exposed, to allow the selective processing of the substrate (Fig 2.1).

When the photoresist material is exposed to the ultraviolet light the resist undergoes a change in its solubility, the soluble areas being removed with an etchant solution. Depending on the resist type some areas of the wafer are exposed while others are covered, therefore protecting against further processing. Resists that become less soluble on exposure to radiation are termed negative resists, while the reverse are called positive resists. The graphical illustration highlights these effects.

Fig. 2.1 Patterning techniques using negative and positive resists[132].
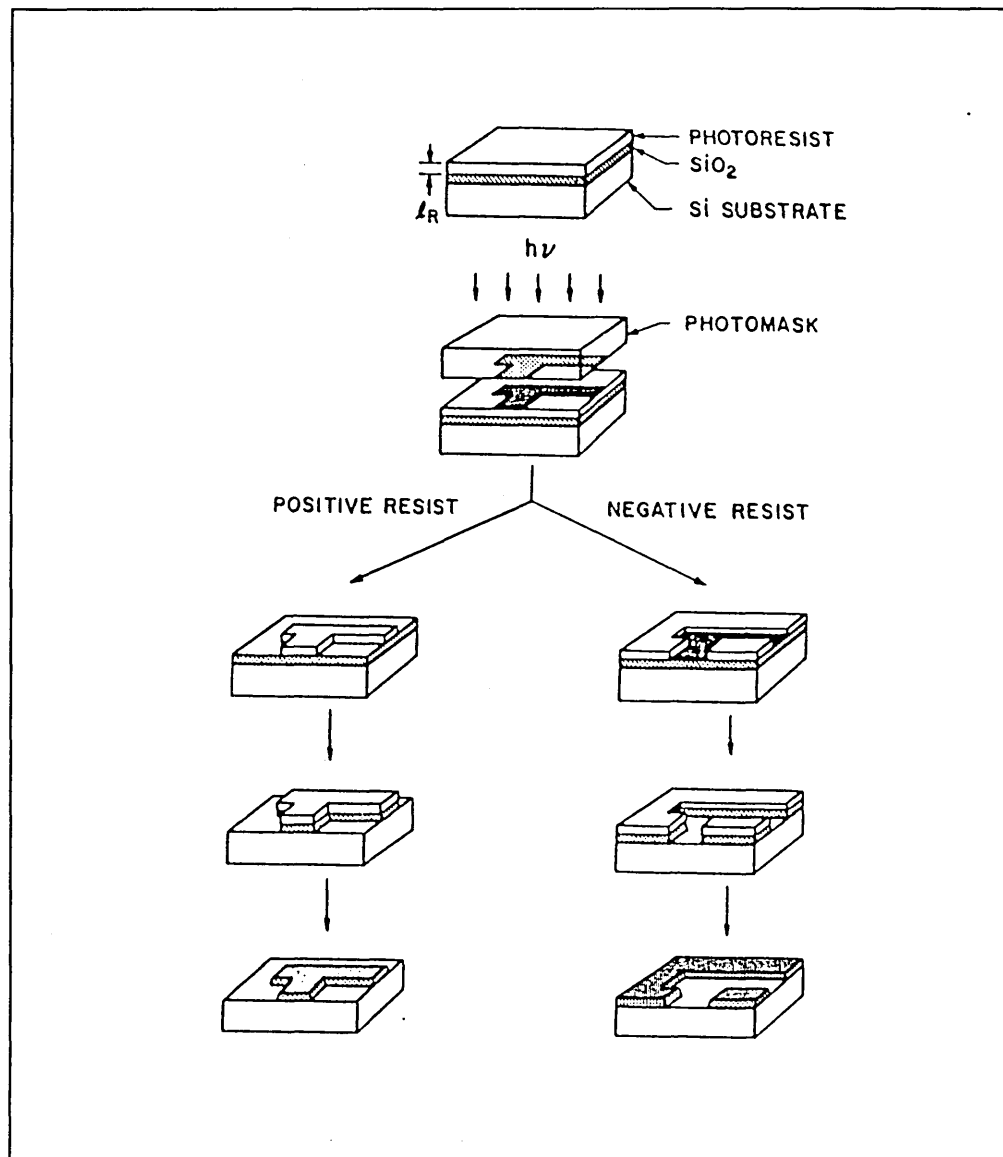
2.2 Experimental

The initial design information was provided by Neotronics Ltd. and consisted of a $7mm^2$ substrate, an adhesive tungsten layer, a gold deposition surface and a CVD nitride passivation layer. The gold surface on the substrate design was separated by a $10\mu m$ insulated gap across which the conducting film was to be deposited thus forming an electrical circuit. The exposed areas in the passivation layer were the two electrical contacts and the area for film growth (i.e. working electrode with a surface area of 7.5 $x10^{-3}cm^2$).

The design was reproduced on a computer aided design package called Autocad whereby the information is stored and generated using a series of vectors. This information was transferred to magnetic tape and converted to Electromask format. This is known as fracturing, i.e. where an image from Autocad is broken down into a series of rectangles. The instrument used for mask generation is an Electromask Combo which is compatible with tapes in the Electromask format. This system has both pattern generating and image repeat facilities. The image is projected onto a photographic plate and built up by repeated exposure of that plate at high resolution (AgX gain size = 30nm). The production of the substrates required the initial preparation of two sets of plates to transfer the patterned design onto the wafer during the production process.

The process of vacuum deposition was used to deposit the metal layers onto the dioxide surface of the wafer. In this process a substance is melted under low vacuum(10^{-5} -10^{-6} torr) and then boils to deposit a layer of that substance within the range of the source. The metals used were held in a basket and a current applied until they vaporised. Initial studies, vaporising gold (99.99%) directly onto the dioxide wafer surface, highlighted the need for improved adhesion between the two surfaces. There were several ways in which this could be addressed, sputtering gold onto the wafer, roughing up the silica layer, or application of a bonding layer. For commercial reasons the latter was decided upon, the potential choices of material being either chromium, titanium, or tungsten.

The use of chromium was discounted on the basis of its potential to form unwanted oxides or nitrides. Titanium was chosen as the University facilities favoured the deposition of this material.

The first method of transferring the substrate design onto the wafer involved a technique called 'lift off'. This involves the patterning of the resist material before the vacuum deposition of the required metal layers. Photoresist strippers were then used to remove the unwanted resist thereby exposing the patterned design.

A series of wafers were coated with negative resist (HNR120) and soft baked at 85°C for 45 seconds. In each case the resist was then exposed to ultraviolet light for three seconds, then developed. A titanium layer then a gold layer were deposited onto the wafers, with the thickness of the titanium layer being varied to determine its effect on adhesion. On removal of the negative resist it was expected that the corresponding metal layers would be removed leaving the desired pattern. Photoresist stripper in conjunction with an ultrasonic bath was used to remove the unwanted resist. Results from these experiments showed that this technique would prove unacceptable due to poor edge definition and removal of sections of the gold layer, although there was an obvious improvement to the gold adhesion with thicker titanium layers(< 100°A).

Wet etch techniques were considered[131,132], involving vapourisation of metal layers onto the gold surface, then patterning the material using photoresist. Etches can be used to remove the unwanted metal, leaving the desired design; the remaining resist is removed via an oxygen plasma. Initial wet etch techniques centred on the use of a positive resist (HIPR 6512), the etching process being repeated for the individual metal layers, ensuring that there was good alignment during patterning procedures. The etchant compositions varied depending on the metal. For removal of the unwanted gold a potassium iodide/iodine etch was used, whilst the titanium required a hydrofluoric acid etch. The concentrations of the etches were varied to obtain etches which gave the

41

best edge definition of the metal layers. The remaining positive resist was removed using a plasma asher.

Analysis of these wafers showed poor edge definition and it was felt that this could be improved upon by the use of negative resist. The masks used for generation of the photolithographic plates were redesigned, such that the area around the electrode design was shaded. Wafers with the respective metal layers already deposited were treated with negative resist and patterned with the new masks. The exposure of the monomer resist to ultraviolet light allowed the radical polymerisation of the monomer to the polymer in the unshaded areas. A series of washes was used to remove the unwanted resist and the wafer was hard baked for sixty seconds at 135°C to harden the polymer. The etching processes were performed as before and between each etch the wafer was hard baked to ensure that the resist was dry. The negative resist was finally removed by using the oxygen plasma.

The study of various photolithographic techniques confirmed that the wet etch techniques using the combination of negative resist was the most successful approach. The inclusion of an adhesive titanium layer considerably improved the bonding of the gold layer. Careful monitoring of the etchant concentrations improved the edge definition of the patterned substrates. The final stage of depositing a passivation layer was completed using a negative resist as the facilities for CVD nitride are not available at the University. The results gained during this brief investigation into the feasibility of substrate production proved valuable to the commercial company who undertook the continued development of substrates based on the investigations reported here.

2.3 Surface Analysis of deposited metal layers

Two techniques were used in the analysis of the metals deposited by the Edwards Vacuum deposition instrument. The first and most useful of these was GDOS (Glow Discharge Optical Spectroscopy). This technique provided quantitative and qualitative information on the elemental composition of the deposited metal layers. Wafers prepared using the various forms of processing were also examined under a SEM (Scanning Electron Microscope), which highlighted the improved edge definition of the patterned design using negative resist processing techniques.

2.31 Glow discharge optical emission spectroscopy

The GDOS technique utilises an argon glow discharge that causes removal and stable excitation of atoms from the test sample and allows quantitative and qualitative analysis of the sample components as a function of depth. If sufficient energy is transferred to a sample atom via an argon atom from the glow discharge, a higher energy level or orbital transition takes place. This provides an excited state and also a vacancy in a lower energy level. The higher energy state is unstable and when the atom relaxes back to the lower energy ground state (by the transition of an electron), the excess energy is normally liberated in the form of a photon of characteristic wavelength, defined by the equation below.

$$(E_1 - E_2) = hc \backslash \lambda$$

where E_1 = energy in the excited state E_2 = energy in the ground state

    h = Planck's constant

    c = speed of light

    λ = wavelength

Due to each element having different electron orbital energy levels, the wavelength of the photon emission will be characteristic of the elements present in the sample. The intensity of the emission lines will be proportional to the number of emission quanta and therefore representative of the elemental concentration[133].

43

The GDOS equipment used was a LEO 750-GDS which consists of a water type glow discharge source[134] with a standard 4mm diameter aperture and a hollow cylindrical anode under vacuum (Fig. 2.2). The cathodic sputtering process of the source is created by applying a voltage to the sample (cathode) under a controlled argon pressure across the sample surface. The surface atoms affected by the source are removed by the sputtering process and diffuse into the argon plasma where excitation and photon emission occurs. The separation of the removed atoms and their excitation provides spectra with a linear relationship between elemental concentration and spectral intensity[135].

Fig. 2.2 The glow discharge lamp and polychromator
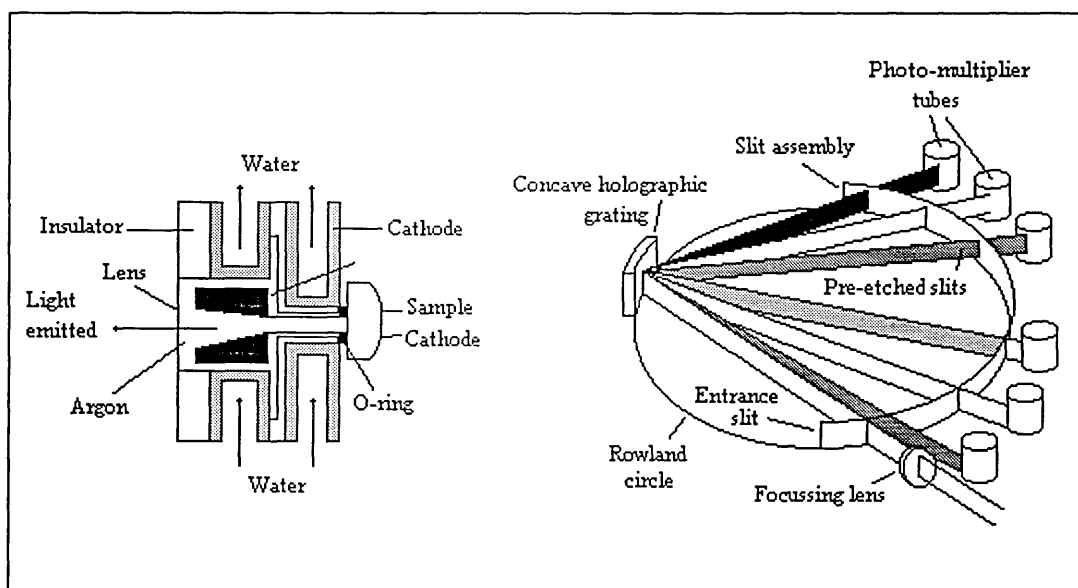
The emitted light passes from one end of the glow discharge lamp through an entrance into the polychromator. The spectrometer is of the Paschen-Runge configuration and the polychromator is based on a Rowland circle, which contains a series of pre-etched slits, enabling a range of spectral wavelengths to be focused on a surface simultaneously (Fig. 2.2). This allows the detection of up to 44 elements through a series of photo-multiplier tubes positioned around the spectrometer periphery. The system is operated either in a constant current or voltage mode, certification is provided by testing against a series of standard reference materials of known

44

concentration. The depth profile analysis has to be considered with care as certain parameters can affect the results significantly e.g. surface roughness and non-uniform crater shape.

The following page (Fig. 2.3) illustrates a typical result using GDOS to analyse the elemental composition of a wafer with and without a bonding titanium layer used to adhere a gold surface. The analysis shows the presence of further elements at certain points in the depth profile particularly sulphur and carbon accruing in the region of the silicon dioxide /gold interface. This further indicated that there was trace contamination affecting the purity and potential adhesion of the two applied surfaces. To reduce this it was proposed to introduce a mechanical shutter over the basket in the Edwards Depostion equipment, as trace contamination is thought to occur during the initial stages of the evaporation process due to the vaporisation of contaminants with lower melting points. The introduction of the bonding titanium layer also reduced the level of contaminants observed

Fig. 2.3 Glow discharge optical emission spectra of precoated wafers
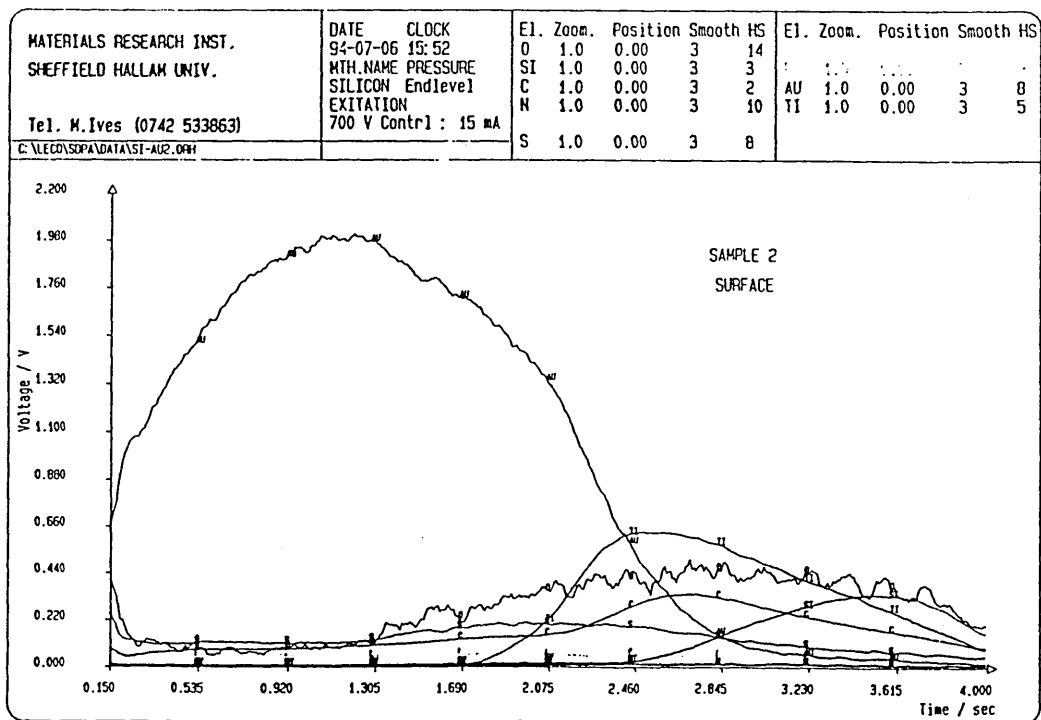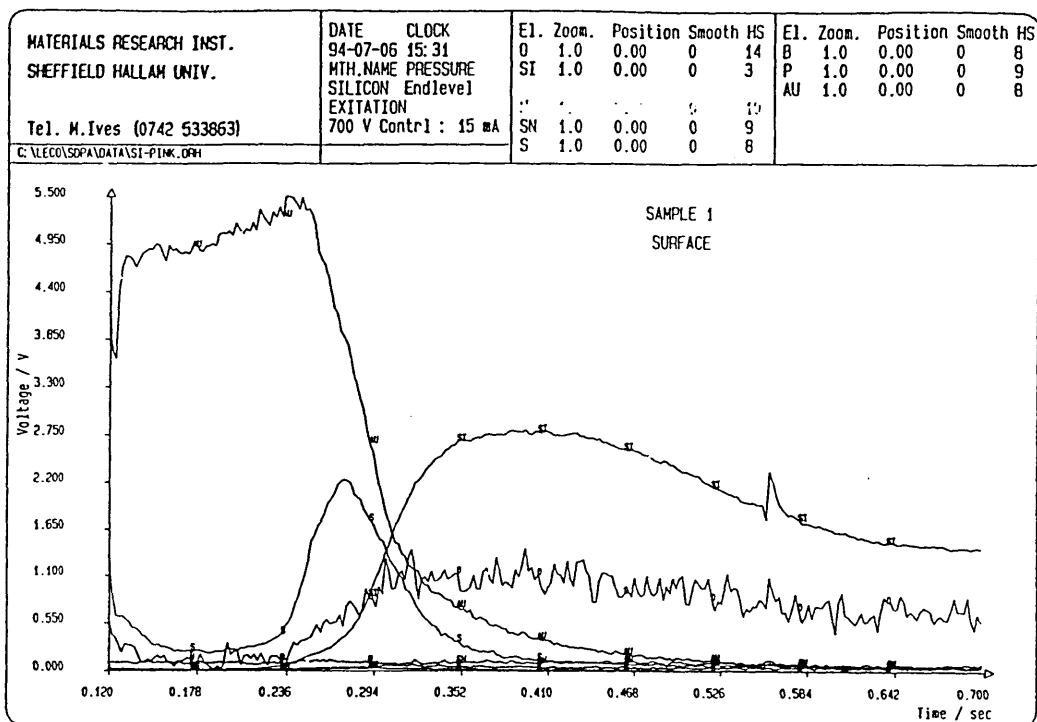
2.4 Substrate design and continued development

The Bass Warwick Sensor Mk2 was the initial design that was approved for use in conjunction with NOSE technology. After studies using this design it was decided that it could be optimised further. Following this decision it was decided to reduce the design and minimise the surface area of the gold on the substrate, hence optimising the number of substrates per wafer, reducing the unit cost per substrate. This led to the development of the current design Sensor Mk3 illustrated below (Fig. 2.4). This design was used throughout the experimental studies in this thesis.

Fig. 2.4 Sensor Mk3 Design

Sensor Mk III (mm)
General Tolerance +/- 0.1mm
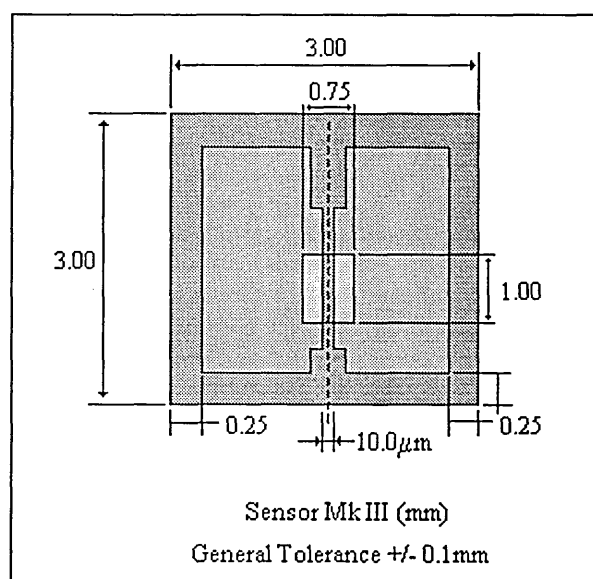
At present this design is proving to be adequate for the electrochemical deposition of polymer based films. But it is felt that the development of a design incorporating an interdigitated format may further enhance the quality and long-term stability of thin polymeric based films and may also increase the overall sensitivity of the instrument. There is already a variety of commercially available interdigitated microsensor electrodes (IME's)[136] that are microfabricated from vapour deposited gold or platinum and available with a variety of space dimensions in the micron region. They are already widely used in research and development predominantly for chemiresistive chemical and biological sensors, electroactive polymeric films, and for impedance

47

sensors based on Langmuir-Blodgett technology. The possible advantages of incorporation of these designs into the NOSE technology include:

1. Greater control during film formation allowing the deposition of uniform thin films.

2. Increase in overall surface area providing a larger area for analyte interaction.

3. Maintaining required resistance levels whilst increasing surface area.

4. Increasing the total gap length reducing the probability of sensor failure due to shrinkage occurring with long term use or faults caused during deposition.

The designs illustrated highlight some of the ideas which could be exploited to improve the existing NOSE based technology.
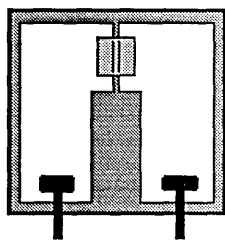
a.   b.
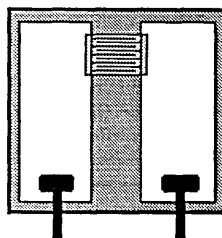
c.
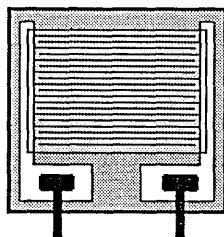
a. Standard design

b. Standard design incorporating interdigitation, comparable growth area, increased gap
    length

c. Interdigitated substrate with increased growth area and increased gap length

Chapter 3 Experimental

3.0 Introduction

This chapter describes the instrumentation, materials and procedures used in the electrochemical deposition of conducting polymer films, and also includes experimental parameters for the cyclic voltammetry performed. The first synthetic section (3.2) includes details of the counter ions used in the formation of the chemiresistors; these can be found in the text and the appendices (Appendix 1) where a more comprehensive list can be found detailing the abbreviations used. The synthetic section outlines the formation of tetraalkylammonium salts for the deposition of chemiresistors in non-aqueous media, and the corresponding elemental analysis data for the compounds prepared.

The main organic section (3.4) contains the synthesis of the β–substituted pyrroles, 3-methylpyrrole, 3,4-dimethylpyrrole and 3-pyrrylacetic acid Their synthesis was aimed at the investigation of simple substituted pyrroles leading to films with suitable conductivites but more for diverse sensing properties than polypyrrole itself. The final synthesis is that of a chiral monomer from which it was proposed to investigate films which were potentially chirally active, and were considered for use in chiral discrimination of optically active analytes.

The final section discusses the characterisation techniques which were used in the analysis of conducting polymer films. The use of cyclic voltammetry provides an insight into a film's redox properties and overall stability. Scanning electron microscopy information was used to study the topology of films, and, via linkage to an Energy Dispersive X-ray analyser, it was also possible to study the elemental composition of some films. The use of reflection absorption FT-IR provided spectroscopic information on the films but was limited due to the hygroscopic nature of

49

the films. The NOSE technology provided information on variations in sensor responses and discriminatory properties.

3.1 Electrochemical deposition of thin polymer films

3.11 Instrumentation

The galvanoastatic and potentiostatic electrochemical polymerisation of pyrrole, 3-methyl thiophene, azulene and substituted pyrroles was performed using an EG&G PAR 362 Scanning Potentiostat/Galvaniostat interfaced with a Time Electronics 2003 DC Voltage Calibrator. The majority of the potentiostatic depostion was performed on an Oxford Potentiostat Model connected to a Bryan Instrument X-Y plotter. All cyclic voltammetry was completed using this equipment.

3.12 Materials

The pyrrole was supplied by Aldrich and stored in the fridge under nitrogen. Before use it was passed through a series of pipette columns containing alumina to remove any polar oxidation products present. The 3-methylthiophene and azulene were used as supplied from Aldrich. All aqueous solutions were prepared using distilled water which had been passed through a Milli-Q (Millipore) water purification system. The other solvents used were HPLC grade acetonitrile, butanol, and propylene carbonate all supplied by Aldrich and stored over molecular sieves. The reagents which were used in the preparation of the electrolyte solutions were used as received from Aldrich and are listed with their corresponding abbreviations in Appendix 1. The exception to this was tetraethylammonium tetrafluoroborate which was recrystallized from methanol. All the tetrabutylammonium salts were prepared as explained in the experimental section (3.3) along with the preparation of 1,1-ferrocenedisulphonic acid disodium salt (see section 3.4). The substrates used to deposit the thin films were the Mark 3 sensor type with a total analytical deposition area of (7.5x10^{-3} cm^2) (see section 2.5). The counter electrodes were either Pt foil or coil, and the reference electrode used was a saturated calomel electrode (SCE) both supplied by Russell pH Ltd.

50

3.13 Procedures

The deposition surface of the prefabricated substrates was cleaned prior to use. An initial wash with Milli-Q water was followed by a separate wash in propan-2-ol, after which they were individually dried under nitrogen. Each substrate was then used as the working electrode in a standard three electrode electrochemical cell, which also contained a Pt coil and SCE which had also undergone similar cleaning procedures. The electrolyte solution was prepared using the desired solvent and counter ion at a predetermined concentration and 25mls of the prepared solution was pipetted in to a 50ml beaker. The desired monomer was added at the required concentration and the system was agitated by stirring to obtain a near homogeneous a solution as possible. The solution was then used in the electrochemical deposition process; the electrodes were lowered into the solution with the working electrodes deposition surface clearly below the meniscus. The films were deposited individually in the growing medium. Details of concentrations and growth conditions are outlined in Chapter 4.

Depending on the conditions required for the formation of the desired thin polymer film either a fixed potential, or constant current was applied for a specific time. After this process had been completed the working electrode remained in the electrolyte solution for a further thirty seconds after being switched to open circuit or stepped to zero volts, this process controlling the oxidation state of the formed film and also allowing the current to decay until the system reached a stable state. The substrate was then removed from the growing solution and washed in fresh solvent (as used in that particular growth process), then finally the film was dried under nitrogen, labelled and stored. The preparation of devices required fresh electrolyte solutions for each series of films produced. No more than ten to fifteen devices were prepared from one electrolyte solution.

The base resistance of each device was recorded within the first ten minutes of the deposition process, and again 24hrs later. This measurement was then recorded on a weekly basis, providing information on the continued stability of the films. The

resistance was measured using a standard digital volt meter (DVM) where the circuit's internal resistance was measured at 0.33 ohms.

3.14 Cyclic voltammetry

All redox scans obtained were performed in a comparable manner using the same electrochemical cell configuration as follows. The cell was cleaned rigorously between individual scans which used different electrolytes. Freshly deposited films were prepared for each scan. The cyclic voltammetry was performed in 25mls of a comparable electrolyte solution to that which the chosen film had been deposited in, but without any monomer present. The thin polymer films were cycled between two fixed potentials -1.00 and + 0.50V vs SCE unless otherwise stated; the scan rate was nominally $50mvsec^{-1}$. Films were scanned in a negative direction starting at a slightly positive potential due to their initial oxidation state For each film the initial scan was performed and subsequently further scans were recorded to monitor the overall stability of the redox system. The ratio of current to voltage link via the X-Y plotter was $100\mu A/V$.

3.2 The synthesis of tetrabutylammonium salts from compounds with the sulphonic acid functionality

3.21 Introduction

It is generally accepted that poly(pyrrole) films form via radical cation intermediates (c.f. Section 1.8)[119]. It is apparent, therefore, that the process occurring at the anode interface will be sensitive to the presence and nature of ionic species (especially anions) in the surrounding anion medium (e.g. dissociation constants, ionic strenghts, softness/hardness, nucleophilicity and basicity). Variables in the medium will encompass the solvent as well as the electrolyte. The generation of this particular series of compounds was to enable the deposition of thin films in the aprotic solvent acetonitrile, which is a poor nucleophile. The electrolyte salt used in the electrochemical deposition must be highly soluble and show a good degree of dissociation to anions which are compatible with organic cations[119]. Some lithium salts are soluble in aprotic systems, but have a tendency to aggregate; sodium and potassium salts are only slightly soluble. Tetraalkylammonium salts are commonly used in aprotic systems since they are soluble and highly dissociated. The use of acetonitrile was paramount in determining the contributory effect that the solvent system had on the growth parameters, morphology and sensing characteristics of electrochemically deposited thin polymeric films. Tetraalkylammonium sulphonates were prepared from the corresponding sodium salts by ion exchange.

3.22 Experimental Methods[137-138]

Each tetraalkyammonium salt was prepared by taking a known quantity of the corresponding sulphonic acid sodium salt (normally 0.015mols) and dissolving it in a minimum amount of Milli-Q water (approximately 50mls was used). Once dissolved a stoichiometric amount of tetrabutylammonium hydrogensulphate was added (relative to the number of sulphonic acid groups present in the system) and dissolved. The product was extracted from the aqueous solution using dichloromethane, in which all the desired tetrabutylammonium salts were soluble. The dichloromethane was washed with

water, dried using $MgSO_4$ and concentrated on a rotary evaporator. The product in some cases instantaneously formed white crystals but most required the further addition of diethyl ether to aid the crystallisation process. The white solids were dried and their masses recorded. The resulting salts are listed here with their respective yields. Elemental analysis was also obtained (Table 3.1 Note the shorthand abbreviations for the compounds, they appear listed in the same order as follows).

Tetrabutylammonium benzenesulphonate: (5.34grm, 89.1%)

Tetrabutylammonium acetylbenzenesulphonate: (6.31grm, 95.2%)

Ditetrabutylammonium 1,3-benzenedisulphonate: (8.96grm, 82.8%)

Tetrabutylammonium dodecylbenzenesulphonate: (7.28grm, 85.3%)

Tetrabutylammonium 2-naphthalenesulphonate: (6.17grm, 91.5%)

Ditetrabutylammonium 1,5-naphthalenedisulphonate: (10.27grm, 88.8%)

Tetrabutylammonium 4-toluenesulphonate: (5.79grm, 93.3%)

The following were also produced but not used

Tetrabutylammonium dodecylsulphonate - crystallisation particularly slow.

Tetrabutylammonium nitrobenzenesulphonate - this system proved to have a particularly low melting point and was only a solid below room temperature.

3.3 The synthesis of 1,1'- ferrocenedisulphonic acid disodium salt. (137,139)

Sulphuric acid (100%) (18.25g; 0.33mol) was added to a slurry of dicyclopentadienyl iron (ferrocene) (23.25g; 0.125mol) in acetic anhydride (250ml) The mixture was left to stir for 1 hour whilst allowing the temperature to rise to 46°C. The dicyclopentadienyl iron went into the solution and after a further 2 hours, 1,1'-disulphonic dicyclopentadienyl iron started to crystallise from the solution. It was filtered and washed with acetic anhydride and petroleum ether (40:60). The yellow crystals are moisture sensitive and were rapidly placed into a solution (200mls) of sodium

54

hydroxide (10.0grms; 0.25mol) (to obtain the disodium salt). The water was removed and the crude product was dissolved in ethanol (200mls), filtered, and yellow crystals precipitated upon addition of benzene. (Yield 28.96g; 62.9%)

Elemental analysis calculated for $C_{10}H_{14}N_2O_6S_2Na_2$ Theoretical: H, 2.07; S, 16.44; C, 30.79: Experimental: H, 2.14; S, 15.77; C, 30.63%.

Table 3.1 Elemental analysis of tetrabutylammonium sulphonates

Compound	RMM	Melting Pt. /°C	Elemental Content	Analysis Element	C	H	N
Bu$_4$NBzS	399.619	33-35	C$_{22}$H$_{41}$NO$_4$S	Theory	66.12	10.34	3.50
				Found	65.84	10.46	3.51
Bu$_4$N4-AcBzS	441.655	113-115	C$_{24}$H$_{43}$NO$_4$S	Theory	65.27	9.81	3.17
				Found	65.26	9.98	3.16
(Bu$_4$N)$_2$ 1,3-BzDS	721.130	115-117	C$_{38}$H$_{76}$N$_2$O$_6$S$_2$	Theory	63.29	10.62	3.88
				Found	62.97	10.80	3.84
Bu$_4$NDDBzS	568.939	61-63	C$_{34}$H$_{66}$NO$_3$S	Theory	71.78	11.69	2.46
				Found	71.74	11.73	2.50
Bu$_4$N 2-NapS	449.675	129-131	C$_{26}$H$_{43}$NO$_3$S	Theory	69.44	9.64	3.11
				Found	69.60	9.73	3.12
(Bu$_4$N)$_2$ 1,5-NapDS	771.186	197-199	C$_{42}$H$_{78}$N$_2$O$_6$S$_2$	Theory	65.41	10.19	3.63
				Found	65.58	10.35	3.63
Bu$_4$NTS	413.645	38-40	C$_{23}$H$_{43}$NO$_3$S	Theory	66.78	10.48	3.39
				Found	66.82	10.60	3.40

56

3.4 The synthesis of pyrrole derivatives

3.41 General Information

All reagents were used as received from Aldrich and Lancaster, the solvents used were dried using molecular sieve unless otherwise stated(diethyl ether was sodium dried). The instruments and separation methods used for the analysis of samples prepared were:-

[1]Hnmr spectra obtained using a Jeol JNM PMX-60 SI 60MHz spectrometer or a Brucker 250 AC spectrometer operating at 250MHz, [1]Hnmr data is given on the δ ppm scale using tetramethylsilane as the internal reference. Abbreviations for the form of the signal are as follows: s = singlet d =doublet, dd = double doublet, t = triplet, q = quartet, m = multiplet and b = broad. Samples were prepared in deuterated chloroform.

Mass spectra were obtained on a VG Micomass 7070F

Melting points were obtained on an Electrothermal melting point apparatus

Thin layer chromatography (TLC) was performed on Merck 555 Alufolien Kieselgel $60F_{254}$ plates. Flash chromatography was performed using Sorbsil C-60H (40-60mm) silica gel and the solvents used were distilled.

All reactions requiring inert atmospheres were performed under nitrogen.
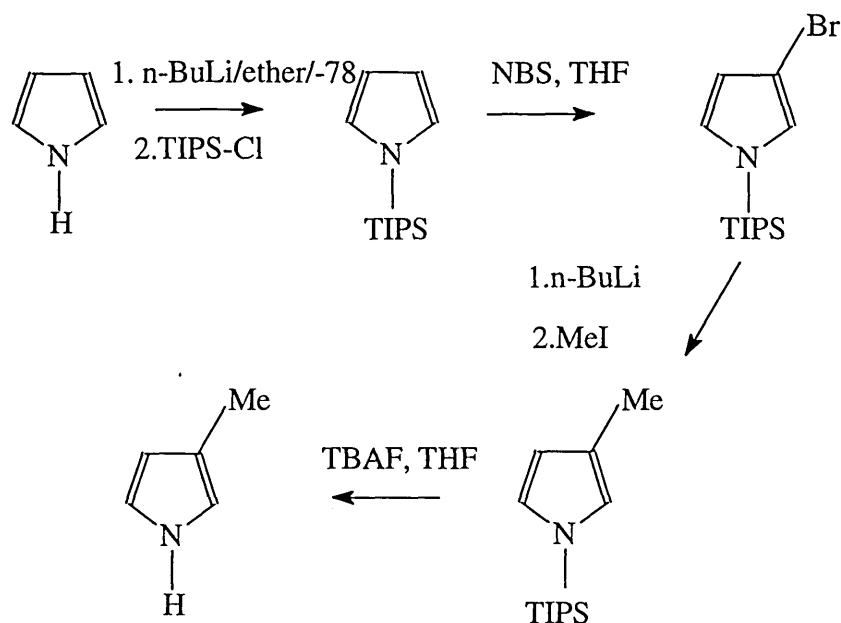
TIPS = -Si(CHMe$_2$)$_3$ (triisopropylsilyl)

Preparation of N-TIPS pyrrrole

To a solution of pyrrole (18.0mls, 259mmol) in distilled THF (250ml) was added 1.6M n-BuLi (178ml, 285mmol) at -78°C The whole system was maintained under nitrogen and stirred. After 10-15 mins triisopropylsilyl chloride (50.0g, 295mmol) was added dropwise via a syringe. After a further 15mins at -78°C the reaction was allowed to gradually warm to room temperature. The reaction mixture formed into a cloudy brown suspension and was diluted with water (100ml), and extracted into diethyl ether (3x100ml). The organic layers were combined and washed with further water. The organic layer was then dried over MgSO$_4$ and evaporated to a brown oil. (Yield 56.41grms: 97.47%) ^{1}H nmr showed the sample to be pure.

^{1}H nmr δ 1.00 (d. 18H) 1.45 (sept, 3H) 6.30 (t. 2H) 6.8 (d. 2H)

Preparation of 3-bromo-1-TIPS-pyrrole

To a stirred solution of 1-TIPS-pyrrole (24.8g,111mmol) in distilled THF (200ml) N-bromosuccinimide (NBS) (20.8g, 117mmol)recrystallized from ethanol was added in one portion at -78°C The suspension produced was stirred under nitrogen for a further 1.5 hours then allowed to warm to room temperature overnight. The solution produced was treated with pyridine (3.1ml) and hexane (250ml). The suspension which resulted was filtered down a prepared alumina column and the filtrate was evaporated to a reddish/brown oil containing a pale solid, which was shown to be succinimide. The filtration process was repeated and the solid removed completely, leaving a clear brown liquid. (Yield 29.91g, 89.1%)

^{1}H nmr δ 1.10(d, 18H), 1.40(sept, 3H), 6.30(dd, 1H), 6.70(dd, 1H).

Preparation of 3-methyl-1-TIPS-pyrrole

To a stirred solution of 3-bromo-1-TIPS-pyrrole (25.0g; 84.7mmol) in distilled THF (250mls) was added n-BuLi (56.8ml; 90.9mmol) at -78°C under nitrogen. After a period of fifteen minutes at this temperature iodomethane, (12.0g, 84.7mmol) was added dropwise over the course of five minutes. The reaction vessel was stirred for a further fifteen minutes at -78°C then allowed to warm to room temperature. The reaction mixture was quenched with water (100ml) and extracted with diethyl ether (2x100ml). The organic extracts were combined, dried with MgSO$_4$, filtered and evaporated under vacuum. The residue was purified using column chromatography eluting with petroleum spirit (40:60): ethyl acetate (4:1). The major fraction was collected. (Yield 19.63 g, 97.6%)

^{1}Hnmr δ 1.10(d, 18H), 1.40(sept, 3H), 2.10(d, 3H), 6.20(m, 1H), 6.60(m, 1H), 6.70 (t, 1H

A solution of 3-methyl-1-TIPS-pyrrole (4.0g;16.8mmol) was stirred at room temperature in 150mls of THF and to this solution was added tetrabutylammonium fluoride as a 1.0M solution in THF (16.8ml, 16.8mmol). After half an hour the reaction mixture was diluted with 100ml of diethyl ether. The organic layer was washed with successive quantities of water, then dried over $MgSO_4$ and evaporated to a brown oil. The brown oil was vacuum distilled with the desired product being collected at 44°C (0.5mmHg) (Yield 0.76g; 53.5%)

[1]Hnmr δ 2.20(s, 3H), 6.10(s, 1H), 6.55(s, 1H), 6.75(s, 1H).

3.43 Synthesis of 3,4-dimethylpyrrole (140)
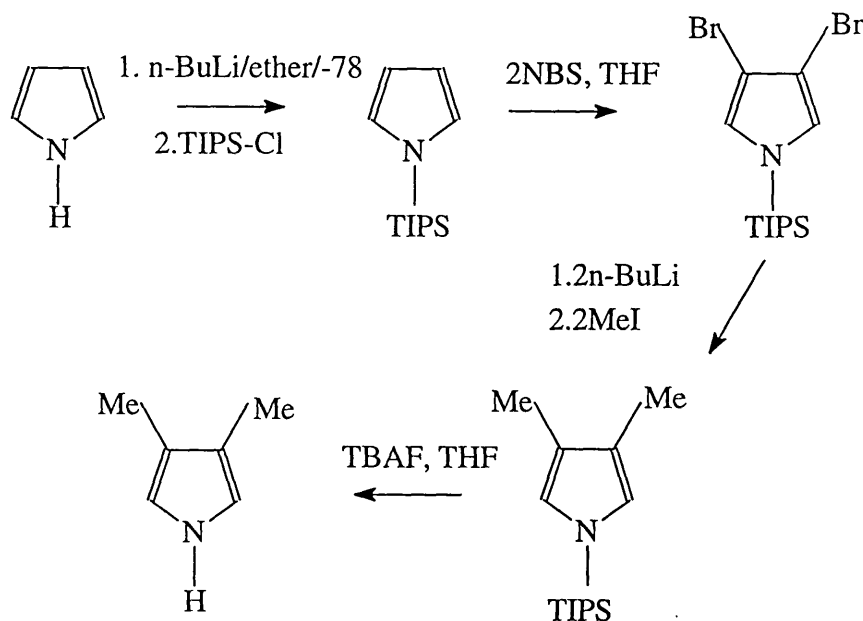
Preparation of n-TIPS-pyrrole as before.

Preparation of 3,4 dibromopyrrole

To a solution of n-TIPS-pyrrole (15.0g, 67.1mmol) in anhydrous THF (200ml) at -78 C under nitrogen, NBS (24.49g, 137mmol) was added. After 1 hour at this temperature the reaction mixture was allowed to reach room temperature. Into this was poured 10% aqueous sodium bicarbonate solution (150ml). The product was then extracted into diethyl ether via several extractions. The organic residues were combined and washed with saturated sodium chloride solution, dried over $MgSO_4$ and evaporated under vacuum. The residue crystallised at 0°C to give the product as a solid. Yield (24.48g, 95.6%) M Pt 76-78°C. M/z 380.9 (M$^+$)

^{1}Hnmr δ 1.10(d, 18H), 1.40(sept, 3H), 6.70(s, 2H).

Preparation of 3,4-dimethyl-1-TIPS-pyrrole

A stirred solution of 3,4-dibromo-1-TIPS-pyrrole (20.0g; 52.3mmol) in distilled THF (250mls) was treated with 1.6n-BuLi (66.6ml; 104mmol) at -78°C. After a period of fifteen minutes at this temperature the solution was treated with iodomethane (15.2g 104mmol), added dropwise over the course of five minutes. The reaction vessel was stirred for a further fifteen minutes at -78°C then allowed to warm to room temperature. The reaction mixture was then quenched with water (100ml), extracted with diethyl ether (2x100ml) and then the organic extracts were combined and dried with $MgSO_4$. The solution was filtered and concentrated under vacuum. The product underwent column chromatography using petroleum spirit (40:60): ethyl acetate 5:2. The product was collected as a brown oil. (Yield 11.17 g, 84.9%)

^{1}Hnmr δ 1.10(d, 18H), 1.40(sept, 3H), 2.00(s, 6H), 6.40(d, 2H)

Preparation of 3,4-dimethylpyrrole

A solution of 3,4-dimethyl-1-TIPS-pyrrole (5.00g; 19.8mmol) was stirred at room temperature in THF (150ml) was added . To this solution, tetrabutylammonium fluoride (1.0M solution in THF) (19.8ml; 19.8mmol) was added. After half an hour the reaction mixture was diluted with 100ml of diethyl ether. The organic layer was washed with successive quantities of water, then dried over $MgSO_4$ and evaporated to a brown oil. At this stage despite taking all possible precautions, the samples prepared continued to polymerise during any purification procedures attempted.

3.44 Synthesis of N-(3-pyrrolyl-acetyl)-(L)-valine methyl ester[141-143]
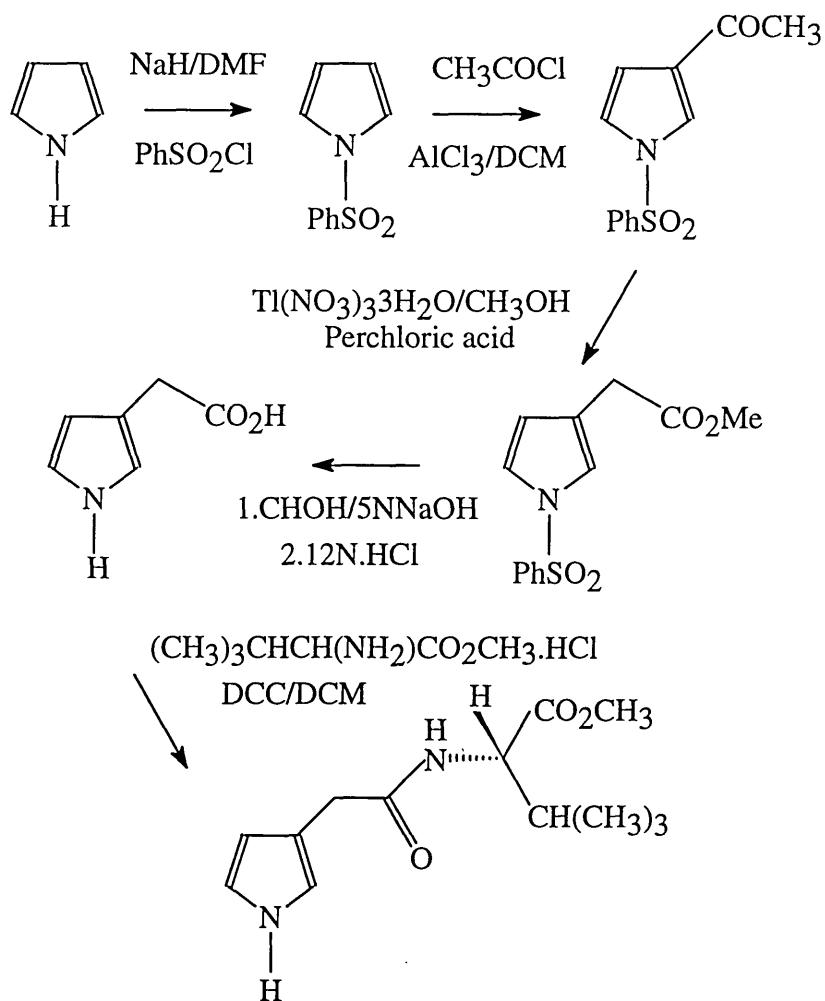
Preparation of 1-(phenylsulphonyl)-pyrrole

A mixture of pyrrole (20.12g, 0.30mols) and sodium hydride (60% dispersion in mineral oil) (12.00g, 0.30mols) was stirred in dimethylformimide DMF (150ml) for 10 minutes. To this phenylsulphonyl chloride (57.19g, 0.30mols) was added dropwise over the course of 15 minutes. The reaction mixture was allowed to stir for a further 2 hours, after which time it was carefully quenched with water (200ml). The product was extracted with dichloromethane (3x100ml), the organic extracts were combined and washed with water, then dried with MgSO$_4$ and evapourated under vacuum to an oil. (Yield 58.9g, 95.0%). M/z 207.1 (M$^+$)

^{1}Hnmr δ 6.30(d, 2H), 7.15(d, 2H), 7.75(m, 3H), 7.90(d, 2H).

Preparation of 1-(Phenyl sulphonyl)-3-acetylpyrrole

To a suspension of anhydrous aluminium chloride (40.0g, 0.30mol) in dichloromethane (400ml), acetic anhydride (15.3g, 0.15mol) was added slowly The resulting suspension was stirred at room temperature until the aluminimum chloride had dissolved. A solution of 1-(phenylsulphonyl)pyrrole in dichloromethane (40ml) was added slowly to the mixture. This was stirred overnight then carefully quenched the following morning with ice/water. The volume of solvent was reduced and the reaction mixture was washed with water, dried using MgSO$_4$ and reduced under vacuum to give a crystalline solid. (Yield 11.72g, 94.1%) M Pt 97-99°C. M/z 249.0 (M$^+$)

^{1}Hnmr δ 2.40(s, 3H), 6.70(dd, 1H), 7.10(dd, 1H), 7.40-7.70(m, 3H), 7.75(dd, 1H), 7.80-8.00(m, 2H).

Preparation of 1-(Phenylsulphonyl)-3-(carboxymethyl)pyrrole

A mixture of 1-(phenylsulphonyl)-3-acetylpyrrole (10.8g; 43.4mol), thallium trinitrate trihydrate (21.14g, 47.6mol) and perchloric acid (3ml) in methanol (300ml) was stirred for 48hrs. The reaction mixture was filtered, and the filtrate was concentrated at a reduced pressure and temperature (less than 40°C), then cooled under nitrogen. The remaining solution was diluted with diethyl ether and filtered. The filtrate was washed with water and 10% aqueous sodium carbonate, then dried using $MgSO_4$ and evaporated. The remaining brown oil was chromatographed using an eluent of petroleum spirit (40:60): ethyl acetate 4:1 mixture. This gave a yellow/orange crystalline solid. (Yield 6.02g, 49.7%) M Pt 53-55°C. M/z 279.2 (M^+)

^{1}Hnmr δ 3.60(s, 2H), 3.70(s, 3H), 6.30(t, 1H), 7.10(d, 2H), 7.40-7.80(m, 5H)

Preparation of 3-Pyrrolylacetic acid

A mixture of 1-(phenylsulphonyl)-3-carbomethoxymethylpyrrole (2.0g, 7.0mmol) in 5N NaOH (15ml) and methanol (15ml) was refluxed for 2.5 hrs at reduced pressure. The aqueous residue was washed with ethyl acetate, acidified using 10-11N HCl, then saturated with NaCl(solid) The product was extracted into ethyl acetate (2x50ml). The organic extracts were combined, dried using $MgSO_4$ and concentrated at reduced pressure to give a solid residue . This was triturated with hexane overnight, and the solid residue collected and filtered, then recrystallised from hexane-toluene. (Yield 0.79g; 90.2%) M Pt 89-91°C. M/z 125.2 (M^+)

^{1}Hnmr δ 3.30(s, 2H), 6.00(m, 1H), 6.70(m, 2H), 10.0-12.0(br., 2H)

Preparation of N-(3-pyrrolylacetyl)-(L)-valine methyl ester

A mixture of 3-pyrrolylacetic acid (1.25g, 0.01mol) and L-valine methyl ester hydrochloride (1.67g, 0.01mol) was dissolved in THF (100ml) To this solution triethylamine (1.01g, 0.01mol) followed by dicyclohexylcarbodimide (DCC) (2.06g, 0.01mol) was added, and the reaction mixture was stirred for two hours. The reaction

was filtered, and water added (100ml). The product was then extracted into dichloromethane (2x100mls). and the organic extracts were combined and washed with 2N HCl, water and sodium bicabonate solution, then dried over $MgSO_4$ filtered and reduced under vacuum. The solid residue formed was triturated using hexane and the product collected (Yield 0.86 g, 36.1%). M/z 238.1 (M^+)

^{1}Hnmr δ 1.10(d, 6H), 2.10(s, 1H), 2.20(m, 1H), 3.55(s, 3H), 3.70(d, 1H), 5.60(br., 1H), 6.15(s, 1H), 6.75(s, 1H), 6.95(s, 1H).

3.5 The characterisation of thin films using Cyclic Voltammetry.

Cyclic Voltammetry is an instrumental method which can be used to characterise the thermodynamic and kinetic parameters of charge transfer processes in redox systems[144]. It has found increasing use in the analysis of both the electrochemical and redox properties of thin conducting polymeric films. The thin films are prepared by an electrochemical oxidation process, whereby each polymer chain develops in a polycationic form and this is charge compensated by the inclusion of counter ions from the electrolyte medium. The properties of these dopant species can dramatically alter the physical, mechanical and electronic properties of the film. Prepared in the oxidised conducting state the polymer films can readily undergo reduction under certain conditions. When reduced the polycationic chain tends towards neutrality with a complementary ion migration to balance the charge within the system, in keeping with the principal of electroneutrality[145],

Oxidised state   Reduced state
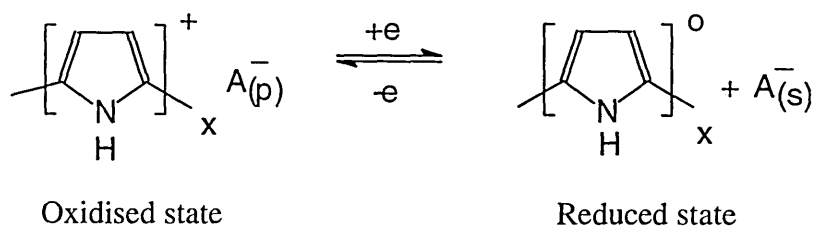
with $A_{(p)}$ representing the anion in the polymer matrix and conversely $A_{(s)}$ the anion in solution. In cyclic voltammetry[146,147] the potential is swept between two potential limits across the solution/film interface. The cycle is based on a triangular waveform and individual or multiple cycles can be performed across the interface (Fig. 3.1). The scan limits are influenced by the solvent system, as it is only the redox properties of the polymer interface in question that are of interest (not those of the solvent). The samples prepared for analysis were in the oxidised state so all cyclic voltammetry was initiated at a slightly anodic potential scanning in a negative direction. In cyclic voltammetry a scan is completed when the potential is swept to a minimum potential (E_{min}), then inverted and swept up to a maximium potential (E_{max}), the potential then returning to

the initial potential E_i. Important parameters to consider when using cyclic voltammetry are -

- the initial potential E_i

- the initial sweep direction

- the sweep rate (scan rate $mvsec^{-1}$)

- the minimum potential, E_{min}

- the maximum potential, E_{max}

- the final potential E_f (influencing the films redox state)

Fig. 3.1 Variation in the applied potential with time in cyclic voltammetry[(146)]
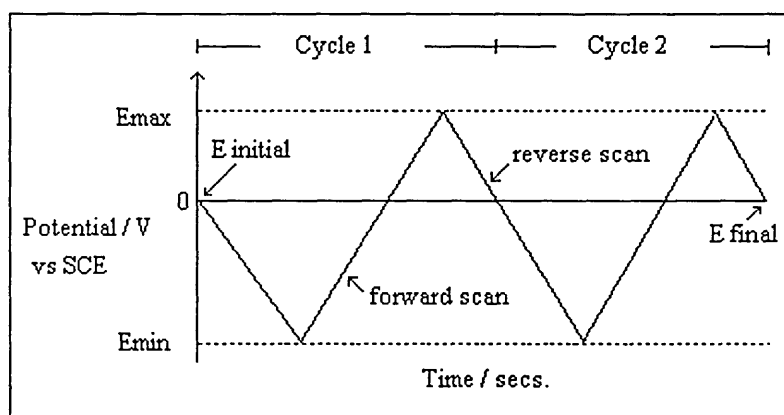
The current is monitored with respect to the applied potential and this information is transferred to an X-Y plotter. The important information gained from a cyclic voltammogram concerns the magnitudes of the peak currents i_{pc} and i_{pa} and the potentials at which these occur, E_{pc} and E_{pa}. Ideal behaviour is represented by the classical shape of a completely reversible cyclic voltammogram which has anodic and cathodic waves of equal amplitude(Fig. 3.2). The initial sweep in the negative direction leads to a cathodic wave, where the polymer interface reaches a potential at which the flim is reduced. Instead off levelling of at the wave's peak the current decreases as the potential is lowered further. This is due to a depletion in the electroactive species around the electrode surface. On reaching E_{min} the current has decayed to a smaller value which is maintained on reversal of the potential. The cathodic current still flows

67

as the potential is negative enough to continue film reduction. At a sufficiently positive potential the electrode surface begins to oxidise and an anodic wave forms, leading to a complete removal of the reduced species present in the system. In a reversible system the redox reaction occurs at a rate such as to maintain equilibrium conditions at the electrode surface as the potential is cycled. The difference in potential between E_{pa} and E_{pc} is given by the equation:-

$$E_{pa} - E_{pc} = 2.22 \, \frac{RT}{nF} = \frac{56.6}{n} \, (mV)$$

where n is the number of electrons involved in the reaction, and F represents Faradays constant $9.6485 \times 10^4 Cmol^{-1}$.

For reversiable systems $E_{pa} - E_{pc} = 56.6/n$ (mV) and $[I_{pa}/I_{pc}] = 1$

Fig. 3.2 A cyclic voltammogram for a reversible system[147]
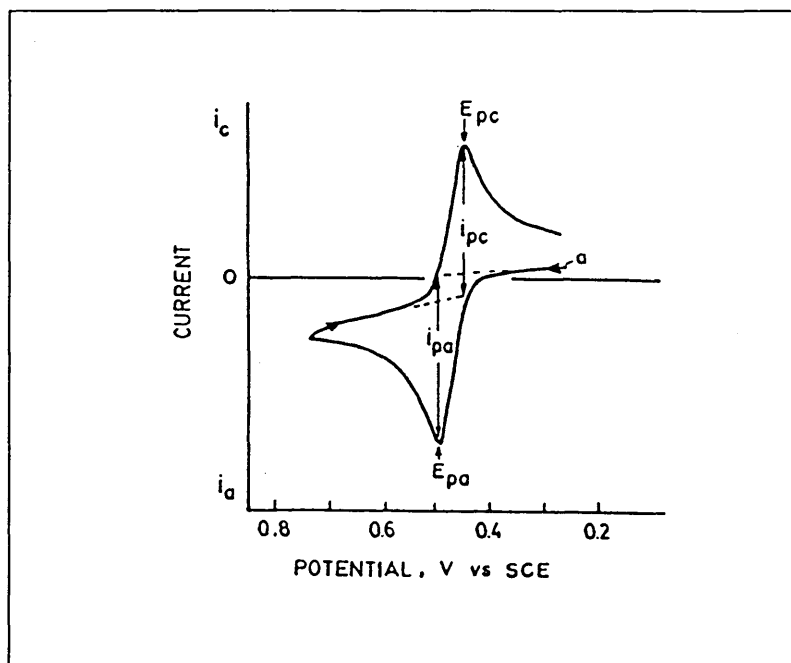
During the scan the film undergoes a number of changes; the conductivity, the film composition and its morphology change. For most of the systems which have been addressed in this thesis the cyclic voltammograms are of a similar overall structure due to the consistent parentage of the films and the mild conditions used. Many theoretical

and practical studies have been performed investigating electrolyte motion (both anion motion and cation motion in opposing directions). Cyclic voltammograms depend on very many factors, for example the preparation of the thin film, the solvent system, the identity and concentration of electrolyte, the electrochemical deposition parameters and the scan rate. When performing a comparative study as many of these parameters as possible need to remain the same as the problems of irreproducibility are extensive with conducting polymer based systems.

As the scan rate is increased there is a shift from the symmetrical shape of a voltammogram (i equals v) to the classical asymmetric shape with i proportional to v $^{1/2}$. As the extent of irreversibility increases there is a decrease in I_{pc}, and an increase in the separation of the anodic and cathodic peaks (quasi-reversible systems) (Fig. 3.3). The occurrence of quasi-reversible systems in conducting polymer films is related to the layer thickness of sample. The diffusion kinetics suggest that the charge transport of a film is dependent on the electron exchange reactions occurring between neighbouring oxidised and reduced sites on a polymer chain and the relative influx of counterions into the film matrix to balance this. This may be enhanced by increased sweep rate as the system is less able to counter the required movement of charge .
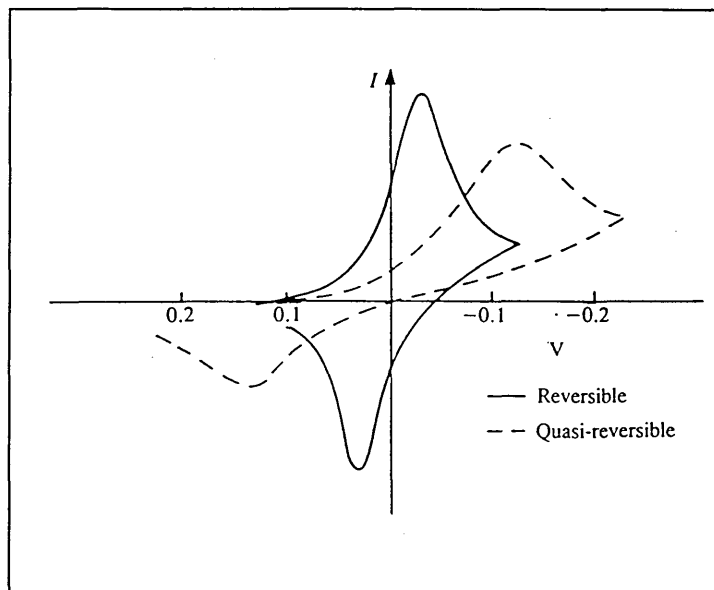
3.6 The characterisation of thin films using Scanning Electron Microscopy (SEM) coupled with Energy Dispersive X-ray analysis (EDX)

The use of Scanning Electron Microscopy(SEM) allowed comparative studies of the change in the morphology of electrochemically deposited thin films with variations in growth conditions such as the solvent, electrolyte and potentiostatic/galvanostatic deposition parameters. This instrument was coupled to an Energy Dispersive X-ray analyser sometimes referred to as SEM-EDX, allowing basic elemental analysis of the polymer films.

The primary X-rays used in the instrument are generated by a gun consisting of a filament (normally tungsten) positioned above the microscope column. This is heated to incandescence (around 2850K) to become a thermionic electron emitter which operates most effectively at saturation[148]. At a potential of 20-50 keV electrons are emitted from the tungsten cathode. On emission they are affected by an electrostatic field provided by a Wehnelt grid which has a small negative bias applied to it. This has the overall effect of focusing the electrons before they pass a cooled anode (Fig. 3.4).

The electron beam passes through a microscope column which is under vacuum (approx. 10^{-7} mbar), the function of which is the production of an electron beam which can be focused on the sample surface, allowing spot analysis of a $1 \mu m^3$ section of the sample[149]. Along certain points in the column are several electromagnetic condenser lenses and scanning coils to cause the following effects: collimation deflection, demagnification, focusing and synchronous rastering of the electron beam in two orthogonal directions

The electrons bombard the sample resulting in the generation of electronic excitations. The X-rays generated pass through a window of either beryllium or an organic polymer. Every point on the sample area which is scanned generates a signal and it is the efficiency of signal production which gives contrast from which an image can be

71

derived. At the beam pivot an aperture is located which can be used to vary the depth of field and intensity.

The images obtained for the analysis of the variation in thin film topology were generated using the secondary electron signal generated from the sample surface. The secondary electron detector consists of a positively biased grid attached to a scintillator/photo multiplier and positioned at an acute angle to the sample. The images from secondary electrons result from the fact that the secondary electrons are not energetic and are considered to drift from the sample's surface. They are only accelerated to the detector if they experience a field on the grid which is strongly affected by the topographical effects of the sample's surface. Regions of the sample which are in the shadow of the field are not attracted into the detector, and such areas appear dark on the image.

Fig. 3.4 Schematic diagram of a Scanning electron microscope(150)
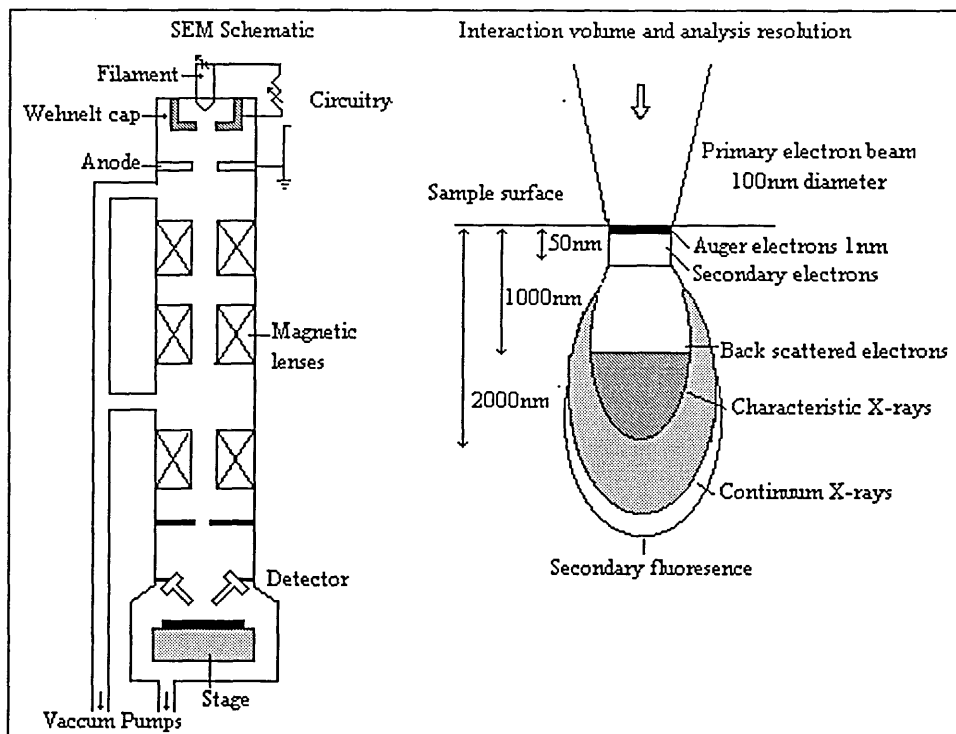
When a sample is bombarded with high energy electrons from the incident beam, the electrons interact with atoms in the sample and an inner shell electron may be removed

causing excitation and a vacancy in the shell. The atom can return to the ground state by an electron transition from a high energy shell to fill the vacancy. This is usually accompanied by the liberation of a photon with a characteristic energy, as determined by the energy gap between the atomic energy levels. Therefore the photon emitted is element specific. The energy dispersive X-ray detectors (EDX) are mounted in the sample chamber, such that sample imaging and elemental analysis can be performed simultaneously. All the EDX experiments were performed at a constant probe current of 3×10^{-9} A , with a sample acquisition period of 50 seconds. The sample analysis of reduced and oxidised polypyrrole films was matched by monitoring the number of gold counts during analysis such that they were comparable. The films which were in the reduced state, showed a slight increase in the intensity of the gold peak, this was due to a reduction in the film thickness due to mass loss i.e. solvent /dopant molecules

The instrument used for all the analyses reported in this thesis was a Jeol 840A microprobe analyser with a Link AN10000 EDX facility.

3.7 The characterisation of thin films using reflection-absorption Fourier-transform infra-red spectroscopy

Fourier-transform spectroscopy[151,152] allows the measurement of a whole spectrum at once. The components of an infra-red spectrum can be written as an infinite sum of sine and cosine components. The use of Fourier analysis splits the $A(v)$ function [where $A(v)$ is absorbance] into component wavelengths [sin (n v) and cos (n v)] each with an appropriate weighting factor.

The instrument relies on an interferometer, within which is contained a beamsplitter. Light is shone onto this device, some of which is transmitted to a stationary mirror and the remainder to a movable mirror. The rays which are reflected by the mirrors travel back to the beam splitter, where half of each ray is transmitted and half reflected, one recombined ray travels to the detector and the other to the source. The distance between the two mirrors can be varied so that the phase difference of the waves reaching the detector can be changed. Therefore it is possible for the waves to interfere either constructively or destructively. The difference in pathlength between the two waves is called the retardation. An interferogram can be obtained by plotting the light intensity versus the retardation. From Fourier analysis of an interferogram the spectrum from which it was obtained is produced.

The analysis of thin films was performed using a reflection-absorption technique (Fig. 3.5). The sample is placed perpendicular to the incident light a fraction of which is reflected back from the sample to the detector. Since the sample absorbs certain wavelengths of light, a background interferogram of the substrate's gold surface was obtained and recorded as a reference. Interferograms of the films were then obtained, each containing the spectrum of the reference minus the spectrum of the sample

The information so obtained did prove useful in the analysis of very thin films (<500°A), giving spectra with good clarity and resolution. But the technique became

less useful as sample thickness increased and was also hampered by the hygroscopic nature of the films even after considerable efforts had been made to provide dry samples.

Fig. 3.5 FT-IR reflection-absorption analysis of polymer films.[152]

FT-IR Microscope in reflectance mode

- MCT Detector
- Detector Objective
- Relay Optics
- Aperture
- Reflectance Focusing Mirror
- Polymer Sample
- Support
- Flip mirror
- Ellipsoidal Mirror
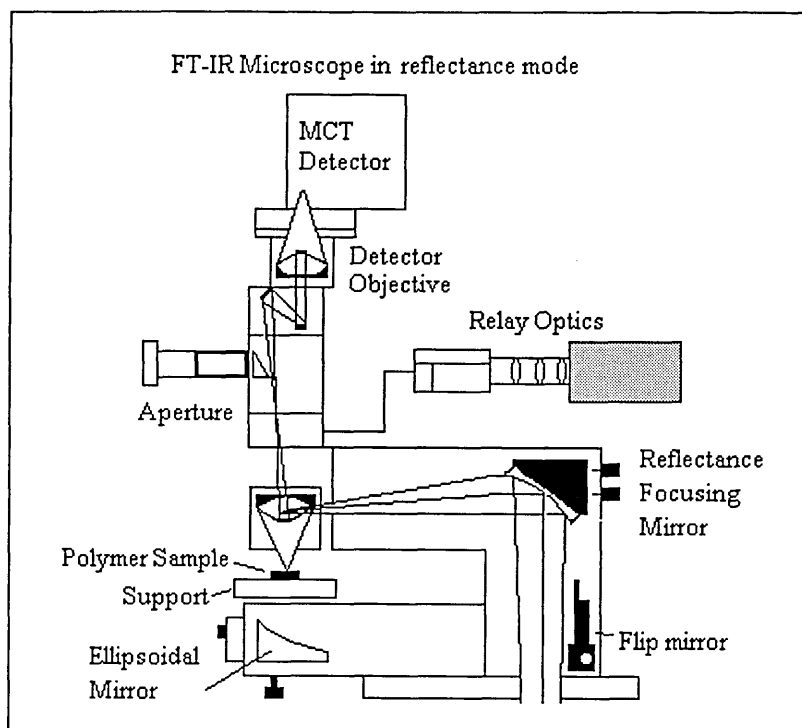
3.8 The characterisation of the sensing properties of polymer films using the Neotronics Olfactory Sensing Equipment (NOSE)

3.81 Introduction

The electronic nose provides a rapid and reliable means of characterising and comparing odours using a series of conducting polymer sensors (chemiresistors). The electronic nose relies on sensory components having broad ranging sensitivities together with discriminatory ability. The instrumental analysis of the data obtained from the sensory components relies on sophisticated data processing techniques to optimise the sensory information obtained. The properties of electrochemically prepared conducting polymers are well suited to the needs of array sensing devices. As a series of individual, uniform, non-specific devices, they have overlapping sensitivities but each contributes uniquely to the overall analysis of a sample. Each device changes resistance selectively when exposed to volatile components in the vapour phase. The individual sensors when optimised show reversible conductivity changes at room temperature enabling rapid sample analysis. The generation of a patterned response allows the discrimination of a complex aroma without the requirement to analyse individual components.

3.82 The Neotronics Olfactory Sensing System (NOSE)

The system[153] is designed to hold a maximum of twelve operating sensors if required, but sample discrimination may be obtained with a lot less depending on the complexity of the analysis. The sensors are arranged in a circular formation in a sensor head with the polymer films facing inwards. The sensor chips are of a 'push fit' variety enabling easy assembly and replacement. The sensors are electrochemically grown under tightly controlled conditions which have been optimised to enable the replacement of a particular sensor type without compromising any subsequent analysis. It has been shown that this is the case from repeated exposure of sensors to standard test conditions.

The electronics used in the NOSE consist of an integral dc power supply which is maintained at a constant current through each of the individual sensor devices. When a chemiresistor is exposed to an analyte its resistance changes. The corresponding voltage change across the sensor is measured and the resultant analogue signal digitised and converted via signal processing systems to sample data output.

3.83 Calibration

The sensor head assembly and the sample vessel are sealed in separate compartments within the NOSE design (Fig. 3.6).

Fig. 3.6 Simplified system design
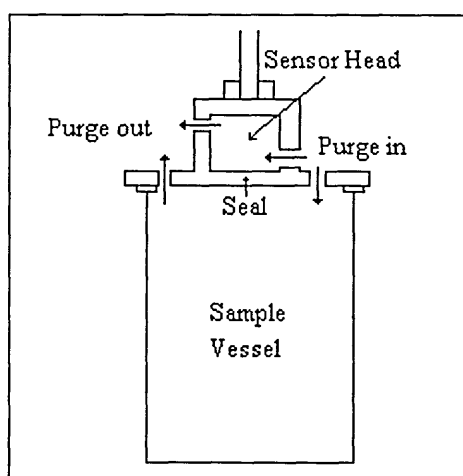
Before any sample analysis is undertaken the system must be calibrated. The calibration process involves the selection of the required head for sample analysis, which is then located in the head compartment in the NOSE. The sensor head is then configured, whereby each individual sensor is labelled, formatted and made active. The potentiostatic controls on the instrument are then used to bring the individual sensors into range. A calibration programme is then performed where the sensors are exposed to air dried by passage through silica gel (reference and standard purge gas). The standard programme purges the sensors for 7 minutes, after which they are exposed for a further 4 minutes to dry air in the sample vessel, this process is repeated five times. Throughout this calibration programme the sensors are being optimised to obtain a uniform baseline.

3.84 Sample Acquisition

The operator assigns the following information to a sample: a description (test identification number), class (product group); substance (member of class); taints (known impurities in the sample); method (defines the sensors and the acquisition method to be used). The analyte is then placed into the sample vessel prior to the sensor head being purged. After the head purge defined by the method, the sensor head is lowered into the sample vessel and analysis begins. The operator is then able to view a real time graphics profile of the emerging acquisition. After completion of the sample analysis the graph is automatically scaled. Further sample analysis can then take place; repeated analysis can be performed acquiring more sample data. Templates can be created when three or more sample acquisitions have been performed and graphs of average response against time are then obtainable. Standard deviations can also be calculated for each test point for each individual sensor, and they can be displayed against time providing further information on result validity. The % relative deviation can also be calculated and this is thought to be of more use than the standard deviations which are obtained. Response data can also be normalised to the individual response of a sensor, and multiplied by a desired factor (e.g. 1,10 or 100).

3.85 Sample Analysis

The NOSE software includes a Windows based analysis package that is used to provide comprehensive information on sensor response. The sensors are individually colour coded enabling easier sensor identification. During sample analysis information is portrayed in the graphical format but, following analysis, it may be displayed in any one of a number of formats (Fig. 3.7)

Fig. 3.7 Graphical analysis of test results
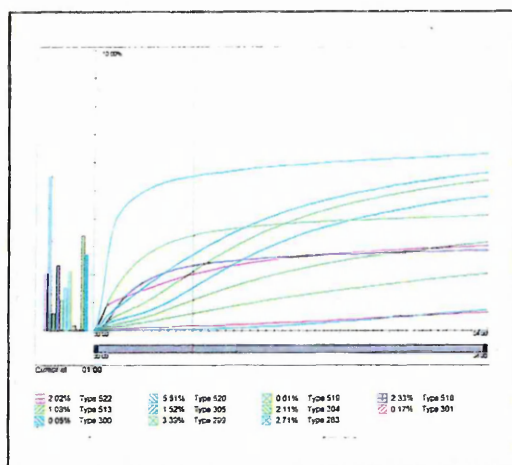
A graphical plot of resistance against time, showing the % resistance change of each colour coded sensor. The vertical cursor can be moved along the horizontal time scale to determine the analysis point. Parallel to the plot is a bar graph showing the amplitude of each sensor response, defined by the analysis point.
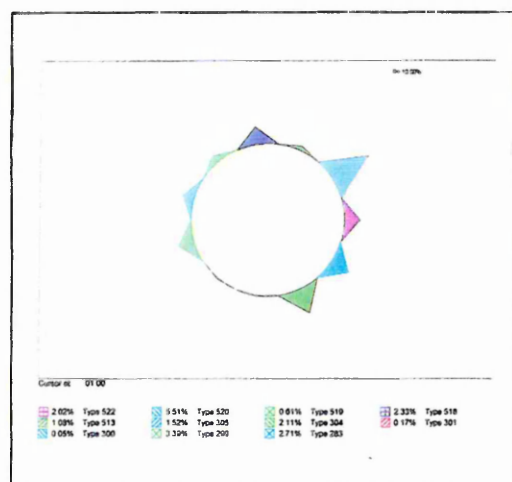
The polar plot represents the resistance change of the sensors as scaled vectors. Each of the twelve sensor responses is spaced at 22.5°(radial) If sensors are removed from the array the angular position is compensated for. Depending on sensor response the shape of the polar plot varies, the disadvantage with this form of graphical analysis is that negative responses can not be visualised.
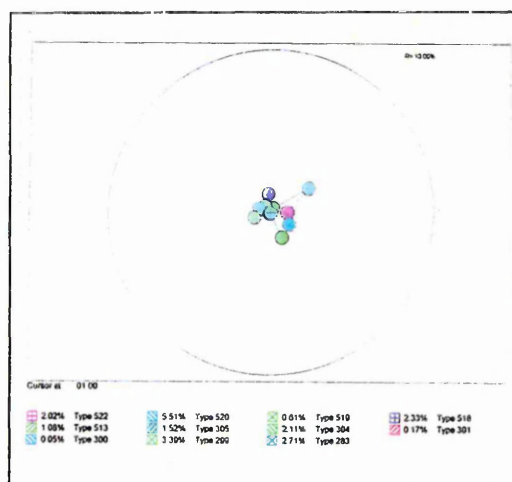
The offset polar plot is a variation on the polar plot. This format allows the representation of positive responses as vectors outside the circle, with the reverse being true for negative responses. As with the other plots the same colour is used to represent each sensor throughout the analysis package, enabling easy comparison.

3.86 Statistical Analysis

The current e-NOSE 4000 model offers a comprehensive range of data manipulation techniques. The first of two statistical packages available is NOSESTAT. This offers a variety of discrimination techniques including PCA (Principal Components Analysis), MDA (Multiple Discriminate Analysis) and LDA (Linear Discriminate Analysis). The information obtained on the instrument during sample analysis can be exported directly to these statistical analysis packages. They are particularly useful when analysing a group of like samples; the use of PCA (Section 1.5) enables the operator to discover trends in the sample analysis by emphasising the structure of the data. The technique maximises the sample variance enabling sample groups to be distinguished and therefore made identifiable. The use of MDA places an additional weighting to each sample depending on the sample subset, this improves sample discrimination. This package also offers the advantage of allowing the sample analysis of unknowns within that group, since it will determine the closest fit of the sample related to the grouping of the known subsets within the group.

Neural Analysis is the most advanced data analysis option. This is ideal when sufficient sample data is available such that the NOSE can be 'trained' to recognise a standard sample based on its characteristics. After the network has been trained the instrument can identify unknowns based on comparisons of information contained in its database. Sample information processed on the e-NOSE 4000 can be directly exported to this network.

Chapter 4 Development of conducting polymer chemiresistors

4.0 Introduction

The development of new conducting polymer chemiresistors was based on initial studies carried out by *Bartlett et al*[49]. They developed a series of twelve sensors based on potentiostatic electrochemical deposition of conducting polymers onto gold substrates. These systems differed by the inclusion of different counter ions and by variation in the solvent system used during the deposition process. It is widely reported in the literature that the properties of cationic conducting polymer films can be significantly altered depending on the nature of the counter-ion included in the system. These changes can be effected by simply changing the electrolyte salt used during electropolymerisation. The anion affiliated with an oxidised polymer system produces changes in both the redox and electron transport properties of the films produced. This method of chemically altering the properties of prepared film provides a practical alternative to the more time consuming and commercially expensive process of modification of the monomer used. Although it is expected that the combination of both these approaches would aid in the development of a wide range of chemiresistors having increased diversity and enhanced sensitivity to volatile components in aromas.

The nature of the chemiresistor formed is primarily based on the monomer used in the electrochemical deposition process. The level of oxidation of the polymer formed governs the quantity of anion in the film. The anion is directly associated with the cationically charged polymer film and films nominally contain 10-35% weight of anion[119], but this factor is directly governed by the nature of the monomer. For the conducting polymer chemiresistor to be effective in the NOSE technology, the resistance of the fabricated films is required to be in the region of 1-100 ohms. The monomers used need to form highly conductive films when grown electrochemically. From the literature it is possible to obtain information on the oxidation levels, the % anion content and the overall general conductivity of films formed using different

monomers (Table 4.1). This information proved valuable in giving some initial direction to the project.

Table 4.1 Anion content and respective conductivites of a series of conducting polymers

Film	Oxidation level	% Anion Content (% weight)	Conductivity $(\sigma) / \Omega^{-1} cm^{-1}$	References
Polypyrrole	0.25-0.33	25-30	30-100	154
Poly n-methypyrrole	0.23-0.29	20-28	0.001	154,155
Poly 3-methylpyrrole	0.25	20-30	4	154,155
Polythiophene	0.06	7-25	$10^{-2} - 10^{-1}$	156,157
Poly(3-methylthiophene)	0.12-0.30	-	1-100	156,157
Polyazulene	0.25	15-28	$10^{-2} - 1$	157
Polyaniline	-	-	$10^{-2} - 10$	158

The use of different monomers can greatly affect the overall conductivity of an electrochemically formed polymer film. From this selection of available conducting polymers it was decided to concentrate on the heterocyclic monomers of pyrrole and 3-methylthiophene due to their relatively high conductivity and the ease with which the anion could be varied. Further studies also addressed the electropolymerisation of the bicyclic hydrocarbon monomer azulene.

All the systems used were aromatic in nature and could be easily oxidised at relatively low oxidation potentials[119]. This alleviated problems of oxidative decomposition of both the electrolyte and the solvent systems. The monomers all undergo film formation via radical cation intermediates, their aromatic natures being maintained in the subsequent films. This approach to polymerisation led to highly conjugated systems with extensively delocalised π–electron systems. The monomers used are listed below

along with their respective peak potentials and the apparent stoichiometries of the electrochemical reactions (Table 4.2). The n values quoted for a film forming reaction are generally between 2.0-2.5 where two electrons per molecule are involved with the excess charge (0-0.5) associated with the reversible oxidation of the polymer. The quantity of excess charge is related to the electrochemical deposition conditions i.e. monomer, solvent and anion inserted during oxidation.

Table 4.2 Electrochemical peak potentials and apparent deposition stoichiometry

Compound	Peak potential (vs SCE)	n	References
Pyrrole	1.2	2.2 - 2.4	154
Thiophene	2.07	2.06	159
3-Methylthiophene	1.86	2.4	119
Azulene	0.91	2.2	155

The anions used in the formation of the chemiresistors have a strong influence on the mechanical properties, electroactivity, morphology, and conductivity of the resultant polymer films. The overall size and charge of the anion affect both the stability and electrical properties of the film. The types of anion which can be incorporated into polypyrrole films are vast and the literature available[118,119] gives indications of the relative conductivites produced by anions commonly incorporated into these types of films. It has generally been found that perchlorate and perfluorate anions give films that are more conducting $(30-200Scm^{-1})$, than films containing e.g. fluoroborate, hexafluorophosphate, nitrate and p-toluenesulphonate anions $(20-100Scm^{-1})$. The films with the lowest conductivities appear to arise with triflates, sulphates and the carboxylate anions $(0.01-10\ Scm^{-1})$. The initial objective of the project was to extend, diversify and improve the current list of chemiresistors available for use with the NOSE technology. Running parallel with this task was the search for an understanding of what properties created the ideal sensor.

The ideal chemiresistor based on the principal of variation of the incorporated anion had to possess the following properties[118].

- High conductivity (with resistances in the region 1-100 ohms).

- High doping amount per unit weight and unit volume.

- Maintain long-term chemical and mechanical stability on exposure to the atmosphere.

- Stability with respect to the electrolyte solution.

- Strong adhesion to the gold substrate.

4.1 Electrochemical deposition conditions for the formation of conducting polymer chemiresistors

The early work on chemiresistors based upon polypyrrole films containing alkyl sulphonates[49] was replicated to ensure that it was possible to reproduce the results accurately. As a result a series of variables that could be altered to affect the nature of the conducting polymer film was highlighted. They are as follows:-

- the nature of the monomer
- the nature of the solvent
- the nature of the counter-ion
- the deposition process i.e. potentiostatic or galvanostatic
- the growth period
- the relative concentrations of the monomer and counter-ion
- electrode material.
- the temperature
- the pH of the system
- storage of the chemiresistor

The number of possible variables was considerable and a series of standard conditions was adopted based on the experimental protocols currently in use. The standard method for electrochemical deposition had been via potentiostatic deposition, i.e. applying a fixed potential for a known time period. Neotronics Ltd felt it desirable to pursue this method of deposition as it had proved effective. The monomer concentration in previous studies had been 0.10M but after a series of tests it was found that a slight increase to 0.15M improved the reproducibility of the chemiresistors obtained. Previous research[160] into the effect of pH on film formation indicates that the best quality films are produced in neutral or weakly acidic/alkaline media; in very acidic media films become powdery and, in highly alkaline media, only very thin films can be formed. The temperature at which electrochemical deposition was performed was based

85

on literature studies[161,162] where it was shown that at low temperatures ($< 15°C$) the solubility of counter ions is reduced, which tends to lower the conductivity of the chemiresistors formed. This phenomenon was particularly noticeable with some alkyl and aryl sulphonates especially the large (amphiphilic) surfactant based counter-ions which required sonication to produce homogeneous solutions at room temperature. Literature[163] has shown that conductivities can be increased by polymerising below $10°C$ for certain PPy systems due to an increase in conjugation; this was also observed in our experimental studies. For the development of NOSE chemiresistors electrochemical deposition temperature was investigated to determine the effects that temperature had on chemiresistor conductivity.

A study of the experimental variables of an individual chemiresistor was performed, using a PPy/BzSA(Na)/H_2O system (BzSA(Na) is benzenesulphonic acid sodium salt). The experiments monitored the corresponding change in film resistance as a function of electrochemical deposition temperature, the increase in the applied potential, and also the concentration of electrolyte in solution during deposition. The experimental parameters which remained fixed were the growth potential at two minutes, and the deposition process. The pH of the solutions remained fixed during the tests (electrolyte pH = 6.82). Deposition temperature was controlled via a water bath and an ice/water bath for the lower temperature (Table 4.3). At each temperature five chemiresistors were grown and the resistances monitored over the first 24hrs, the average resistance quoted is after the 24hr stabilisation period, along with the corresponding % relative standard deviation.

Table 4.3 Chemiresistor resistance variation relative to electrochemical deposition temperature

Deposition Temperature / °C	Average Resistance / Ω	% Relative Standard Deviation
10	7.32	7.38
20	10.87	8.19
30	4.55	9.37
40	13.64	8.78

The experimental evidence shows that the conductivity of the chemiresistors formed is affected by electrochemical deposition temperature but no proportional trend is discernible. The main factor not evident from Table 4.3 is that at lower temperatures the rate of polymerisation is visually slower than at higher temperatures. The films formed more slowly at lower temperatures than at the higher temperatures (30-40 °C) where the films formed rapidly, with an increased mass of polymeric material being deposited. At temperatures between 30-40°C there was a deterioration in the conductivity of the chemiresistors formed, probably due to an increase in structural irregularities (see Section 1.8) and the formation of a more disordered structure (consisting of a network of shorter polymeric chains) occurring during the polymerisation process. The topology of the films also varied significantly with the lower temperature chemiresistors having a less nodular surface than higher temperatures where extensive nodular growth was observed in SEM studies.

The method-development work for electrochemical deposition required a procedure which could be replicated easily in an industrial environment. Therefore all polymerisation reactions were temperature monitored and performed within a temperature region between (16-24°C) to produce chemiresistors with compatible conductivites required for operation with the NOSE technology. The effect of

temperature on film growth, conductivity and sensor response is currently under further investigation.

Initial studies on the effects of growth potential and electrolyte concentration were also performed. In the first the change in the applied potential was monitored and varied slightly. The second study concentrated on the conductivity of films formed at varying electrolyte concentrations, the deposition potential remaining constant at 0.85V The results are tabulated below and are based on the resistance reading 24hrs after formation (Tables 4.4 and 4.5). Each analysis was replicated five times and average, maximum and minimum resistances are shown along with the corresponding % relative standard deviation.

Table 4.4 Variation in resistance obtained as a function of the applied potential

Growth Potential / V	Average value / Ω	Minimum value / Ω	Maximum value / Ω	% Relative. standard deviation
+ 0.75	9.70	2.76	21.91	79.38
+ 0.80	3.84	1.65	4.46	37.23
+ 0.85	7.65	5.14	9.26	21.70
+ 0.90	42.82	2.30	128.3	124.47
+ 0.95	160.48	8.04	278.19	69.02
+ 1.05	376.25	274.8	525.1	24.29

Table 4.5 Variation in resistance obtained as a function of electrolyte concentration

Electrolyte Conc /mL^{-1}	Average value / Ω	Minimum value / Ω	Maximum value / Ω	% Relative standard deviation
0.010	1097.5	310.7	2595.9	80.74
0.025	112.4	76.03	164.2	32.11
0.050	15.29	11.42	17.98	16.80
0.100	7.65	5.14	9.26	21.70
0.250	5.63	3.57	7.41	28.06

The results show regions in which the production of chemiresistors was more reproducible and within the limits for use within the technology. Later studies on the response characteristics of the developed chemiresistors led to re-optimisation of the deposition conditions used. These initial studies however, demonstrated the feasibility of a particular chemiresistor and gave an indication of the overall stability of each system and likely response characteristics. Based upon initial findings from these tests, together with further comparative studies performed on other systems, the experimental conditions were defined. It was felt that the conditions for research purposes should be within close limits enabling direct comparison between the different sensor types which were developed. The method of electrochemical deposition was also developed to enable its replication in an industrial environment

The conditions which were decided upon were an electrolyte concentration of 0.10M and a growth potential of between 0.75 - 0.85V for pyrrole and 1.55 - 1.65V for 3-methyl thiophene. These conditions proved effective in the search for a wider range of chemiresistors available for use with the sensing technology.

4.2 Polypyrrole based chemiresistors from aqueous electrolytes.

The first report of a polypyrrole based film obtained in an aqueous medium was by *Dall'Olio et al*[164] in 1968. They reported the anodic deposition of a conducting polypyrrole termed 'pyrrole black' from the electrochemical oxidation of pyrrole in aqueous sulphuric acid. Further work highlighted the value of the electrochemical approach and there has been a considerable amount of literature published in that area,[118,119] that has identified numerous potential dopant species which can be incorporated into polypyrrole based films. The use of aqueous deposition media offers a larger selection of dopant anions which can be utilised in comparison with non-aqueous systems. The incorporated anion influences both the structural properties and the overall electroactivity of polypyrrole based films. The level of oxidation of the polymer chains determines the amount of incorporated dopant which is normally 0.25 - 0.32 per pyrrole unit corresponding to a doping level of one anion every 3-4 units. The literature evidence shows that the level of oxidation is a property of the polymer and is not effected by the anion (Table 4.6).[165]

Table 4.6 Polypyrrole films with different anions

Anion	Oxidation level	Density (g/cm^{-3})	σ (Ω^{-1} cm^{-1})
Tetrafluoroborate	0.25-0.32	1.48	30-100
Hexafluorophosphate	0.25-0.32	1.48	30-100
Perchlorate	0.30	1.51	60-200
Trifluoromethanesulphonate	0.31	1.48	0.3-1
p-Toluenesulphonate	0.32	1.37	20-100
Trifluoroacetate	0.25	1.45	12

The anions which prove least effective in the production of good quality films are those which are highly electron rich (and thus easily oxidised), for example the halides. Further nucleophilic species which produce poor films are anions such as cyanide, hydroxide, acetate and benzoate that produce soluble products which colour the

electrolyte solution. Most of the initial study had centred on the use of alkylsulphonates but it was felt that this could be expanded to include a range of arylsulphonates, and an investigation of a more diverse selection of electrolytes was also envisaged. It was hoped that the experimental investigation would lead to a clear understanding of the type of aqueous media which would produce stable films with reproducible sensor responses.

From Table 4.6 it is clear that the conductivity of PPy films is strongly influenced by the nature of the incorporated counter ion. This is not surprising since the counter ions are able to interact electrostatically with the charge carriers, hence affecting the conduction pathways in the film. From conductivity and SEM studies it is apparent that two categories of counter ion[166] are emerging from studies of films prepared from aqueous media. The smaller, rather spherical, univalent inorganic counter ions (BF_4^-, PF_6^-, ClO_4^-, NO_3^-) and the small organic ions (CH_3COO^-, $CF_3SO_3^-$) promote isotropic structures in which the films are more open and less ordered i.e. more nodular in appearance (Fig 4.1). The surface topologies observed are similar although variations are observed depending on the particular counter-ion used during deposition. The reason for the more disordered structure is related to the adherence of the planar PPy chain to the electrode surface. This requires a distribution of negative charge during film growth and spherical counter ions lead to a disruption of the growth face at a molecular level leading to less uniform growth. The second category, anisotropic counter ions (e.g. planar aromatic systems), lead to a layered and more ordered system (Fig. 4.2). *Warren et al*[167] concluded that substituted benzene sulphonates and large amphilic counter ions promoted the highest degree of order within a film. This was also deduced from the experimental results observed with counter ions containing multiple fused aromatic units (e.g. naphthalenesulphonates also showed similar order in product films).

The results showed that films with isotropic structures exhibited the lowest conductivites and showed increased degradation kinetics in ambient atmosphere when

91

compared to anisotropic films (alkyl and aryl sulphonates). The low conductivity of isotropic systems and their instability in an ambient atmosphere reduced their effectiveness as chemiresistors.

Many of the useful dopants contain the sulphonate functionality As the number of sulphonate groups increased in a comparable dopant system, the conductivities of the films produced under comparable conditions decreased, e.g. 1,5-NapDSA(2Na) < 2-NapSA(Na). This can be explained in terms of charge localisation on the polymer chain, the increase in the number of sulphonate groups causing a stronger attraction to the cationic polymer chain[168]. The resistances of films containing increased numbers of sulphonate groups could be lowered by reduction of the growth potential. This approach produces films which may contain polymer chains having increased molecular weight and reduced cross-linking, therefore leading to more uniform growth and charge balance within the film This approach can also explain the reduction in the conductivity of films containing smaller dopant anions which exhibited the similar trends.

The molecular size, orientation and bulk of a dopant molecule also influence the conductivity of a film. Larger dopants can interfere with the planarity of the polypyrrole chains formed during electrochemical deposition as they can have a disruptive effect on the molecular organisation of the film. Combined with this disruptive effect is the reduction in counter-ion mobility due to molecular size, leading to lower doping levels. These factors lead to a decrease in the conductivity of films formed, and large counter ions also increase the separation of PPy chains presenting an obstacle to interchain charge transport processes (e.g. electron hopping).

A camphorsulphonate anion also exhibits an ordered anisotropic structure despite its non-planar structure. This is thought to be related to the hydrophobic nature of the counter ion; counter ions which are strongly hydrophobic are generally located near the electrode surface during aqueous deposition, encouraging the growth of PPy chains

parallel to the electrode surface thus producing an anisotropic film[169]. The use of large alkyl amphililic surfactant based molecules (OcSA(Na), DDS(Na), DOSS(Na) - see Appendix 1) generated high conductivites irrespective of their precise size; this may be due to the linear planar shape of these dopants and the presence of hydrophobic groups leading to the formation of highly ordered, dense, uniform films.

The incorporation of large transition metal containing anions[170] such as 1,1-ferrocene (II) disulphonate (2Na) and copper (II) tetrasulphophthalocyanine tetrasodium salt (MPcT), into PPy films to produce chemiresistors proved unsuccessful. This is probably due to the size of these species which may be too large to be readily incorporated into PPy films, the size also producing packing inconsistencies in the films facilitating degradation. The conductivites of these films were relatively low due to their low anion concentration in the films as a result of a large number of sulphonate groups per dopant, particularly with the MPcT. The adhesion of the films was poor and this is also probably related to the size of the incorporated dopant. Similar problems were also experienced with polymeric anions such as poly(sodium 4-styrene-sulphonate)

The nodular nature of some films made measurement their thickness difficult. Measurements using a Vickers Optical Microscope showed them to be between 2-10 microns in thickness. All experimental results for the systems quoted have been based on a series of five chemiresistors described in Table 4.7.

Fig. 4.1 SEM photograph of a PPy/LiClO$_4$/H$_2$O film surface
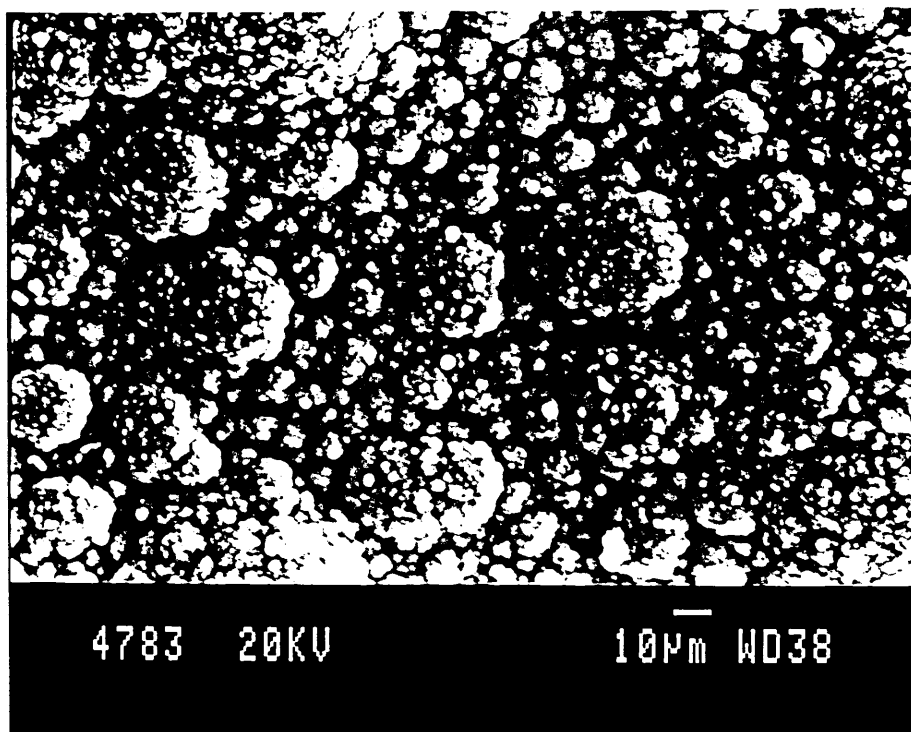
Fig. 4.2. SEM photograpgh of a PPy/DDBzSA(Na)/H$_2$O film surface
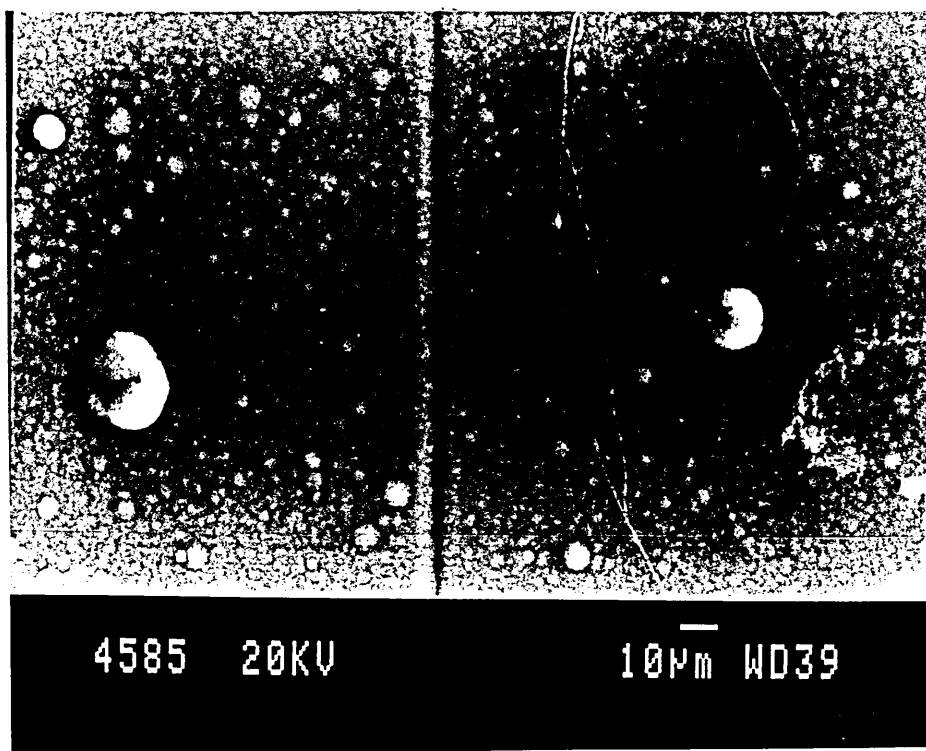
Table 4.7 Details of conducting polymer chemiresistors

Index number	Polymer system	Monomer concentration / moldm^{-3}	Electrolyte concentration / mol dm^{-3}	Solvent	Growth potential / V Period /secs	Av. Resistance / Ω	Standard deviation
280	PPy-LiClO$_4$	0.15	0.10	Water	0.75, 120s	27.83	5.89
282	PPy-LiNO$_3$	0.15	0.10	Water	0.85, 120s	9.48	3.51
284	PPy-TEATFA	0.15	0.10	Water	0.85, 120s	474.8	38.66
281	PPy-LiPF$_6$	0.15	0.10	Water	0.85, 120s	312.8	59.92
270.	PPy-TEABF$_4$	0.15	0.10	Water	0.85, 120s	80-200	*
274	PPy-LiTFMS	0.15	0.10	Water	0.75, 120s	28.31	2.93
547	PPy-2M-2PSA(Na)	0.15	0.10	Water	0.85, 120s	60.87	5.97
257	PPy-BuSA(Na)	0.15	0.10	Water	0.85, 120s	11.53	2.922

Five chemiresistors used to obtain each data set
* Films repeatedly failed due to poor adhesion

95

Table 4.7 (cont.) Details of conducting polymer chemiresistors formed using aryl sulphonates

Index Number	Polymer system	Monomer concentration / mol dm^{-3}	Electrolyte concetration / mol dm^{-3}	Solvent	Growth potential / V, Period / secs	Av. Resistance / Ω	Standard deviation
263	PPy-pTSA(Na)	0.15	0.10	Water	0.85, 120s	2.58	0.13
283	PPy-BzSA(Na)	0.15	0.10	Water	0.85, 120s	8.64	0.87
300	PPy-2-NapSA(Na)	0.15	0.10	Water	0.85, 120s	1.70	0.26
301	PPy-DDBzSA(Na)	0.15	0.10	Water	0.85, 120s	7.55	1.29
513	PPy-4-ABzSA(Na)	0.15	0.10	Water	0.85, 120s	2.93	0.23
514	PPy-NBzSA(Na)	0.15	0.10	Water	0.85, 120s	4.90	1.34
304	PPy-1,3-BzDSA(2Na)	0.15	0.10	Water	0.85, 120s	12.66	1.69
305	PPy-1,5-NapDSA(2Na)	0.15	0.10	Water	0.85, 120s	23.00	1.51
546	PPy-4-OcBzSA(Na)	0.15	0.10	Water	0.85, 120s	4.96	0.88
540	PPy-3-SuBz(Na)	0.15	0.10	Water	0.85, 120s	5.23	0.99
541	PPy-5-SuIA(Na)	0.15	0.10	Water	0.85, 120s	8.05	1.07
542	PPy-DM-5-SuI(Na)	0.15	0.10	Water	0.85, 120s	14.84	3.78

96

Table 4.7 (cont.) Details of conducting polymer chemiresistors

Index number	Polymer system	Monomer concentration / moldm^{-3}	Electrolyte concetration / moldm^{-3}	Solvent	Growth potential / V	Av. Resistance / Ω	Standard deviation
297	PPy-(1R)-(-)10CSA	0.15	0.10	Water	0.85	16.33	0.40
298	PPy-(1S)-(+)10CSA	0.15	0.10	Water	0.85	15.04	1.89
515	PPy-FDSA(2Na)	0.15	0.10	Water	0.85,30s	14.46	3.02
302	PPy-DDS(Na)	0.15	0.10	Water	0.85	2.56	0.25
543	PPy-n-t-(2SP)N(Na)	0.15	0.10	Water	0.75,60s	27.33	4.93
545	PPy-DOSS(Na)	0.15	0.10	Water	0.85	3.19	0.15
544	PPy-OcS(Na)	0.15	0.10	Water	0.85	2.35	0.31
-	PPy-Cu(II)PTSA(4Na)	0.15	0.0125	Water	1.10, 120	20-30	-
-	PPy-P(St-4-NaS)	0.15	0.0050	1:3 MeOH:H$_2$O	10-30	-	

4.3 Polypyrrole chemiresistors based on non-aqueous electrolytes.

The potential importance of non-aqueous media became apparent from a communication by *Diaz et al*[109] in 1979 which reported the anodic oxidation of pyrrole in acetonitrile (albeit containing 1% water). This led to the formation of continuous, free standing, air stable films of polypyrrole. Their electrical conductivity was significantly higher than had been achieved previously (50-100 $\Omega^{-1}cm^{-1}$).

The development of conducting polymer chemiresistors in non aqueous media has not been studied to the same extent as in aqueous media. This is predominately due to the reduced availability of more complex electrolytes which are soluble in these solvents. It is possible to overcome the solubility problem by the synthesis of tetraalkylammonium salts as described in Section 3.2. The formation of good films is greatly dependent on the nature of the solvent system which in itself affects the mechanical and electrical properties of a film. The diversity of aprotic solvents available to perform electrochemical depositions of pyrrole is vast, a key factor being the nucleophilicity of the solvent, which has to be low. Therefore films are not produced in nucleophilic aprotic solvents such as dimethylsulphoxide and dimethylforamide, unless the nucleophicity of the system is reduced by the addition of a protic acid. Solvents which have intermediate properties between those of water and aprotic solvents, like alcohols and mixtures (water/aprotic solvents), will produce films with intermediate conductivites and reasonable physical strengths These too can be improved upon by the addition of protic acids to reduce the nucleophilic character[119].

The initial approach was to develop chemiresistors using acetonitrile as the non aqueous medium. A number of studies have been completed of the deposition of conducting polymer films using acetonitrile or acetonitrile/water as the solvent.[171-173] These have highlighted the fact that, under strictly anhydrous conditions, the films which are formed are poorly adhesive to the anode surface (Pt). This problem was rectified by the addition of 1% water to the system leading to reduced structural

disorder in the films and higher conductivities with the same degree of doping. A significant contribution was made by *Diaz and Hall*[171] who studied polypyrrole/toluenesulphonate films using a variety of solvent systems. It was found that the conductivites of the films could vary from $0.5-100\Omega^{-1}cm^{-1}$ due to variation in the percentage water content. Moreover, the films grown with 1% water content were seven times stronger than films grown in a solution containing 25% water. It was hypothesised that the improvement was due to reduction in the chain lengths within the films, as there was no obvious visual difference or apparent chemical explanation. The most successful systems were those using an acetonitrile/toluenesulphonate system, where the solvent was not dried or deoxygenated and the electrolyte salt, which is particularly hygroscopic, was not dried prior to use. The films formed had high conductivites, excellent mechanical properties and a significantly higher degree of oxidation (0.43), for which there was no apparent reason. These results indicated that film formation relied on the hygroscopic nature of the acetonitrile/counter ion system. The fact that a certain percentage of water did not need to be added to the solvent system reduced the likelihood of irreproducibility in the level of water present in the system. This method was adopted as the standard procedure for acetonitrile based chemiresistors, after tests had showed that it produced stable and uniform chemiresistors.

Other solvents including propylene carbonate and 2-butanol were also considered. The films formed using the former showed high conductivites but, during stability testing they were prone to adhesion problems with the film peeling from the gold surface.

The lower alcohols proved to be somewhat inflexible as solvents for electrochemical deposition. There were solubility problems with some of the salts, and the films formed using ethanol proved to be of poor quality. 2-Butanol was investigated as a racemic solvent (with a view to using both its enantiomeric forms), and the potential incorporation of a chiral solvent into chemiresistors was envisaged. Initial studies used the racemate of 2-butanol to investigate film formation with the anion from (1R)-(-)-10-

camphorsulphonic acid and tetraethylammonium toluenesulphonate. The inclusion of a chiral anion with the corresponding enantiomer of the solvent was intended to produce an enhanced system with chirality exhibited in both anion and solvent. Butanol based systems incorporating camphorsulphonic acids proved successful and a series of films were formed with high conductivities, good mechanical properties and excellent long-term stability as shown in Fig. 4.3. The corresponding electrochemical deposition procedure using the tetraethylammonium toluenesulphonate proved less successful with the reproducibility of the chemiresistors initial resistance proving somewhat variable, although the long-term stability was again good.

Fig. 4.3 Stability data for PPy/(1R)-(10) CSA/Butanol films

Stability data for PPy/(1R)-(-)10 CSA/Butanol films
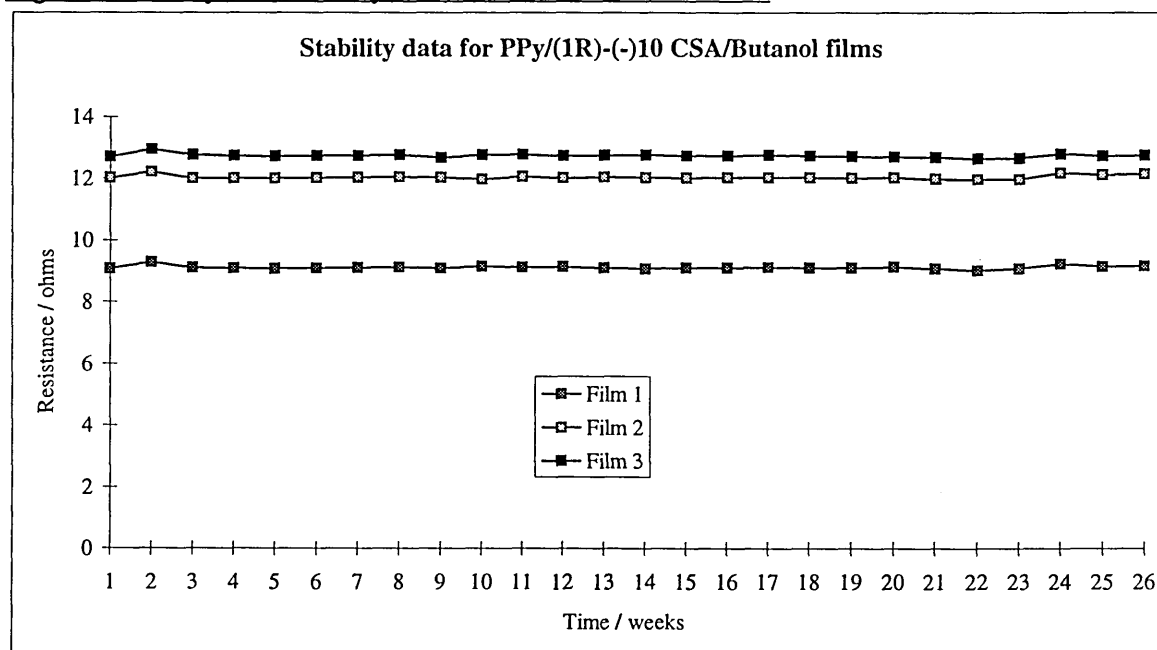
From the results obtained it is apparent that, in contrast to aqueous media, the anion/solvent combination and not just the anion significantly influences the nature, stability and morphology of films obtained. Films prepared in non-aqueous media generally have lower conductivites, even when the deposition period is reduced leading to the formation of thinner films (Table 4.8). The film thickness was measured at around 0.5-2.0 microns for non-aqueous systems.

Table 4.8 Details of conducting polymer chemiresistors using aryl sulphonates in non-aqueous media

Index number	Polymer system	Monomer concentration / moldm^{-3}	Electrolyte concentration / moldm^{-3}	Solvent	Growth potential / V Period/ sec	Av. Resistance / Ω	Standard deviation
279	PPy-TEATS	0.15	0.10	Acetonitrile	1.20; 30s	7.66	1.98
299	PPy-Bu$_4$NBzS	0.15	0.10	Acetonitrile	1.20; 30s	8.56	0.36
518	PPy-Bu$_4$NDDBzS	0.15	0.10	Acetonitrile	1.20; 30s	13.83	2.30
519	PPy-Bu$_4$-2-NapS	0.15	0.10	Acetonitrile	1.20; 30s	3.52	0.12
520	PPy-(Bu$_4$N)$_2$-1,3-BzDS	0.15	0.10	Acetonitrile	1.25; 30s	9.05	0.73
521	PPy-(Bu$_4$N)$_2$-1,5-NapDS	0.15	0.10	Acetonitrile	1.20; 45s	15.13	0.60
522	PPy-Bu$_4$N-4-ABzS	0.15	0.10	Acetonitrile	1.20; 30s	13.74	2.79
527	PPy-Bu$_4$N-(±)10CS	0.30	0.10	Acetonitrile	1.45; 45s	13.82	2.92
516	PPy-(1R)-(-)-10CSA	0.30	0.10	(±) Butanol	1.65;180s	11.56	1.69
525	PPy-TEATS	0.30	0.10	(±) Butanol	1.65; 180s	10-300	*
266	PPy-TEATS	0.15	0.10	PC	1.10; 120s	2.58	0.51

Five chemiresistors used to obtain each data set

* films irreproducible

101

4.4 Polypyrrole chemiresistors based on aromatic dyes as the incorporated anion.

Experimental evidence confirmed that conducting polymer chemiresistors incorporating either alkyl or aryl sulphonate anions showed increased stability and reproducibility. Although the reasons behind this are not fully understood, important aspects are thought to be the anion size, the aromatic ring system and its substituents which help control the effect of the localised electronic field within the film. For example, well ordered films seemed to arise from planar aromatic systems (Section 4.3) having one or more sulphonic acid functionality. A readily available group of compounds which have these properties are aromatic dyes, compounds in the substituted arylsulphonate category. The energy levels of the delocalised ring based orbitals are variable (hence determining the colour), and the anion groups (predominately the sulphonate) confer water solubility.

Our research developed around this class of compounds in order to investigate the incorporation of dye anions into the polymeric matrix of chemiresistors, and to study the resulting stability and spectrum of response to analytes of interest. The further possibility existed that the dyes in the conducting polymer films might be responsive to light, so that resistance change could be monitored in response to the intensity of light absorbed by the film.

The majority of the dyes investigated are visual-indicators for acid-base titrations, and are structurally based on three groups: phthaleins, sulphenophthalins and azo compounds[174]. The dye group which was found to posses the best overall qualities for incorporation as an anion was the azo dye group. The following Table 4.9 illustrates the dyes investigated in aqueous conditions and the baseline resistances obtained along with the corresponding standard deviation based on five chemiresistors. The aromatic dyes were only investigated using pyrrole as the monomer, it may also be possible to include these species as counter-ions with different monomer systems. Minor changes in the electrochemical polymerisation conditions significantly altered the resistances and stabilites of chemiresistors formed, as seen with the dye Orange G.

The electrolyte solutions also required considerable sonication as the solubility of certain dyes in water was low.

With the exception of PPy/Napthol Yellow S the chemiresistors formed using aromatic based dyes had rather low conductivites. The reason for this is related to the nature of the counter-ions incorporated into the chemiresistors. The size, shape and the expected doping levels obtained from these molecules determines the conductivites of the films formed. The dye based dopants (Fig. 4.4) are predominantly less planar by comparison to previous aromatic systems incorporated. Combined with the size effects of larger counter-ions, these factors may cause a disruption to the molecular organisation of the film (leading to a more disorganised film). A further factor is the restricted mobility of these large non-planar molecules during film growth, which may be leading to a reduction in the doping levels within the film and a decrease in the charge to volume ratio of counter-ion units within the polymer matrix. These factors may be contributing to the decrease in conductivites observed. The exception mentioned was Napthol Yellow S which contains a planar naphthalene ring system, this may promote anisotropic growth and hence produce the higher conductivites observed.

Fig. 4.4 Examples of dye based counter-ions incorporated into polypyrrole films.

Tropaeolin O

Nitrazine Yellow
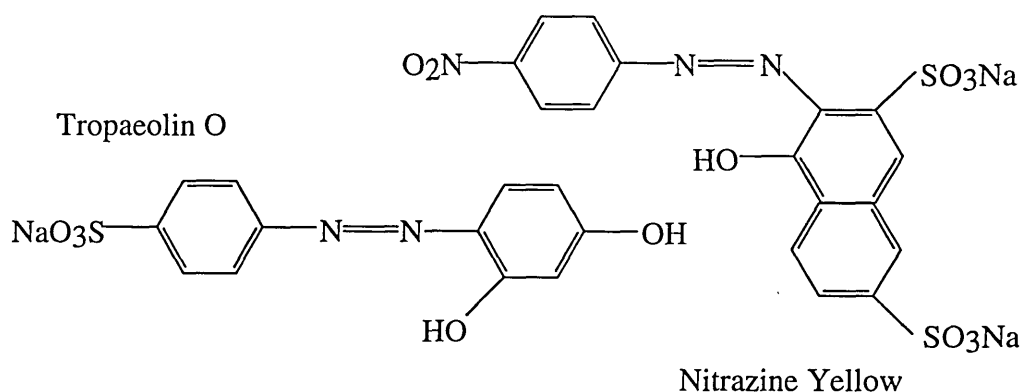
Table 4.9 Details of conducting polymer chemiresistors formed using aromatic dyes

Index Number	Polymer System	Monomer concentration / mol dm^{-3}	Electrolyte concetration / mol dm^{-3}	Growth potential / V ; period / secs	Av. resistance / Ω	Standard deviation
769	PPy-Methyl Orange	0.15	0.10	0.75, 120s	43.91	15.64
770	PPy-Nitrazine Yellow	0.15	0.10	0.75, 120s	199.19	104.91
774	PPy-Napthol Yellow S	0.15	0.10	0.75, 120s	10.35	1.48
773	PPy-Orange G	0.15	0.10	0.75, 120s.	56.50	19.98
773	PPy-Orange G	0.20	0.10	0.73, 120s	33.66	3.21
-	PPy-Tropaeolin O	0.15	0.10	0.75, 120s	243.18	23.77

Five chemiresistors used to obtain each data set.
All systems electrochemically deposited in aqueous media.

4.5 Poly(3-methylthiophene) chemiresistors

The use of polythiophene to form chemiresistors provides a further polyheterocyclic polymer closely related to polypyrrole. Advantages in using thiophene monomers include the possible preparation of a wide variety of β-substituted thiophenes, and the high doping levels achievable. The mechanism of polymerisation is also well understood and can be related to that of polypyrrole based on α–α'-linked monomer units. Polythiophene was first prepared electrochemically in 1982[156,157], and further studies showed that a series of β-substituted thiophenes could also be polymerised[175,176]. One of the most conductive polymers was from 3-methylthiophene, its high conductivity and ease of electrochemically deposition were the main reasons for investigating its potential as a chemiresistor. Literature has shown[119] that bulkier substituents in the β–position hinder chain propagation due to steric crowding, leading to systems with decreased molecular weight and reduced conductivity due to a decrease in film planarity.

The comparative cyclic voltammograms for polythiophene and poly(3-methylthiophene) (P3MT) indicate a comparative cathodic shift (a cathodic shift indicating that a film is more easily oxidised) in the switching potential for P3MT compared to the parent polymer; these studies were performed using tetrafluoroborate as the counter-ion. Hence, although films produced using P3MT may have increased conductivity over the parent polymer, the long-term stability of some systems may suffer due to their increased ability to oxidise. This comparative increase in conductivity has been related to the ability of the β-substituent to reduce the number of β–linkages between monomer units, this in turn imparting an increased linearity and planarity of the film produced. It has further been suggested[157] that the electron-donating properties of the methyl group may itself increase the number of potential charge carriers in the polymer and hence the conductivity.

The monomer appears to provide an easy route to expand the range of chemiresistors available but the incorporation of many dopant anions used in polypyrrole films is not possible. Initial studies performed highlighted that the following dopants produced successful films: perchlorate, tetrafluoroborate, hexafluorophosphate and trifluoromethanesulphonate, the preparation of films incorporating either alkyl or aryl sulphonic acid based systems proved less than successful when tried in a number of solvents. There was particular interest in these dopants as the study on polypyrrole based chemiresistors had highlighted these anions as being particularly stable. As the corresponding section on stability shows (see section 4.8), P3MT films formed had very poor long-term stability, with their conductivity decreasing rapidly over few months.

These results showed that conductivites were high as expected for P3MT films (Table 4.10), but the chemiresistor was affected by poor film stability. Further literature searches showed that the films may benefit from a reduction in thickness and in some cases electrochemical deposition at reduced temperature may help. The case for the former is a study by *Roncali et al*[176] who showed that the extent of conjugation is increased in thinner films, and that the number of defects in a polymer chain increases rapidly as the growth of a polymer chain proceeds. Several studies[175,176] have also shown that, with certain anions, a reduction in the electrochemical deposition temperature affects the properties of the films. Films formed at temperatures around 5°C were found to be more conductive than those formed at room temperature.

Initial problems encountered with P3MT systems limited the advancement of these chemiresistors. The decrease in conductivity observed during long-term stability tests, combined with the limited range of counter-ions available, hindered their development. This led to an overall scaling down in developmental studies with this particular poly(heterocycle). At some point it is hoped to re-investigate this particular area and incorporate some of the literature based ideas and knowledge gained, to improve the results achieved so far. Some literature sources[177] have reported good long term stability results when trifluoromethanesulphonates have been used as the dopant. The

investigation of other solvents besides acetonitrile have been suggested, in particular propylene carbonate and hexamethylphosphoramide (HMPA).

Table 4.10 Details of Poly 3-methylthiophene chemireistors deposited in aqueous media

Index number	Polymer system	Monomer concentration / mol dm^{-3}	Electrolyte concetration / mol dm^{-3}.	Solvent	Growth potential / V, Period / secs	Av. resistance / Ω	Standard deviation
288	P3MT-LiClO$_4$	0.15	0.10	Acetonitrile	1.65, 120s	2.84	0.17
287	P3MT-LiPF$_6$	0.15	0.10	Acetonitrile	1.65, 120s	5.29	0.37
286	P3MT-TBAPF$_6$	0.15	0.10	Acetonitrile	1.65, 120s	3.92	0.55
285	P3MT-TBABF$_4$	0.15	0.10	Acetonitrile	1.65, 120s	2.96	1.14
-	P3MT-TBATFMS	0.15	0.10	Acetonitrile	1.65, 120s	32.56	9.90

Five chemisresistors used to obtain each data set.

108

4.6 Polyazulene / Polypyrrole based chemiresistors

Literature[178] has shown that the electrochemical properties of the polycyclic hydrocarbon poly(azulene) were notably similar to those of polypyrrole. The electrical conductivities of polyazulene depend on the nature of the counter ions incorporated into films, showing similar electrochemical stoichiometry to that of polypyrrole. The anion concentrations are between 0.25-0.33 per monomer unit, and the electroactivity (both the oxidation potential and the polymerisation scheme) are comparable to that of pyrrole. The polymerisation mechanism involves the linkage of monomer units via the 1- and 3- positions on the five membered ring (similar to polypyrrole); this was discovered from experimental studies[159,179] which showed that 1-substituted azulenes did not electrochemically polymerise. The structure of 'polyazulene' corresponds to poly(1,3-azulenediyl) supporting the theory that polymerisation occurs via radical cation dimerisation, leading to linkages between the 1- positions of azulene monomers, the position of highest spin density[180] (Fig. 4.5). The porous morphology and the reversible anion doping-undoping process are further similarities to polypyrrole. Based on the initial success with pyrrole based systems, it seemed that the use of polyazulene may provide a new series of relevant chemiresistors.

Fig. 4.5 Proposed structure for Polyazulene.

ClO_4^-
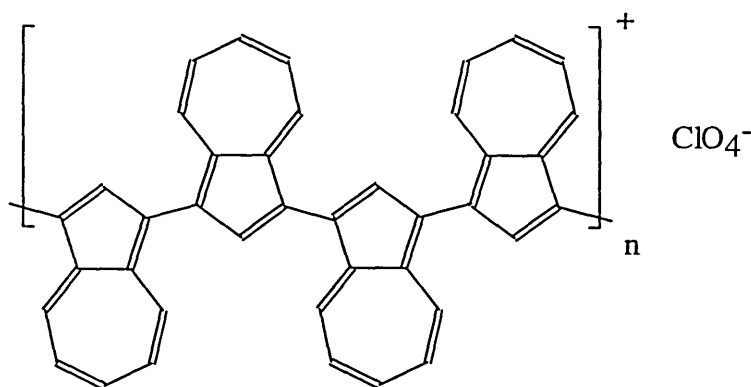
Studies of polyazulene films have been performed in various solvents predominately propylene carbonate and acetonitrile. Literature information shows that the films formed with the highest conductivities are those incorporating the perchlorate and tetrafluoroborate anions[159] whereas with polypyrrole the anions which gave the best overall chemiresistors were alkyl and aryl sulphonates. The preparation of polyazulene/tetraethylammonium toluenesulphonate/acetonitrile films was attempted. The electropolymeriation proceeded smoothly and a series of films was formed varying the deposition potential and the growth period. It was found however that the films were highly irreproducible and, in many cases, the conductivities of the chemiresistors were low and therefore not compatible with the NOSE technology. The films, however, had good adhesive properties to the gold substrate and possessed excellent long-term stability at room temperature.

Experimental studies were promising and so it was decided to co-electropolymerise pyrrole and azulene, preparing a composite based material by mixing the two monomers together in the polymerisation solution. The formation of a composite based material is made possible by the similarities in the properties of the two monomers and the films formed from them. Studies have shown[181,182] that films formed using this technique are polymer composites only on the basis of elemental composition, with little interaction between the two monomers. In this particular case there is a vast difference in the monomer sizes the azulene being far bulkier. It is possible to alter the ratios of the two monomers to alter the film morphology and physical properties of the films formed.

A series of 'copolymer' films was deposited using equimolar amounts of each monomer (0.15M) while the electrolyte concentration remained unchanged at (0.10M). The potentiostatic growth conditions were 1.25V for 30 seconds. The films formed were considerably more reproducible than for polymerisations with the azulene monomer alone (Fig. 4.6). The resistances obtained were now compatible with the

NOSE technology. The long-term stability of these films was outstanding, the variation in conductivity being virtually negligible over the course of six months.

Fig 4.6 Stability data for PPy/PAz/TEATS/H2O films

Stability data for PPy/PAz/TEATS/H$_2$O films
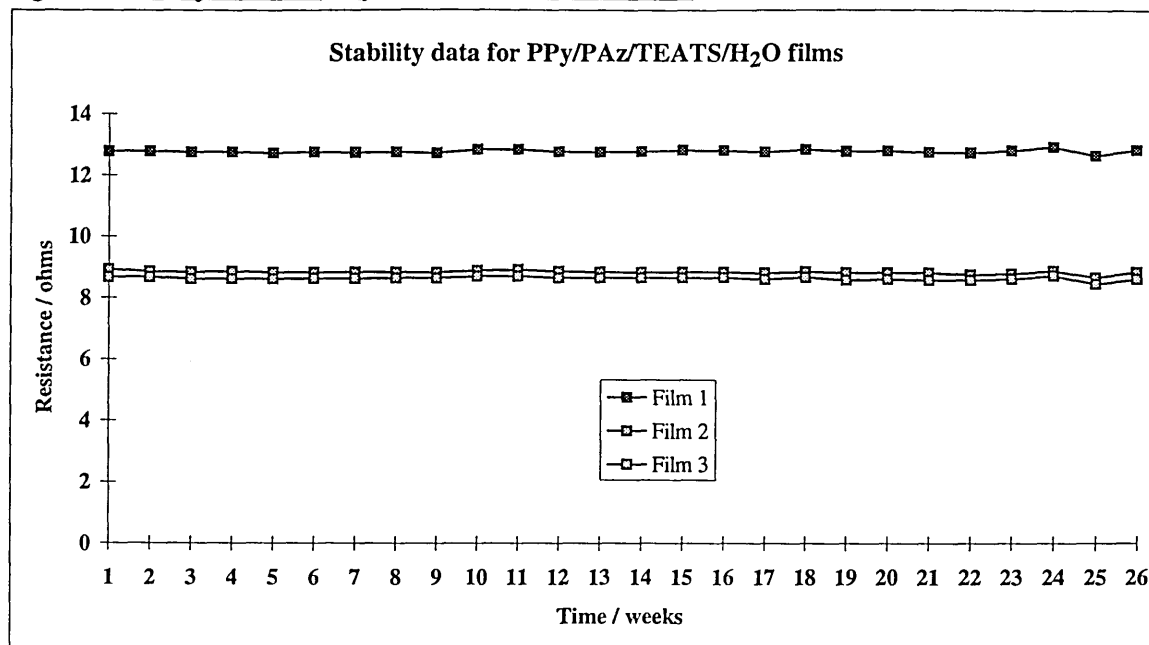
4.7 The stability of conducting polymer chemiresistors.

The stabilities of conducting polymers have been widely investigated[183,184] as significant factors when considering practical applications. Different conducting polymer systems have shown varying stability and the mechanisms of degradative instability are receiving increased attention in the literature. The NOSE technology measures resistance change across the chemiresistor on exposure to an analyte, hence the paramount importance of stability. A conducting polymer chemiresistor which degrades in the ambient atmosphere provides significant problems, predominately response variation and irreproducibility, which invalidate the film as a sensor.

Polypyrrole has been the most investigated of the conducting polymers due to its ease of synthesis and good electrical and mechanical properties. The stabilities of electrochemically deposited thin films vary considerably depending primarily on the incorporated anion, deposition conditions, morphology and film thickness. In general though, many polypyrrole based films have shown reasonable stability with only slow degradation with time[183].

Initial studies completed in conjunction with Neotronics Ltd, found that the rate of conductivity decrease in conducting polymer films was related to the relative humidity of the storage conditions that the sensors were exposed to. A series of controlled experiments demonstrated that, for a variety of sensors stored at reduced humidity, the rate of degradation was reduced. These tests highlighted the fact that moisture content of the surrounding atmosphere played a significant role in the degradation kinetics of polypyrrole films. The reduction in conductivity is therefore probably linked to oxidation by the air, with a synergistic effect involving ambient humidity. The chemiresistors produced were all stored in conditions of relative humidity between 10-15% as monitored by a relative humidity detector. The sensors were stored at room temperature since the literature has shown that at higher temperatures the rate of change

increases for some systems, while others have reasonable stablities up to moderate temperatures $(T < 200°C)$[186].

Following the preparation of fresh polypyrrole based films it is generally accepted that they already contain large amounts of trapped oxygen, and studies have shown that the presence and interactions of oxygen molecules have been the main pathway of conductivity loss. The presence and the rate of diffusion of oxygen into the film (both surface and bulk) significantly inhibit the conduction process by lowering the surrounding local potential of the film so that electrons trapped on adjacent monomer units cannot contribute to the conduction process and hence the route is blocked[187]. Other intrinsic effects leading to conductivity loss are often thermodynamic in origin based upon irreversible chemical reactions. These are predominantly between charged sites on the polymer chain and other counter ions or the π-system of a localised chain. These reactions introduce saturated sp^3 defects along polymer chains distrupting conjugation and hence conduction pathways and other structural defects (as outlined in Section 1.8). The inclusion of an anion which itself has a high proportion of oxygen relative to the molecular weight is more likely to promote rapid changes in its conductivity as highlighted by NO_3^- and ClO_4^- films[186] (see appendix 1 for counter-ion abbreviations). This implicates oxygen, whether present in the system as oxygen rich ions or absorbed from the atmosphere, with degradation. Further to this it is proposed that systems with a more open structure (i.e. increased porosity) are also more likely to deteriorate at an increased rate. The preparation of films with denser morphologies will inhibit the diffusion of oxygen into the film thereby improving stability, but also reducing the effectiveness of the film as a chemiresistor.

Some of the polypyrrole films are inherently hygroscopic due to the presence of hygroscopic anions. It has been proposed[188] that such films may absorb some water vapour from air. A small concentration of hydroxide could be generated from the water leading to the following reaction

$$PPy \ (A^-) + OH^- = PPy \ (OH^-) + A^-$$
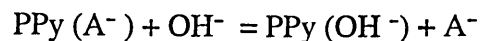
The concentration of OH⁻ present is likely to be rather small, hence the slow degradation in some cases, but it will be enhanced with the increasing relative humidity of the surrounding environment.

The increase in overall thickness of a particular polypyrrole based film is likely to be non-uniform as the film thickness increases. This would lead to a more complex, three dimensional system in which polymer chains of random length are cross linked, therefore leading to an increase in the number of defects in the film. These cross-links usually include N-N linkages, dopant induced acceptor sites, leading to an increase in the oxygen incorporated into the chains and enouraging cross-linking. Results from a series of studies undertaken showed that a marked decrease in film thickness led to a marked reduction in the degradation of the polymer system.

The results shown in Tables 4.11 and 4.12 were gained by monitoring the resistance of a series of three chemiresistors grown under the conditions previously discussed. Their resistances were recorded at regular weekly intervals. The results have been plotted in more comprehensive form in the appendices (Appendix 1 gives details of counter-ion abbreviations used in the text, Appendix 2 provides graphical information relating to the stability of different films). The results shown below highlight some of the trends that were apparent.

The percentage conductivity change relates to the difference between the initial conductivity and that measured six months later (in $\Omega^{-1}cm^{-1}$), calculated from the surface area of the substrate (7.5 $x10^{-3}cm^2$). The results (Table 4.11) are each based on an individual chemiresistor and are representative of the stabilities of the conducting films produced using the electrochemical conditions outlined in Chapter 4

Table 4.11 Stability data for a series of chemiresistors over six months.

Polymer type	Solvent	Initial resistance / Ω	Resistance Six Months / Ω	% Conductivity change
PPy/LiClO$_4$	Water	21.58	175.2	-87.68
PPy/LiNO$_3$	Water	4.86	16.23	-70.94
PPy/TEATS	Water	5.12	7.98	-35.84
PPy/TEATS	Acetonitrile	4.57	5.13	-10.92
PPy/2-NapSA(Na)	Water	2.10	3.74	-44.72
PPy/Bu$_4$N 2-NapS	Acetonitrile	3.18	3.22	-1.24
PPy/DDBzSA(Na)	Water	7.99	7.62	+ 4.86
PPy/DDBzSA(Na)	Acetonitrile	16.42	9.28	+ 76.94
PPy/1,5-NapDSA(Na)	Water	17.96	19.77	-9.16
PPy/Bu$_4$N 1,5-NapDS	Acetonitrile	14.98	19.42	-22.86

For many of the aryl monosulphonates, the films appear to be more stable when grown in acetonitrile. This may be predominately due to the reduced growing period leading to thinner films. Further evidence suggests that the topology of films grown in acetonitrile is more planar and uniform, unlike similar films grown in water which appear to be less uniform and more nodular in appearance. The latter may be more porous in nature therefore having a greater surface area, allowing increased diffusion of oxygen. The topology is also highly dependent on the counter-ion used. The aryl disulphonates seem more stable when aqueous deposition techniques are used, since the corresponding non-aqueous films show a larger decrease in conductivity. Aryl monosulphonates show the reverse characteristics appearing to have enhanced stability in non-aqueous systems. The reason for this is not clearly understood.

One of the more unexpected results was the increase in conductivity of films containing the dodecylbenzene sulphonate anion, the size and hydrophobic nature of this dopant are thought to minimise degradative effects. This also follows another trend which highlighted that smaller dopants lead to films with increased degradation rates due to the more open structure of the resultant films (Table 4.11).

Table 4.12 Further stability results

Polymer system	Solvent	Initial Resistance / Ω	Six Month Resistance / Ω	% Conductivity change
P3MT/LiClO$_4$	Acetonitrile	2.98	17.01	-82.48
P3MT/Bu$_4$NBF$_4$	Acetonitrile	2.19	111.03	-98.03
PPy/PAz/TEATS	Acetonitrile	8.66	8.72	-0.69
PPy/(1R)-(-)10CSA	Butanol	12.71	12.77	-0.50
PPy/(1R)-(-)10CSA	Water	23.71	54.71	-56.66

The results above (Table 4.12) show the rapid degradation experienced by poly(3-methylthiophene) films making them non-functional as chemiresistors for NOSE technology. The following results highlight the stability of the copolymerised system of azulene and pyrrole, where incorporation of a bulkier cyclic monomer (azulene) with a smaller heterocyclic monomer creates a tightly formed film with very little space for the diffusion of oxygen.

The final results for (1R)-(-)-10-camphorsulphonic acid indicate the that effect the solvent system can have on the overall stability. Although many of the variables differed in the electropolymerisation conditions, the solvent has been shown to play a significant role in preventing the degradation of films. Later work showed that the stability of an aqueous system could be considerably improved by a reduction in film thickness; this was used to improve upon earlier results. Another factor which may in some way contribute to the overall stability of a chemiresistor is polymer adhesion.

116

Many forces act on the polymer films due either to ageing (shrinkage) or mechanical expansion-contraction due to repeated exposure to analyte samples occurring when the films act as chemiresistors in the NOSE technology. These processes may lead to a gradual reduction in the physical bonding of the polymer to the gold surface, this in turn reducing the number of conduction routes available from the gold surface across the polymer film, thereby increasing the resistance. The evidence for this derives from films which exhibited poor adhesion to the substrate surface.

To summarise, the main factors that relate to polymeric film stability are the morphology determining the accessibility and susceptibility of deactivating reagents entering the film; the nature and type of counter-ion present, the reactivity of dopant sites to surrounding chains, the environment in which they are stored, the level of structural defects, the conformational state of the polymer backbone (this is highly dependent on the presence of substituents on the monomer), and film adhesion to the gold substrate[184].

4.8 An investigation of the redox properties of doped polypyrrole films.

The nature of the anion affiliated with an oxidised conducting polymer can modify the properties of an electrochemically formed film. The anion produces changes in the redox and electron transport properties, and also affects the morphology, porosity and reactivity of the films. This means that film properties can be altered, providing a viable alternative to the chemical modification of the monomer. It is probable that the combination of both these two methods would produce the most dramatic effects in altering the overall properties and would provide a very wide range of sensor responses.

As already discussed, cyclic voltammetry can be used as a method to monitor the redox properties of conducting polymer films. The change in redox properties can be recorded with respect to the nature of the counter-ion incorporated. The trends emerging from the initial stages of the research performed showed that alkyl and aryl sulphonates were emerging as the most effective chemiresistors. By comparison a second category, small univalent inorganic anions i.e. ClO_4^-, BF_4^-, NO_3^-, PF_6^- (see Appendix 1 for counter ion abbreviations) were less effective chemiresistors, predominantly due to their lack of stability, which is related to film porosity and morphology as discussed in section 4.7. From these two classes of anion a group was selected as subjects of a study of redox properties in aqueous solution. Combined with the cyclic voltammetry information (on redox properties), elemental analysis was performed using SEM-EDX on oxidised and reduced films. The redox behaviour of six polypyrrole films is shown in Figure 4.7 {(a), sodium perchlorate, ClO_4^- (b), sodium hexafluorophosphate, PF_6^- (c), butanesulphonic acid (sodium salt), BuSA(Na) (d), p-toluenesulphonic acid (sodium salt) p-TSA(Na) (e), dodecylbenzenesulphonic acid (sodium salt) DDBzSA(Na) (f), 1,5-naphthalenedisulphonic acid (disodium salt), 1,5-NapDSA(2Na)} [refer to Appendix 1 for identification of counter ions]. All films were electrochemically deposited, and the cyclic voltammetry was performed, as explained in the Chapter 3 (Section 3.2).

From the cyclic voltammograms it is apparent that the anions fall into two classes[189].

The polypyrrole films doped with the small, univalent inorganic counter ions show reversible, stable redox properties exhibiting a broad reduction wave in the scan appearing at -100mV (perchlorate) and -250mV (hexafluorophospate). From the supporting EDX data it can be seen that the prevailing process during reduction of the perchlorate system is expulsion of the anion from the film (see Figs. 4.8 and 4.9), and its corresponding incorporation during oxidation. The EDX data for the polypyrrole/perchlorate system shows a considerable reduction in the elemental chlorine present in the reduced state by comparison with the oxidised state. It is also worth noting that there is no trace of sodium present in the elemental analysis for either the oxidised or reduced forms. For the polypyrrole/hexafluorophospate system (see Figs. 4.10 and 4.11) the EDX shows the emergence of a sodium peak, indicating cation motion into the film to maintain charge balance in the redox process. This highlights the effect that relative migratory apptittude has on counter-ion movement (anion or cation), the anion size being just one aspect of relative migratory apptittude.

The second series of redox voltammograms is associated with polypyrrole films doped with a series of sulphonate anions. These exhibit a variety of redox shapes which are of a similar pattern, but vastly different from those of the small, univalent anions. The voltammograms are quasi-reversible (see Section 3.6) with a significant shift in the redox potentials observed. Both the cathodic and the anodic redox processes have shifted cathodically by comparison with the first group of anions. The cyclic voltammograms for the sulphonates show the initial scan as a solid line, and the second scan as a dashed line. It is clear that there is a significant difference between the initial cathodic sweep and subsequent scans. The reduction peak is sharper and of greater surface area, indicating that there is a chemical/physical change occurring in the system during the first scan. The first cathodic scan of any conducting polymer film involves the process of cation inclusion or anion expulsion (depending on the dopant), film shrinkage, and the movement of solvent through the matrix. The deposited film structures are not regenerated after the initial cycle, even when in the presence of the

original counter-ion. This was apparent from SEM studies which indicated that the polymer matrix has undergone a physical/chemical change. The significant cathodic current (i_{pc}) values for the first reduction scan are related to the physical/chemical change the films have undergone. The magnitude and sharpness of the first reduction peaks are related to the equivalence of redox sites in the film. From the cyclic voltammograms obtained for sulphonate containing films it is possible to suggest that there are more equivalent redox sites present in the film after this first scan. Films deposited with small, spherical, inorganic anions (i.e. ClO_4^-) show broader reduction peaks, than their larger anion counterparts [i..e1,5-NapDSA(2Na)]. The smaller anions have a more porous morphology (apparent from SEM studies) allowing easier diffusion of counter ion species during the redox processes, hence the reproducibility of the cyclic voltammograms obtained[137].

The EDX analyse of p-TSA(Na) doped films (see Fig. 4.12 and 4.13) in its oxidised and reduced states, show comparable peaks in relation to the amount of sulphur present, but in the reduced state we see the emergence of a significant sodium peak not apparent in the oxidised state. This indicates that there are two types of redox behaviour. In the p-TSA(Na) system cation motion (in the opposite sense to anion motion) sees the movement of sodium ions into the film to maintain the balance of charge. For the small, inorganic anions the mechanism for de-intercalculation-re-intercalculation during the reduction-oxidation process involves anions.

The size of anion used in the doping process clearly plays a significant role in the type of redox behaviour exhibited by a film. This is highlighted by the EDX data obtained for DDBzSA(Na) where the large amphiphilic anion again remains fixed in the film and cation motion is again the mechanism of charge balance (see Fig. 4.14). The stability of this system is shown by second EDX trace obtained after the film had been continually cycled for four hours at 50mvsec^{-1} (see Fig. 4.15). It shows no significant change in elemental composition as compared with the composition after just two cycles.

The film thickness and morphology of a conducting polymer film are important factors in determining the redox properties of the chemiresistor. The smaller inorganic anions produce films with a porous nodular morphology, which fits well with the known theory of anion motion. But as seen with the EDX differences between ClO_4^- and PF_6^- it cannot be assumed that a nodular, porous, less ordered structure will lead to anion motion, the overall relative migratory aptittude determines the redox movement of anions, the anion size being part of this. As the anion size increases there is a noticeable change in the film morphology the structure of the films becomes less nodular, with increased space filling, and the surface adopting a more uniform appearance. The less porous, densely packed films containing the larger counter ions appear to have insufficient space for the movement of larger anions through the film, hence the comparative movement of cations instead of anions.

The EDX analysis for BuSA(Na) a medium sized alkylsuphonate showed no marked differences between the oxidised and reduced states. The sulphur peaks remaining comparable, with no presence of a sodium peak in the reduced trace. The film was particularly thin and no conclusive information was obtained, although it is felt unlikely that anion motion was involved in the redox process.

Aryldisulphonate films showed a decrease in their conductivity when compared to films produced with the comparable monosulphonate. The increased number of sulphonate groups enables the dopant to bind more strongly with cationic sites on the polymer chain. With this form of attraction in place the film adopts a more open structure. The elemental analysis of the reduced film (see Figs. 4.16 and 4.17) shows a reduction in the sulphur content and a small influx of sodium into the film. The elemental sulphur loss is possibly due to the migration out from the film of disulphonate anions, counter to polypyrrole cations that are neutralised during the reduction process. Less negative charges are required to satisfy the number of cationic charges associated with the polymer backbone, therefore the percentage of required anion within the film is possibly reduced.

The larger aromatic dyes incorporated into PPy films exhibit a migration of sodium ions into the films during reduction to maintain the balance of charge (see Figs 4.18 and 4.19). The example involves the dye Orange G. The reduced trace also shows a peak related to silicon due to contamination from the CVD nitride layer.

Fig. 4.7 Cyclic Voltammograms of various polypyrrole films.

(a) PPy/NaClO$_4$/H$_2$O

50µA

(b) PPy/NaPF$_6$/H$_2$O

50µA

(c) PPy/BuSA(Na)/H$_2$O

50µA
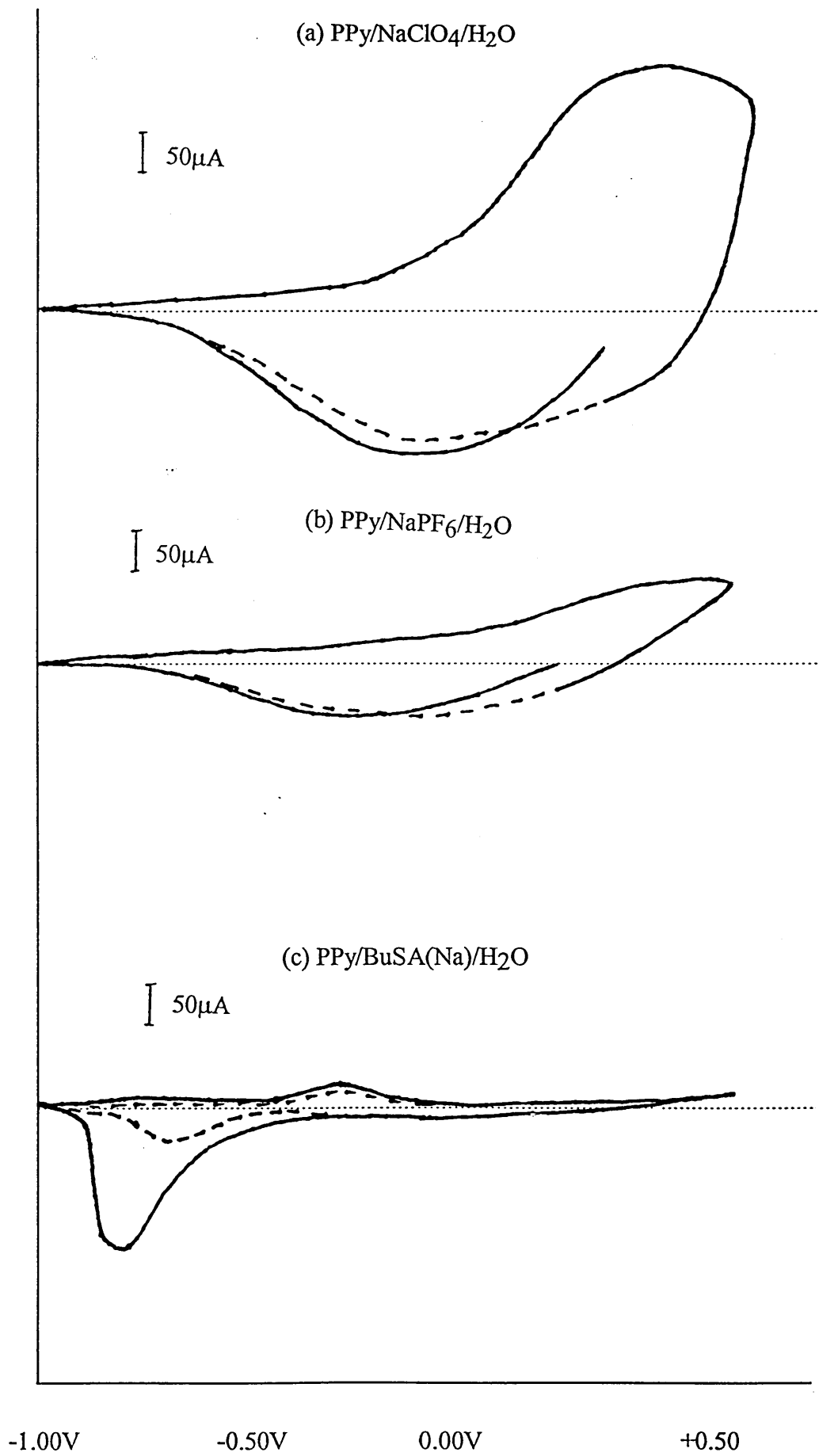
-1.00V   -0.50V   0.00V   +0.50

(d) PPy/p-TSA(Na)/H₂O
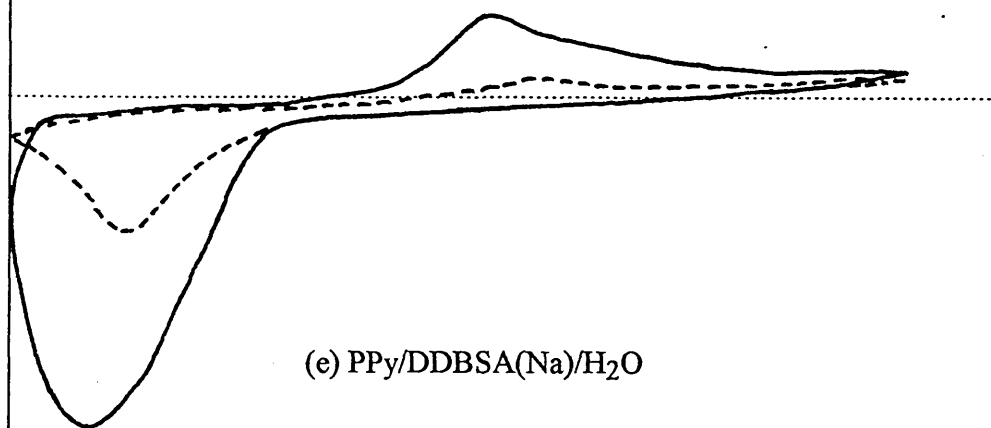
50μA

(e) PPy/DDBSA(Na)/H₂O

50μA
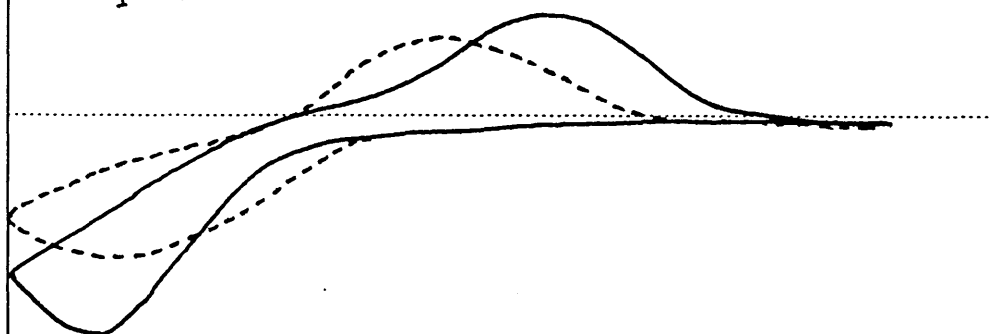
(f) PPy/1,5-NapDSA(2Na)/H₂O

50μA

-1.00V   -0.50V   0.00V   +0.50

124
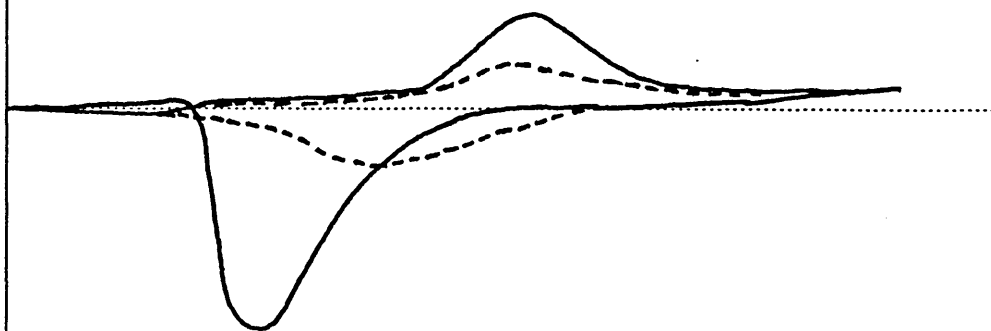
Fig. 4.8 EDX of an Oxidised PPy/NaClO4/H2O film
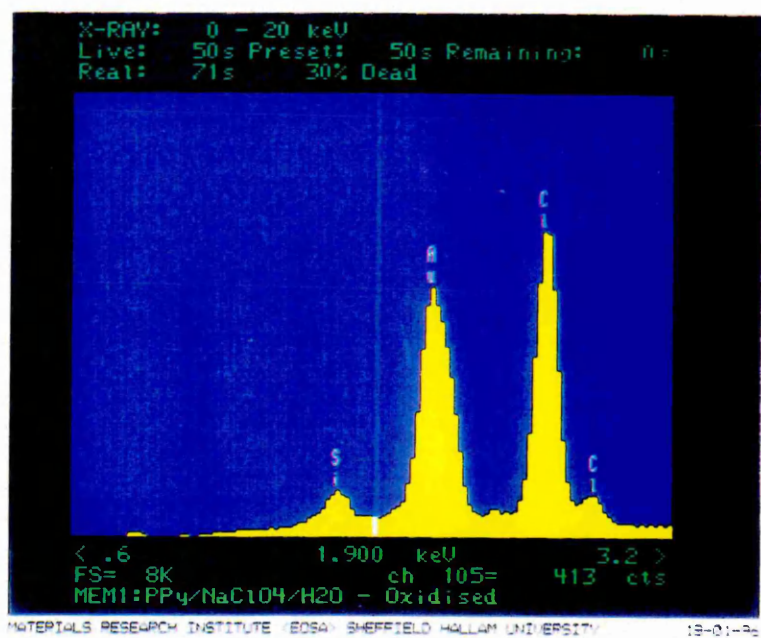
Fig. 4.9 EDX of a Reduced PPy/NaClO4/H2O film
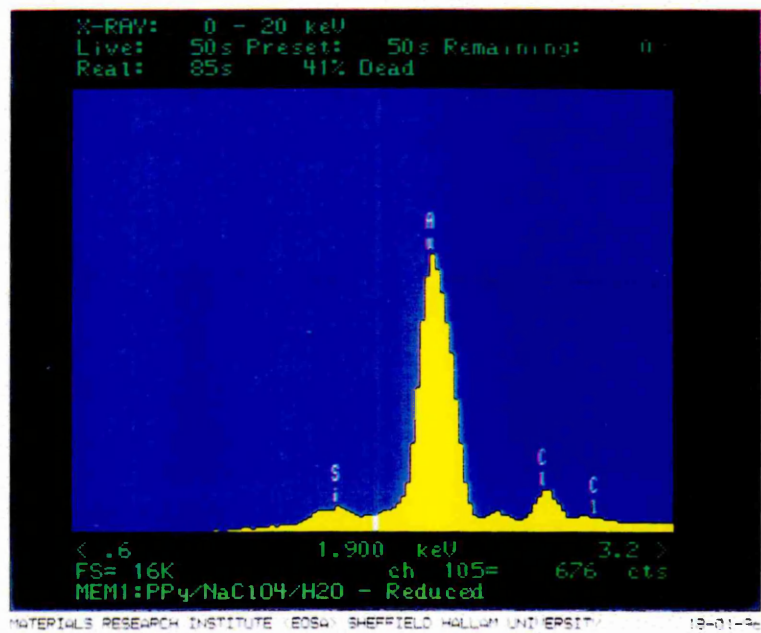
Fig. 4.10 EDX of an Oxidised PPy/NaPF6/H2O film
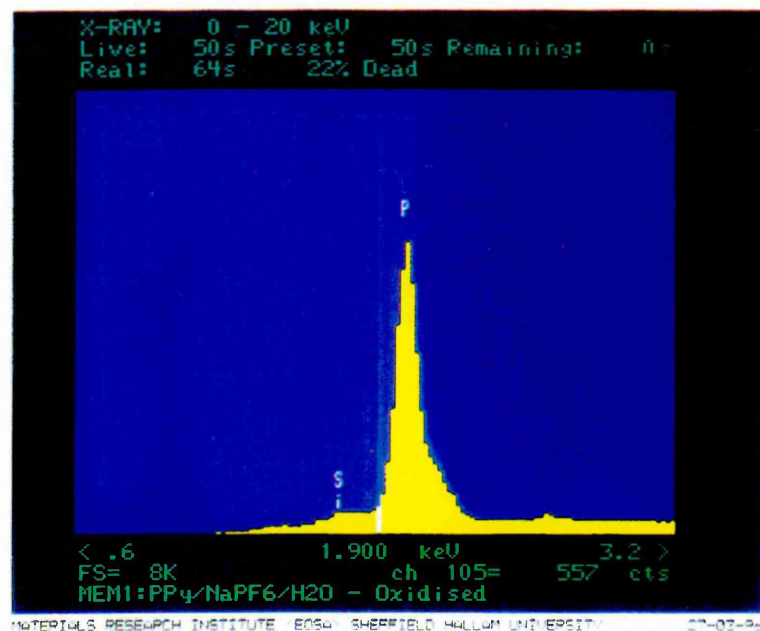
Fig. 4.11 EDX of a Reduced PPy/NaPF6/H2O film
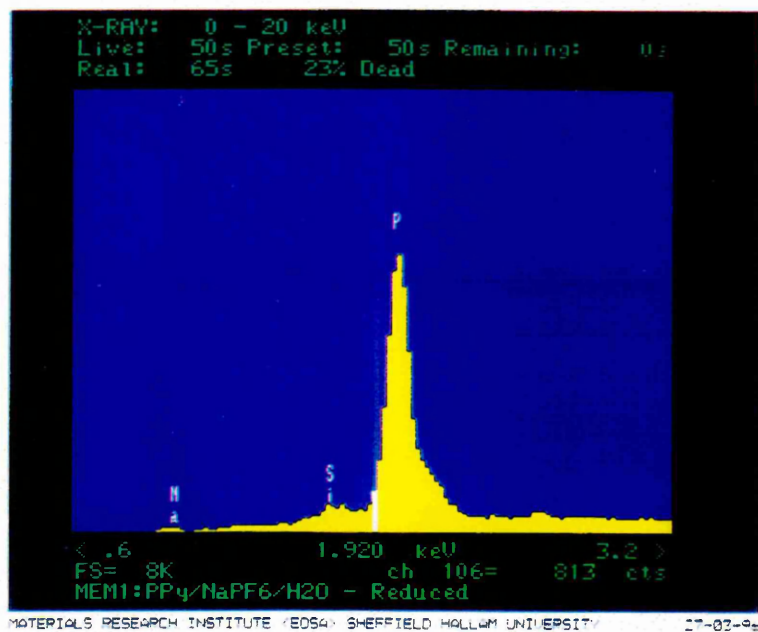
Fig. 4.12 EDX of an Oxidised PPy/p-TSA(Na)/H2O film
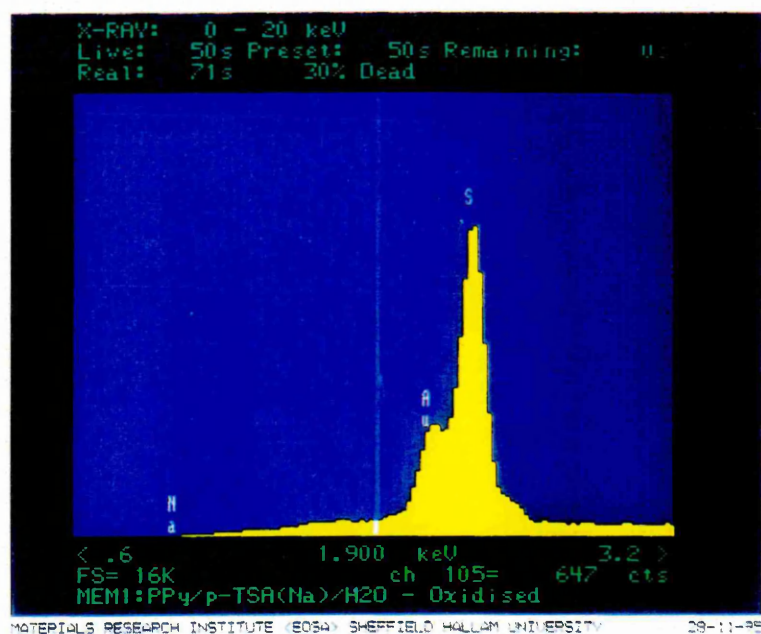
Fig 4.13 EDX of a Reduced PPy/p-TSA(Na)/H2O film
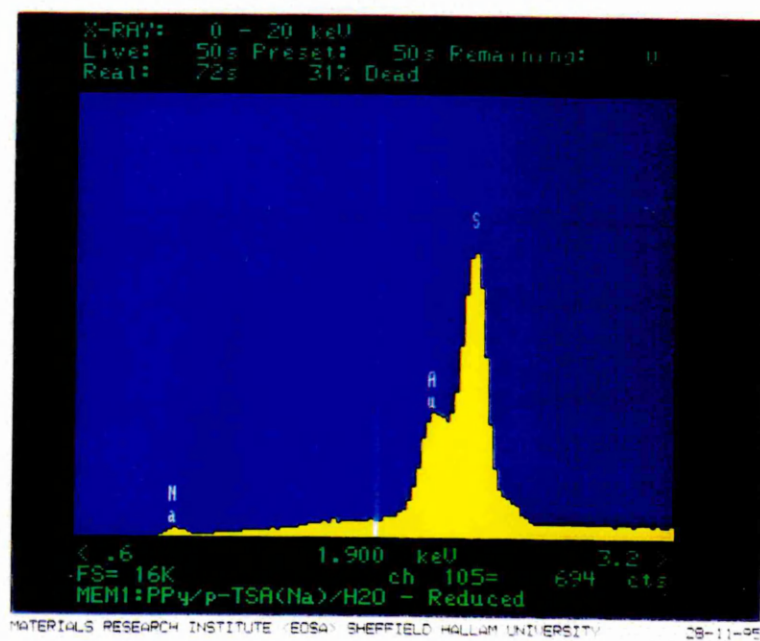
Fig. 4.14 EDX of a Reduced PPy/DDBzSA(Na)/H2O film
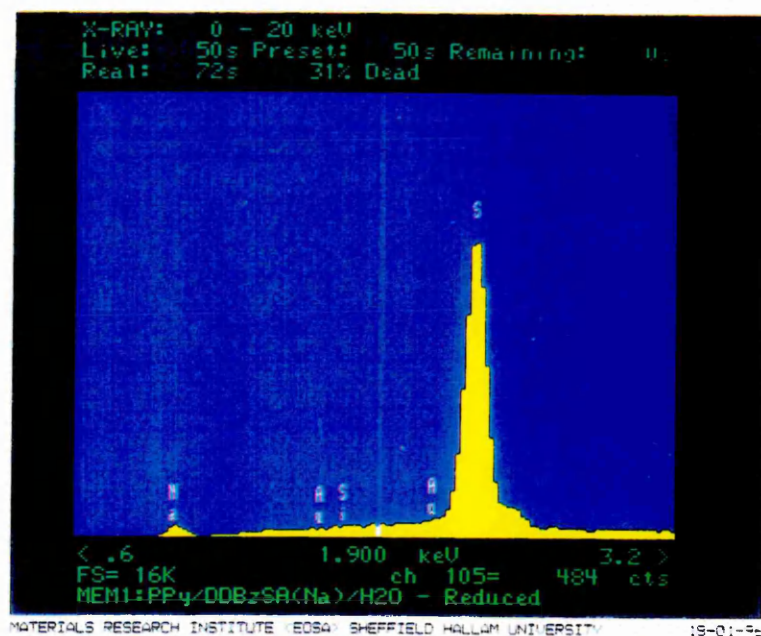
Fig. 4.15 EDX of a Reduced PPy/DDBzSA(Na)/H2O
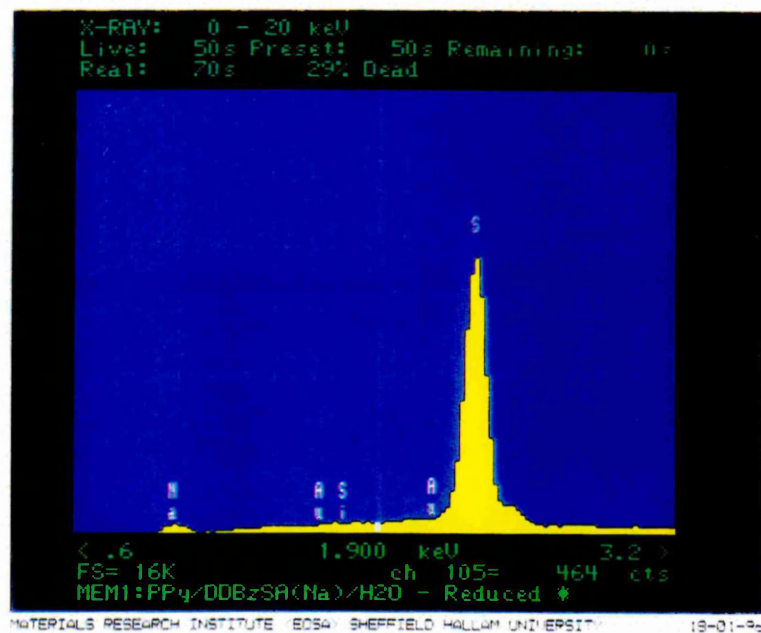
Fig. 4.16 EDX of a Oxidised PPy/1,5-NapDSA(2Na)/H20
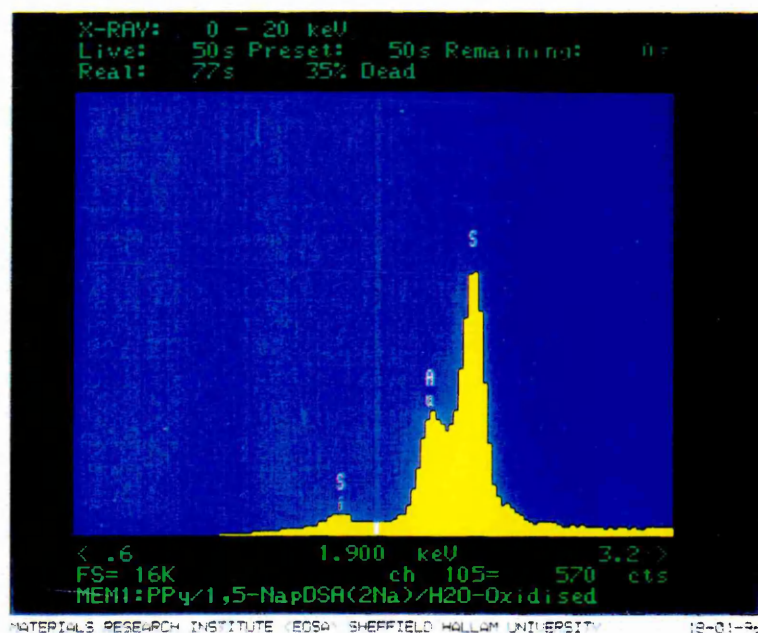
Fig. 4.17 EDX of a Reduced PPy/1,5-NapDSA(2Na)/H2O film
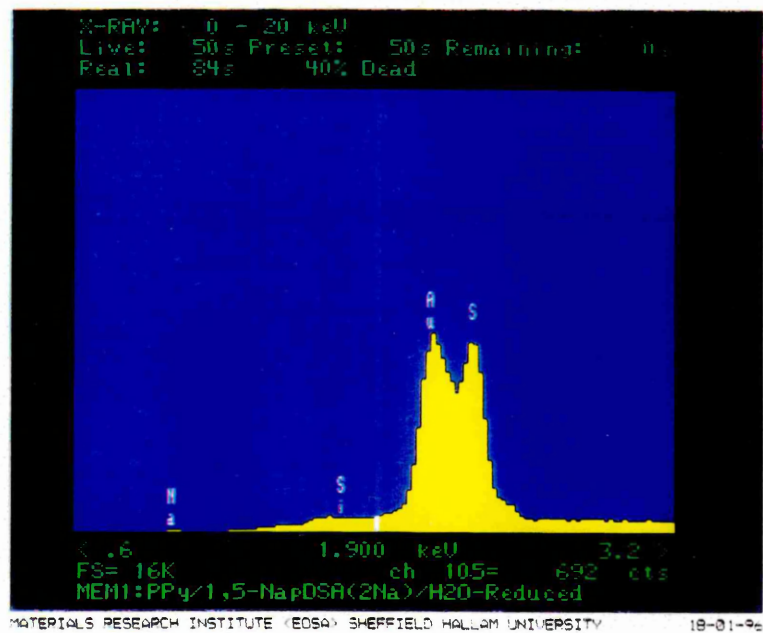
Fig. 4.18 EDX of a Oxidised PPy/Orange G/H20 film
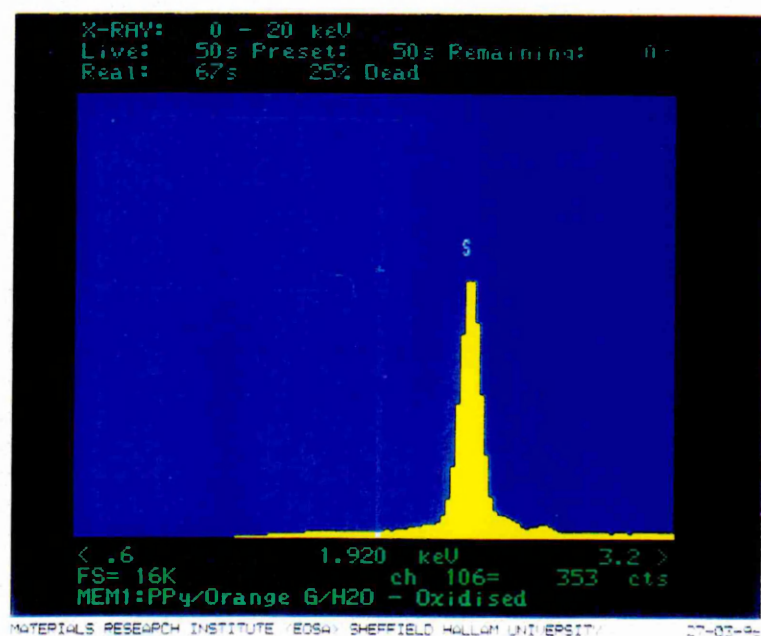
Fig. 4.19 EDX of a Reduced PPy/Orange G/H2O film
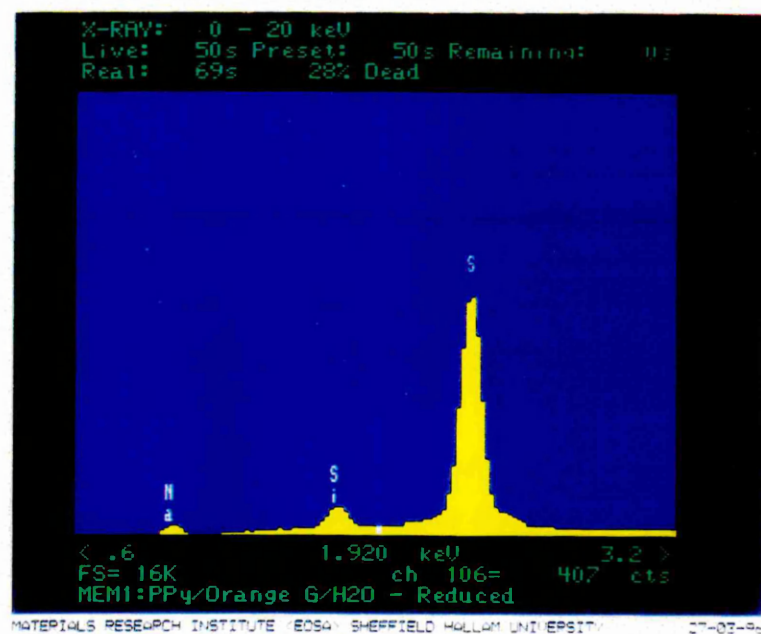
Chapter 5 The modification of conducting polymer films and the optimisation of chemiresistor response

5.0 General Introduction

Preparation of sensors optimised for the NOSE technology required research into many areas of polymer technology. The initial study highlighted areas deemed significant for response characteristics including, baseline resistance relative to response, deposition conditions (both potentiostatic and galvanostatic), variation in film thickness, film morphology and solvent conditions used during deposition.

The relationship between initial baseline resistance and sensor response was an area which had not previously been studied. The e-NOSE 4000 required baseline resistance in the region 1-100 ohms and any chemiresistor not in this region was unusable. This is a particularly limiting factor, requiring the formation of films with high conductivites (therefore only highly conductive polymers were considered). Within the desired region it was necessary to clarify the baseline resistance which gave a high, reproducible percentage change when exposed to analytes.

The alteration of electrochemical deposition conditions enabled the variation of many physical characteristics shown by the resulting sensor films, for example the degree of polymer oxidation, and, thus, the concentration of incorporated anion and the number of polymer chain defects (both of which can affect conductivity). Further physical properties include the structural morphology, porosity, film thickness, solvent incorporation, bulk and surface properties and environmental stability, all of which may play a role in defining the optimum growth conditions for effective and reproducible sensor response.

5.1 The relationship between baseline resistance and optimum sensor response

A pro-gramme of studies was performed (in conjunction with Neotronics Ltd) investigating a series of sensor types grown using predetermined electrochemical conditions. The individual sensor types had baseline resistances which varied between 5 - 40ohms under a predetermined electrochemical deposition protocol. To determine the effect of the baseline resistance the chemiresistors were placed into the NOSE technology and exposed to a reference sample. This enabled the correlation of baseline resistance with sensor response.

Sensors of a similar type, grown in the same experimental conditions are expected to perform comparably when exposed to a standard reference vapour. The baseline resistance of individual sensor types grown in identical conditions was found to vary. A relationship between film baseline resistances and the size of response on exposure to a standard analyte was felt to exist. This research was aimed at showing the link between baseline resistance and the size of sensor response and improving sensor comparability, such that sensor types gave comparable responses to standard analytes. The experiments were performed using a D model NOSE under the experimental parameters listed:-

Vessel Purge	-	2 minutes
Equilibration time	-	7 minutes
Head Purge	-	7 minutes
Sample Time	-	4 minutes
Reference gas	-	Dry air

The gas flow rates were kept constant for the head and vessel purges, and the same standard reference sample used throughout. Sensor responses were recorded one minute after the sample had been exposed to the sensors. The reference sample was prepared (in 100ml batches) from 75% ethylene glycol and 25% water. The presence of the glycol helps to stabilise the response to increased humidity. This industry standard

sample was used throughout the optimisation programme as it leads to high % responses from the sensors enabling easy interpretation of the effects on response characteristics

Similar trends were observed for a large number of alkyl and arylsulphonate doped sensor types, as exemplified by the two types shown in Figure 5.1 and 5.2 (where each graph represents data collected using between 100 - 200 individual sensors

Fig. 5.1 Type 259 PPy/Hexane sulphonic acid(sodium salt)/ Water

Potentiostatic electrochemical deposition conditions used and all standard experimental conditions applied.

Pyrrole concentration   -   0.15M

Electrolyte concentration   -   0.10M

Growth potential   -   0.85V

Growth period   -   60 seconds

The baseline resistance vs response to PG/Water for sensor type 259
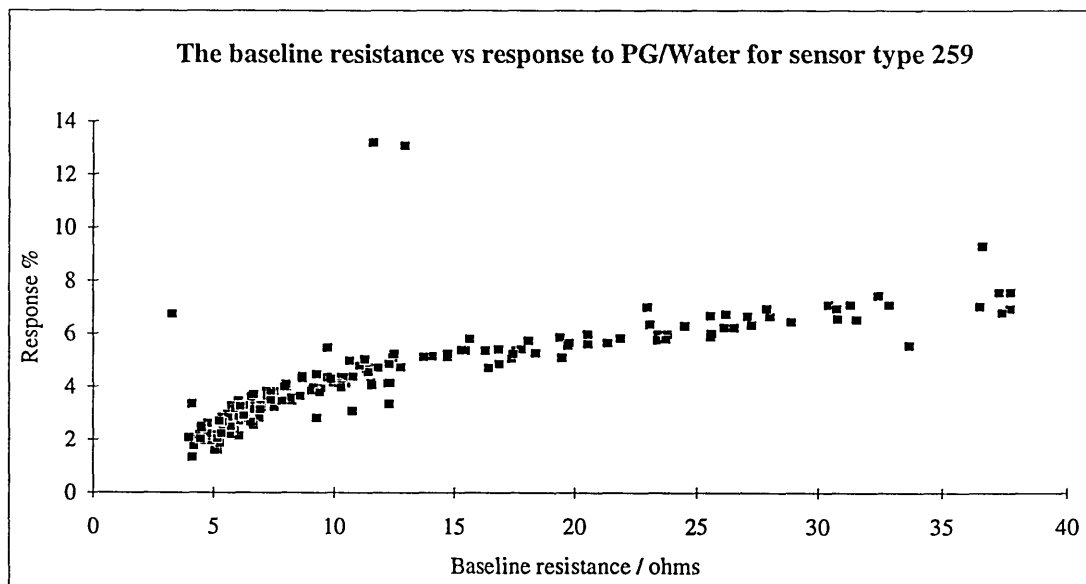
Fig. 5.2 Type 264 PPy/Tetraethylammonium p-toluenesulphonate/Water

Potentiostatic deposition conditions used

Pyrrole concentration	-	0.15M
Electrolyte concentration	-	0.10M
Growth potential	-	0.85V
Growth period	-	60 seconds

The baseline resistance vs response to PG/Water for sensor type 264
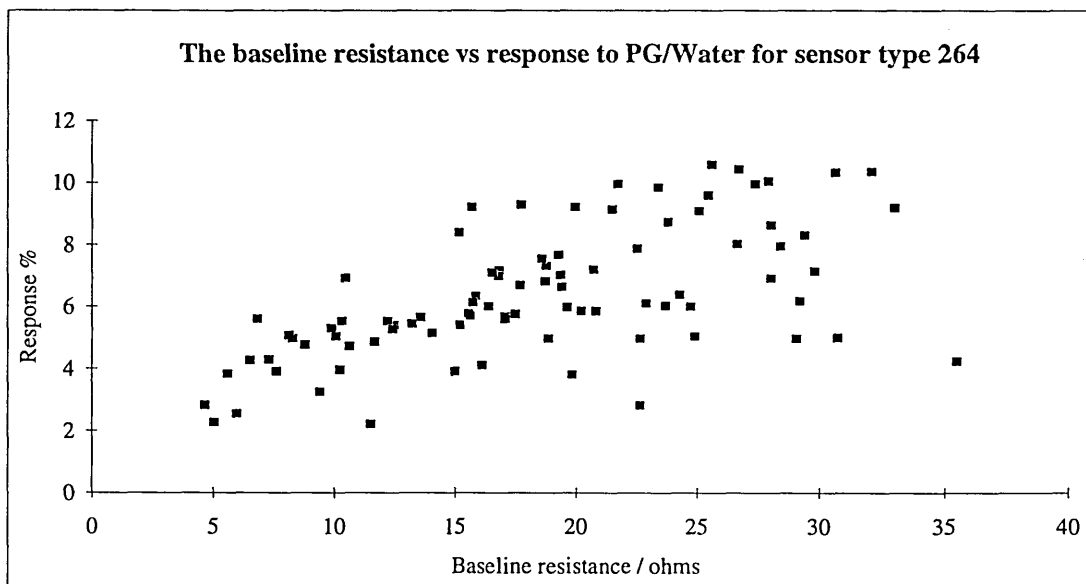
The percentage response graphs indicate that there is a link between the initial baseline resistance and response, Figure 5.1 (sensor type 259) shows that there is a gradual increase in response as the baseline resistance increases from 5 to15 ohms, after which there appears to be a plateau region where response appears to be at its optimum level (a region between 15-30 ohms). A similar trend can be seen for graph representing the sensor type 264, (Fig. 5.2) although it is far less well defined. The cross-section of data obtained and the examination of this data show that there is an upward trend in the response which correlates with an increase in baseline resistance. Further studies completed on other sensor types (263, and 283 see pg96) highlighted this trend. This information led to the introduction of sensor optimisation, whereby all sensor systems were developed within a predefined resistance region (between 15-30 ohms). The electrochemical growth conditions which were used, (i.e. growth potential, growth

134

period and respective concentrations of pyrrole and electrolyte) were varied in the production of each sensor type to achieve this objective. This initial study had shown that comparable sensor response was linked to baseline resistance. Further research proved that this was a minor improvement in the context of total sensor optimisation.

5.2 The relationship between potentiostatic growth conditions and sensor response.

An investigation of growth conditions and their effect on sensor response was required to determine the factors which were significant in controling a sensor's response characteristics. This evaluation indicated whether initial baseline resistance was a significant factor in determining sensor properties. Based upon the number of variables that electrochemical deposition controls, (i.e. porosity, oxidation level, morphology, level of structural defects, redox properties, film thickness and reactivity), it was probable that a range of properties would require optimisation to improve discriminatory ability and variation in sensor response. Factors controlling sensor response relating to potentiostatic electrochemical deposition required a study of film conductivity, morphology, film thickness, environmental stability and response to a standard reference analyte.

The study used a sensor that is in common use (to reflect the range of sensors currently used). The investigation used the sensor type 264 (600 series) as used in the previous baseline resistance vs. response experiments. The sensor type is prepared from the following monomer/electrolyte/solvent system, pyrrole/tetraethylammonium p-toluenesulphonate/ milli-Q-water. Throughout the electrochemical deposition process several variables remained consistent; those were the concentration of pyrrole (0.15 moldm^{-3}) and the electrolyte concentration (0.10 moldm^{-3}). A series of chemiresistors were formed at varying growth potentials and growth periods (Table 5.1), and all standard experimental techniques (Section 3.2) were adopted and maintained throughout the procedure. The chemiresistors initial resistances were recorded and this

135

was repeated on the tenth and twentieth day after deposition (Table 5.2). The relative responses to a reference standard were established on day ten. A D-model electronic nose was used in the tests, and the sensor head was prepared, calibrated, and the baseline response to dry air measured to confirm calibration. Film thickness was recorded using a Vickers optical microscope with a tolerance of +/- 0.30 microns (Table 5.2).

Table 5.1 Growth variables and conditions used during potentiostatic deposition.

Index Number	Monomer conc. mol dm^{-3}	Electrolyte conc. mol dm^{-3}	Potentiostatic dep. potential / V	Growth Period /seconds
600	0.15	0.10	0.85	120
601	0.15	0.10	0.85	60
602	0.15	0.10	0.95	60
603	0.15	0.10	1.05	60

Table 5.2 Resistance and film thickness measurements

Index number	Initial resistance / Ω	Resistance day 10 / Ω	Resistance day 20 / Ω	Film thickness / microns (μm)
600	3.80	3.57	3.29	4.0
600	3.57	3.19	2.99	4.5
600	4.30	3.23	3.28	5.0
601	5.25	4.79	4.26	2.5
601	7.51	6.56	5.84	2.5
601	7.28	6.35	5.70	2.0
602	12.51	11.01	9.63	3.0
602	11.95	10.56	9.61	3.5
602	10.53	9.14	7.90	3.5
603	39.68	30.06	25.12	4.0
603	48.39	35.56	29.52	4.0
603	50.34	37.88	31.34	5.0

The conditions used in the formation of sensor type 600 are those outlined in Chapter 4 (section 4.3) and the stability data can be found in the appendices (Appendix 2). The formation of sensor type 601 was to monitor the effect the deposition period had on initial resistance and film thickness. The conductivity of the films decreased with a reduction in the deposition period, which also saw a reduction in film thickness of approximately half. Sensor types 601, 602 and 603 investigated the effect of an increase in the electrochemical deposition potential. The results showed an decrease in the conductivity of films formed (i.e. increased resistance), a significant decrease being noted between types 602 and 603. The decrease in conductivity observed may be partly due to an increase in polymer structural defects as the potential is increased. The higher potential leading to increased overoxidation, results in more structural defects and a reduction in the effectiveness of conduction pathways in the films. The films formed

were also becoming progressively thicker due to the increasing deposition potential applied.

Increasing the synthesis potential affected the surface and structural properties of films formed. Those deposited at higher potentials exhibited structures which appear to be less ordered and more porous structures (see comparison in Figs. 5.3 and 5.4). The surface morphologies for the films grown at lower potentials appear to be of a more ordered nature, with a generally smooth surface. At higher potentials the films appear to be less smooth, perhaps even slightly nodular, the irregular surface leading to potentially more porous film. A more nodular surface also raises the probability that there will be an increase in the total surface area, thereby leading to a larger area for analytes to interact with.

The nature of the responses to the reference analyte (propylene glycol/water 75%/25%) appears to substantiate the evidence from the morphology study. Three individual sensors grown from each of the four subsets (Table 5.1) were exposed to the reference analyte using the same method used previously (Section 5.1). A series of three consecutive tests was completed to form the template observed (Table 5.3). The graphical profile (Fig. 5.5) shows the responses of the sensors with each set of sensors displaying varying levels of response. The vertical cursor is positioned at one minute, the position from which most sample data gathered from the instrument is analysed (Table 5.3). The most significant result is the large increase in response due to reduction of the growth period from 120 to 60 seconds, resulting in a thinner film. The sample analyte was able penetrate into the thinner film (601) and affect the bulk resistivity of the film more rapidly, whereas the thicker film (600) has appeared to respond to a lesser extent. This may be due to a predominant surface interaction of analyte and film, the analyte having a reduced impact on the bulk resistivity, but it is also feasible, however, that the increase in the overall mass of film present reduced the output value, although this was not possible to prove.

138

The effects of increased film deposition potential suggests that there is a link between film porosity (as observed in the surface studies) and the ability of a vapour to penetrate into the film. The traces associated with the sensor types 601, 602, 603 show a gradual increase in the sensor output. This may be due to the increased porosity allowing deeper penetration of the vapour into the film bulk, which in turn has a greater impact on the film's conduction. The film thickness measurements (Table 5.3) indicate a gradual increase, which may be due to the structure adopting a less ordered appearance with the slightly nodular structure giving the film increased depth. The trends observed with the reference analyte were also seen when further analysis was completed using static sampling for methanol, ethanol and acetone.

Table 5.3 Responses to dry air and reference analyte with related standard deviations

Index number	Head position	Response to dry air / %	Response to reference analyte / %	Standard deviation to ref. analyte / %
600	1	0.00	0.67	0.00
600	2	0.00	0.64	0.00
600	3	0.00	0.66	0.00
601	4	-0.05	1.33	-0.05
601	5	0.00	1.46	0.00
601	6	0.05	1.12	0.05
602	7	0.02	1.39	0.02
602	8	0.05	1.39	0.05
602	9	0.00	1.46	0.00
603	10	0.06	1.57	0.06
603	11	0.06	1.70	0.06
603	12	0.03	1.60	0.03

Fig 5.5 Profile view of sensor variables (600 series) responses

Sample

Class	SENSOR VARIABLES
Substance	1,2-PROPANEDIOL/WATER
Sample	DRY TEM PG/WATER 75%/25%(Template)
Method	N/A
Time	N/A
Calibrated	Some (or all) missing

Cursor at   01:00
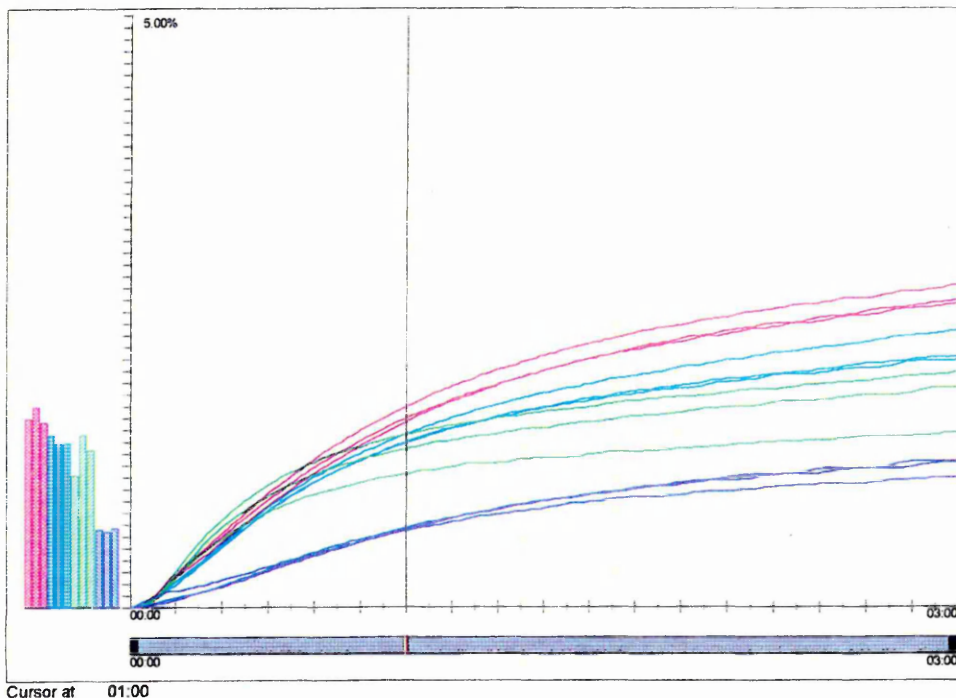
⊠ 1.60%	Type 603	⊠ 1.70%	Type 603	⊠ 1.57%	Type 603	⊞ 1.46%	Type 602
⊞ 1.39%	Type 602	⊞ 1.39%	Type 602	▨ 1.12%	Type 601	▨ 1.46%	Type 601
▨ 1.33%	Type 601	◩ 0.66%	Type 600	◩ 0.64%	Type 600	◩ 0.67%	Type 600

Sample Comments
N/A

Fig. 5.3 SEM photograph of sensor type 601
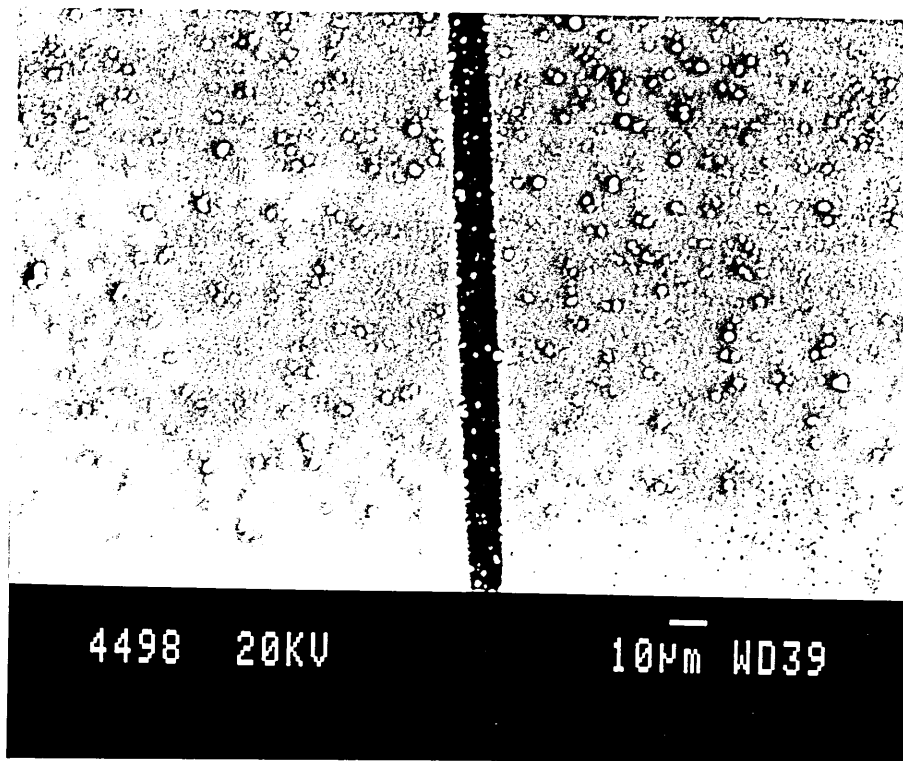
Fig. 5.4 SEM photograph of a sensor type 603
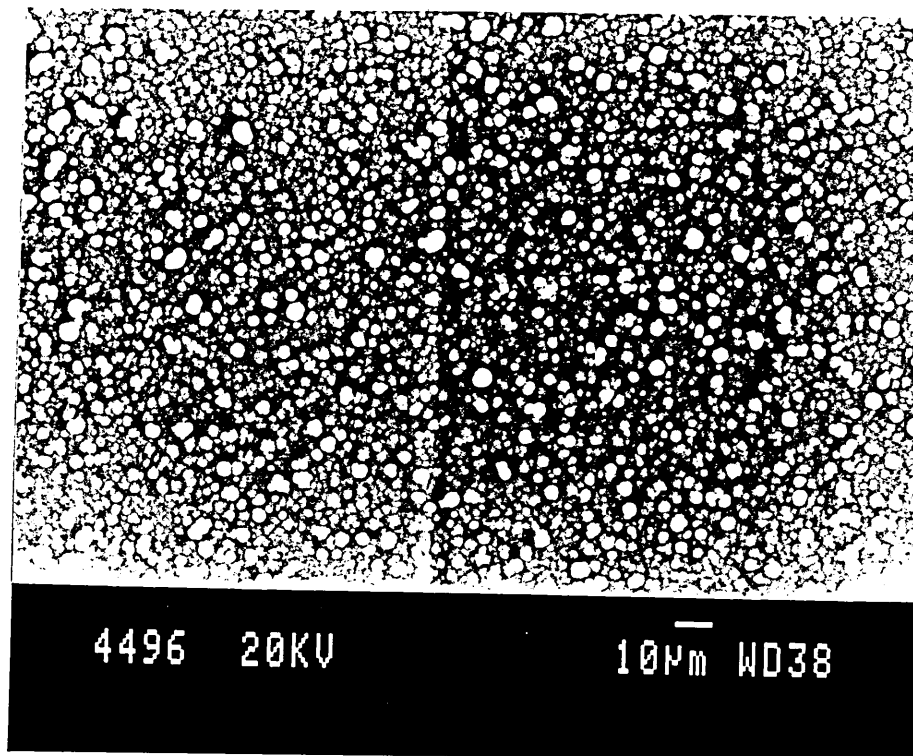
5.3 A comparison between potentiostatic and galvanostaic growth conditions relative to sensor response.

In this section a further variable to the electrochemical growth of films is examined. The last section demonstrated that potentiostatic growth conditions affect the nature and magnitude of sensor responses. Here, we investigate galvanostatic depostion (i.e. constant current) via the preparation of new films (Table 5.4) and comparison with potentiostatic films 600 and 603 (Table 5.3). The main aim was to determine the effect of the electrochemical technique in use (i.e. potentiostatic or galvanostatic growth) on sensor charateristics, concentrating on conductivity, film thickness, sensor response and short term stability (Table 5.5)

Table 5.4 Growth conditions and variables used during galvanosatic deposition.

Index number	Monomer conc. / mol dm^{-3}	Electrolyte conc. / mol dm^{-3}	Current passed / A	Growth period / seconds
604	0.15	0.10	0.080	120
605	0.15	0.10	0.080	60

Table 5.5 Resistance and film thickness measurements

Index number	Initial resistance / Ω	Resistance day ten / Ω	Resistance day twenty / Ω	Film thickness / microns(μm)
604	4.46	3.55	3.28	2.5
604	4.17	3.43	3.04	2.0
604	4.28	3.69	3.33	2.0
605	5.45	4.72	4.53	1.0
605	5.41	4.60	4.46	1.5
605	5.33	4.79	4.58	1.0

The results revealed that the conductivites are relatively high, with film thickness being considerably less than for films grown potentiostatically, although this may be relative to the amount of charge consumed during electrolysis. From the SEM study it appears that the films are uniform with even surfaces, leading to the assumption that the films are highly uniform and regular in their mode of growth.

The most significant result is the manner in which the films responded to the reference sample (Table 5.6 and Fig. 5.5) their mode of response being somewhat different from that of films deposited under potentiostatic conditions. The films grown galvanostatically show a rapid initial response to the analyte vapour, reaching an equilibrium value which is maintained (although the values do increase slightly during the course of the response). The potentiostatically deposited films respond in a slower manner maintaining an ever increasing response during the course of the sample acquisition. As expected the film deposited at a reduced growth potential type 605 has a higher overall output, this being due to the formation of a thinner film which is less dense and of lower mass than type 604.

143

Table 5.6 Responses to dry air and reference analyte with related standard deviations

Index number	Head position	Response to dry air / %	Response to reference analyte / %	Standard deviation to ref. analyte / %
600	1	0.05	0.72	0.04
600	2	0.01	0.73	0.04
600	3	0.00	0.66	0.17
603	4	0.05	1.72	0.11
603	5	0.05	1.80	0.09
603	6	0.05	1.64	0.11
604	7	-0.01	1.09	0.04
604	8	0.05	1.01	0.06
604	9	0.05	0.99	0.04
605	10	0.10	1.17	0.14
605	11	0.05	1.39	0.13
605	12	0.05	1.37	0.09

Fig. 5.5 Profile view of constant current/fixed potential sensor responses

Analysis : Sample (Avg) - Profile view

Sample

Class	CONSTANT CURRENT
Substance	1,2-PROPANDIOL/WATER
Sample	4/12/95 14:45(Template)
Method	N/A
Time	N/A
Calibrated	Some (or all) missing
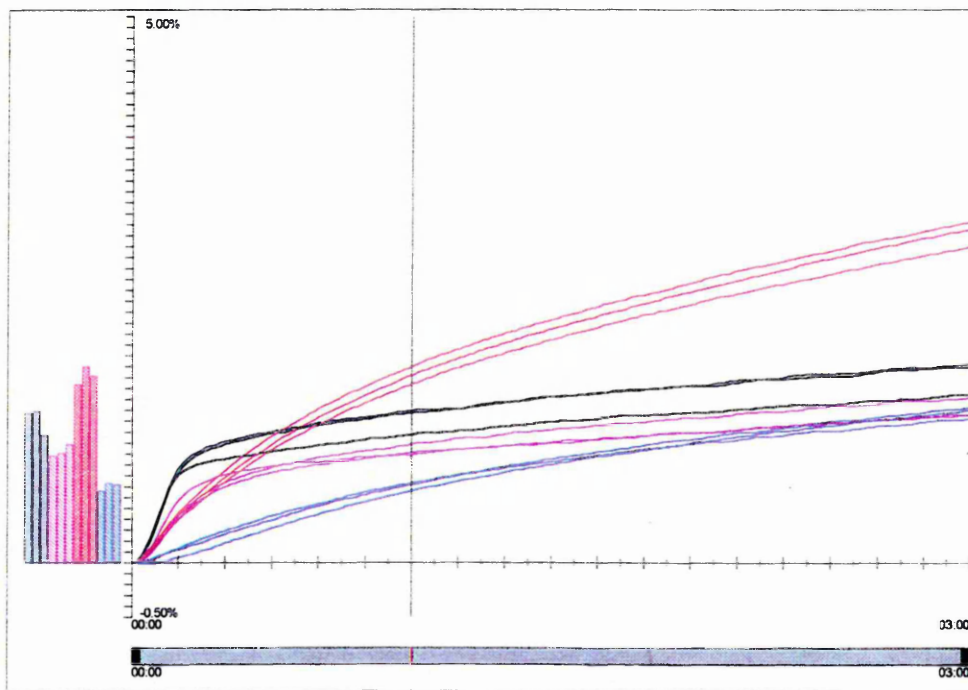
Cursor at   01:00

1.37%	Type 605		1.39%	Type 605		1.17%	Type 605		0.99%	Type 604
1.01%	Type 604		1.09%	Type 604		1.64%	Type 603		1.80%	Type 603
1.72%	Type 603		0.66%	Type 600		0.73%	Type 600		0.72%	Type 600

Sample Comments .
N/A

5.4 Summary of optimisation processes

The optimisation studies have clarified some of the characteristics which affect sensor performance and response. Some of the experimental parameters introduce significant changes in chemiresistor performance. This chapter has centred on the modification of an individual aqueous sensor type. Based upon comparative studies the results obtained can probably be applied to all aqueous sensor types. The study has shown that the polypyrrole system can be altered dramatically to vary the nature and level of response. The fundamental factors essential for these alterations are those mentioned in the introduction to this chapter (i.e. film thickness, morphology environmental stability and baseline resistance). The advantage of such variation being available with an individual sensor type is that an array could be constructed from only a few sensor types. If an individual sensor type was found to be particularly sensitive and discriminating for an analyte of interest, then a specific array containing a limited number of particularly effective sensors could be designed for that analyte type.

The information obtained for aqueous sensors was also compared directly with similar information for non-aqueous systems. This information has not been disclosed in this Section as it proved less significant in the context of multisensor array formation. Section 6.3 discloses the irreproducibility of chemiresistor analysis with non-aqueous systems. A significant discovery was the formation of galvanostatic films giving especially reproducible outputs to the standard reference analyte.

The bulk resistance of chemiresistors is known to be governed by the effectiveness of the interchain transport processes within the matrix (see section 1.8). The increase in resistance observed with increasing deposition potentials and growth periods follows from the increased level of overoxidation and structural disorder, hence lowering the effectiveness of this charge transport process leading to reduced conductivity. These disadvantages may be outweighed by an increase in the film porosity, allowing a greater degree of penetration of the sample analyte into the film bulk, producing an enhanced

146

output. This is due to the ability of the analyte to rapidly modulate the resistance of the film bulk rather than a surface interaction effect dominating the resistance change that is observed. An observed increase in porosity also has disadvantages as it can dramatically affect environmental stability of the chemiresistor in question and hence the reproducibility and life expectancy of the polymer film.

When determining the optimised state of a polymer chemiresistor a considerable number of factors have to be balanced carefully to provide a system with the properties that are desired. It may be the case that the level of output would have to be sacrificed for an increase in response reproducibility and sensor lifetime. The responses of individual sensor types may be varied considerably by altering the electrochemical deposition conditions between potentiostatic and galvanostatic growth.

Chapter 6 Analysis of chemiresistor response data

6.0 Introduction

The characteristic properties of conducting polymers are in many ways ideal for the formation of multisensor arrays. The films can be chemically tailored via control of either the monomer or electrolyte feedstock, or by variation in the electrodeposition protocol. The nature and type of counter ion has a pronounced effect on the physical and chemical properties of electrochemically deposited films, therefore allowing the formation of films with varied sensing characteristics. Films with broad overlapping sensitivities can be produced which exhibit reversible conductivity changes (via modulation in their molecular electronics), at room temperature, when exposed to analyte vapours. The corresponding, detectable resistance changes can then be processed.

The sensing phenomenon is rapidly reversible with the vapour being involved in an absorption-desorption process so that the films return to their initial state soon after exposure. However, some analytes can irreversibly damage the film structure, inhibiting further use as a sensor. The response kinetics are highly reproducible and allow the detection of volatiles in the ppm region[49,190,191].

The interactions occurring when certain polypyrrole sensors are exposed to simple vapours has been reported. Responses of the chemiresistors to these vapours can be interpreted in terms of conductivity changes caused by interactions between the p-type polypyrrole and the vapours. On exposure to electrophilic gases such as nitrogen dioxide the films exhibited an increase in conductivity. This interaction is enhancing the p-doped system by the extraction of electron-density away from the polymer matrix. It was found that nucleophilic gases such as ammonia have the reverse effect with an decrease in conductivity observed due to the donation of electron-density to the polymer matrix, thus reducing conduction pathways. The responses of polypyrrole films

148

to these simple vapours was easily explained and the nature and mechanism of response understood. As the nature of molecules exposed to conducting polymer sensors becomes more varied by means of their size, shape and structure, interactions occurring in the polymer to provide a response are likely to be more complex, probably involving numerous mechanisms[192-194].

To form an effective multisensor array it is important to understanding what characteristics are required to produce an effective chemiresistor. By considering the effect of electrochemical growth conditions, morphology, film thickness and baseline resistance the nature and amplitude of response can be altered (see Chapter 5). The experimental analysis in Chapter 6 was an attempt to determine what characteristics effect a variation in response to complex vapours and the possibility of exploiting these properties within a sensor array. The counter-ion incorporated into the polymer matrix performs a significant role in modifying the sensor response characteristics. From the analysis of response data it is hoped to determine the most effective counter-ions for use in multisensor array systems. Other properties are also important in governing the nature of the response, (i.e. the nature of the solvent system used during electrochemical deposition, the oxidation level of the film, film stability and the mass of analyte absorbed and desorbed in the sensing process)[190].

The response produced by the action of the vapour with the polymer matrix is thought to occur via an number of complex mechanisms. Some mechanisms dominate in responses to certain vapours (i.e. water causes a swelling of the polymer matrix). The following mechanisms have been discussed as potential causes of conductivity change within conducting polymer films during the sensing phenomena.

a.   Physical swelling of the polymer matrix caused by a change in state

b.   The generation and removal of charge carriers in the polymer film

c.   Modification of the charge carrier mobility

d. Interactions with the incorporated counter ion and solvent changing the polymer state

e. Analyte associating with the solvent present altering interchain electron transfer processes

f. Change in the charge transfer rate between the polymer film and the supporting metal contact.

These mechanisms are complex and the interactions between the different polymer matrices (sensor types) and organic vapours require detailed analysis of response data to determine underlying trends. This information may provide further scientific understanding into the different processes involved in gas sensing using multisensor arrays of conducting polymer films.

A further consideration with more complex organic vapours is the nature of the molecular interaction at the polymer interface. The nature of these interactions depends primarily on the type of functionality present in the analyte molecule. It has already been acknowledged that the size, shape and position of functionality play a more significant role in molecular recognition than the nature of the functionality. The molecular interactions (Fig. 6.1) occurring may be a minor in the context of an overall response, but should not be ignored, as the number of interactions occurring increases the sensor may becomes a more selective sensing device[191].

The physical properties of the vapour to be detected also determine the level of response which may be expected. Vapours which have a low molecular weight, high volatility, may be expected to give significant outputs whereas vapours with the reverse properties would be expected to show significantly lower response outputs.

150

Fig 6.1 Molecular interactions

Interaction Type

Ionic

Ionic-dipole

Dipole-dipole(H-bonding)

Ion induction

Dipole induction

Dispersion

151
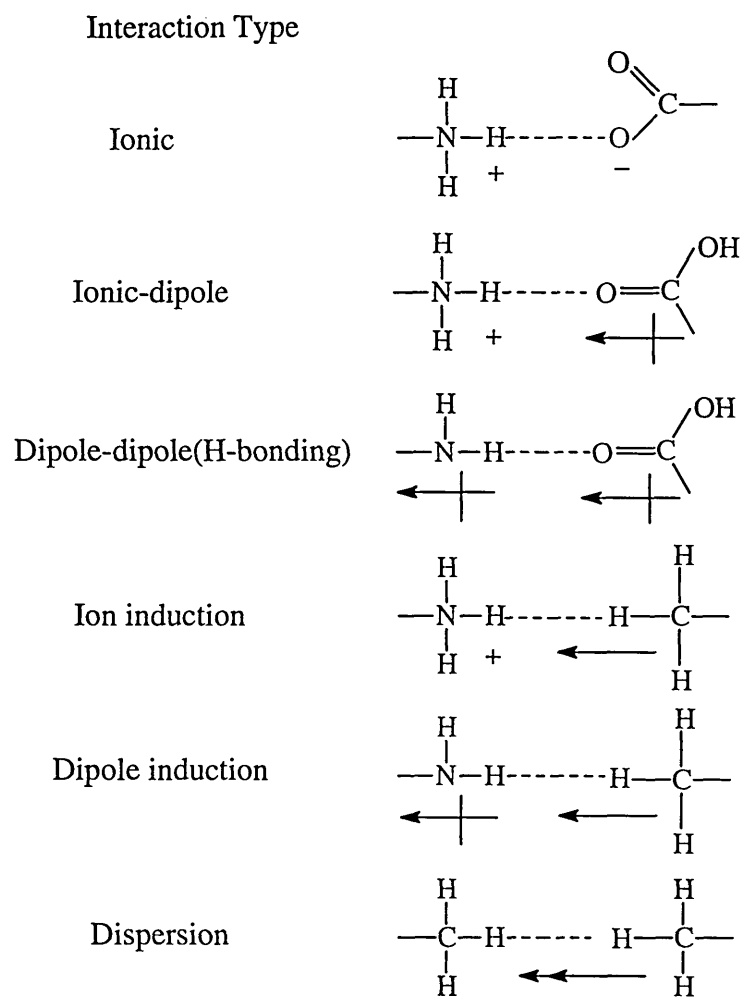
6.1 The formation of effective multisensor arrays

The characteristic properties of effective chemiresistors have already been discussed (see Section 4.0). Some systems have shown promise as conducting polymer films but failed to deliver as effective sensing devices. From an experimental study it became clear that certain anions led to poor chemiresistors when incorporated during electrochemical deposition. These included anions such as perchlorate, tetrafluoroborate, trifluoroacetate, trifluoromethanesulphonate and nitrate, where results were poor for a variety of reasons. The most common reason was environmental instability (see Section 4.7 and Appendix 2) leading to decreasing conductivity of the pre-formed films. This considerably reduced the reproducibility of the results obtained and also the sensors drifted dramatically from the calibration conditions. Another type of failure led to repeated inconsistencies in the nature of sensing results obtained. Literature sources have shown that certain anions especially tetrafluoroborate can decompose, this being perhaps a possible further reason for failure[195]. The effect of sensor failure with a nitrate based device during sensing is shown (Fig. 6.2). The polypyrrole/nitrate sensor that failed shows a sizeable, rapid response which gradually decreases during the sampling procedure. The response is unlike the other sensor types which showed gradual changes in their response to the sample analyte. After the sample analysis was completed the sensor was removed from the array as its resistance had increased dramatically as a result of exposure to the sample analyte

Fig. 3.3 The effect of increasing irreversibility on the shape of a cyclic voltammogram[(147)]
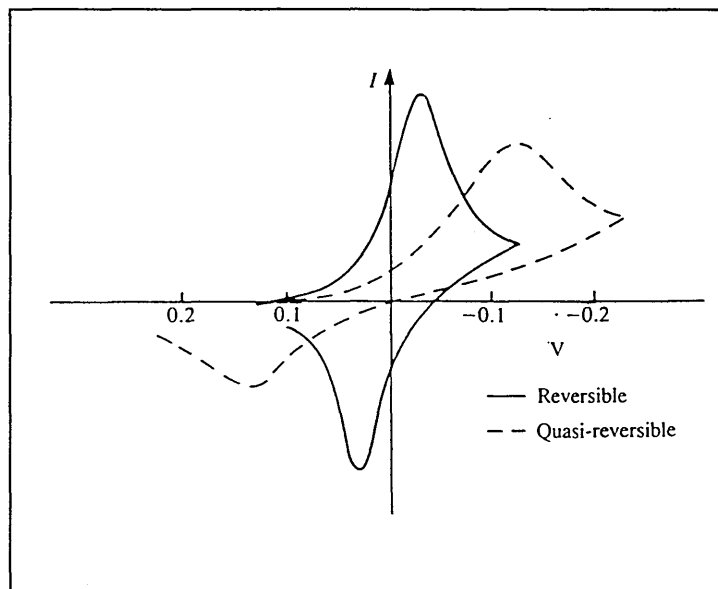
6.2 Response data from polypyrrole chemiresistors doped with aromatic sulphonate anions

The formation of a series of polypyrrole chemiresistors incorporating aromatic dopants was outlined in Section 4.1. The conditions described there were used to prepare a series of sensor types for inclusion into a multisensor array. The characteristic responses of these sensor types had not previously been investigated so, in an attempt to understand the mechanism of sensor response, the array was exposed to a series of individual organic vapours. The investigation involved acquiring information on individual sensor responses to a fixed quantity of analyte, within a controlled environment over an established time period. The array consisted of a series of six sensor types, electrochemically deposited in an aqueous environment, together with the corresponding sensor deposited in non-aqueous conditions to complete the array of twelve sensors (Table 6.1). From this combination of chemiresistors a direct comparative evaluation of sensor reproducibility and output between aqueous/non-aqueous sensors was performed, although its effectiveness was limited due to the variation in electrochemical deposition conditions.

The instrument used was a D-model NOSE. The array was prepared and placed in the sensor head, and the instrument was calibrated using a continuous flow of dry air. The sensors were exposed to one gram of a single, pure, organic analyte and template responses were recorded. Between each template an air test was completed to ensure that there had been no sensor drift or poisoning effect from the analyte. The analytes used covered a range of functionalites and molecular weights (Table 6.2). The experimental parameters used in data gathering are shown and data was obtained in the temperature range 18-21°C. The percentage responses and comparative standard deviations for the template responses, are outlined in Table 6.3. All the sample analysis data was then tabulated and statistical analysis performed using multiple discriminate analysis (Fig. 6.3)

Experimental parameters.

Vessel purge   0 minutes

Equilibration time   7 minutes

Head purge   7 minutes

Sample time   4 minutes

Reference gas   dry air

(The templates were formed by concurrent repetition of this process in triplicate)

Table 6.1 Composition of multisensor array including resistance data.

Head Position	Index Number	Sensor Type	Initial resistance / Ω	Resistance four months / Ω
1	283	PPy/BzSA (Na)/H_2O	8.62	15.92
2	513	PPy/4-ABzSA (Na)/H_2O	9.96	15.09
3	304	PPy/1,3-BzDSA(2Na)/H_2O	17.48	34.64
4	301	PPy/DDBzSA(Na)/H_2O	11.92	14.50
5	300	PPy/2-NapSA(Na)/H_2O	13.67	18.28
6	305	PPy/1,5-NapDSA(2Na)/H_2O	20.92	35.04
7	299	PPy/Bu_4N-BzS/CH_3CN	14.90	26.98
8	522	PPy/Bu_4N-4-ABzS/CH_3CN	32.89	39.03
9	520	PPy/$(Bu_4N)_2$ 1,3-BzDS/CH_3CN	13.69	54.26
10	518	PPy/Bu_4N DDBzS/CH_3CN	35.25	48.32
11	519	PPy/Bu_4N-2-NapS/CH_3CN	7.05	8.43
12	521	PPy/$(Bu_4N)_2$ 1,5-NapDS/CH_3CN	23.41	*

* - Sensor 521 failed after two weeks of sample analysis.

155

Table 6.2 Reference vapours

Reference vapours	Abbreviation	Molecular weight	Polarity / (p[1])	Dipole Moment / (μ)	Boiling Pt. / °C
Propylene glycol / Water*	PG/ HO	18.02	10.2	1.85	100.00
Methanol	MeOH	32.04	5.1	1.70	64.55
Ethanol	EtOH	46.07	4.3	1.69	78.29
Acetone	AcT	58.08	5.1	2.88	56.07
Diacetal	DiA	86.09	-	-	88.0
Propionaldehyde	PropA	58.08	-	-	48.8
n-Butyl acetate	BuA	116.16	-	1.86	124-26
Ethyl acetate	EtA	88.11	4.4	1.78	77.11
Diethyl ether	DiEt	74.12	2.8	1.15	34.49
Tetrahydrofuran	THF	72.11	4.0	1.75	65.97
Toluene	Tol	92.14	2.4	0.37	110.63
Pyridine	Pyr	79.10	5.3	2.21	115.25
Chloroform	CCl_4	119.38	4.1	1.04	61.18
Acetonitrile	CH_3CN	41.05	5.8	3.92	81.60
Camphor	Cam	152.24	-	-	(s)
Dimethyl sulphoxide	DMSO	78.13	7.2	3.96	189.0

* values for water quoted (PG/Water mix consisted of 75grms PG : 25grms Water)

The template responses tabulated (Table 6.3) show that the most significant outputs are shown to the PG/Water reference analyte. This level of output by comparison to the

156

remaining organic reference analytes highlights the need for a tight control on humidity levels during sampling. It also shows that the NOSE technology responds to non-odifirous sample analytes (within the context of a biological system). The standard deviations displayed in the template formed for PG/Water indicates that the responses obtained were reasonably reproducible, however, this was not the case for the responses to individual organic analytes.

The standard deviations for some of the analytes tested are significant. The formation of sample templates from concurrent individual sample analysis showed that the response level would either increase or decrease during individual tests used to form the template. This led to some of the more significant standard deviations which are observed. It may be possible to improve on these values by increasing the purge time between analysis of subsequent samples, allowing the sensors a greater recovery time and minimising sensor drift during repeated analysis.

A significant reduction in the film thickness and mass of polymeric material deposited may also contribute to a reduction in the recovery period required. The tabulated results indicate that the solvent system from which conducting polymer films are deposited influences the level and nature of response to an analyte vapour. From the pattern of template responses it has emerged that films deposited in non-aqueous media give less reproducible responses, (i.e. have higher relative standard deviations). This may be caused by interactions between trapped solvent molecules in the polymer film with the analyte vapour.

Exposure of polymer films to organic analytes causes a swelling of the film. This process probably predominates in the initial stages of the chemiresistors' response to an analyte vapour. The swelling effect probably contributes significantly to sensor response (particularly for small, volatile molecules) more so than the other forms listed in Section 6.0. The extent of this process is governed by the rate at which the polymer swells and the extent of penetration of the analyte into the polymer matrix. The process

occurs within the first seconds of exposure and appears to be a solvent-type effect, which was first noticed during exposure to methanol. The swelling effect is limited by the analyte's size, shape and ability to penetrate into the film matrix. The film thickness also has a bearing on the swelling effect, with the possibility of two processes taking place; first and foremost a surface interaction, but then followed by a bulk interaction depending on the analyte and film morphology and thickness. These properties are governed by the electrochemical deposition conditions and the nature of the counter-ion incorporated into the film. The type of counter-ion incorporated has a bearing on the properties such as morphology and porosity that govern analyte interaction. The control and optimisation of these properties will allow enhanced sensitivity and increased discriminatory ability. The effect of swelling is particularly noticeable using the reference analyte PG/Water, methanol, ethanol or acetone, possibly due to their molecular size and shape and the ease in which they can penetrate the polymer matrix. As the molecular size, shape and volatility of a molecule is reduced so the level of observed response is also reduced. The ability of the outer analyte to penetrate the polymer bulk and effect a response is less, therefore the outputs observed are lower. In some templates the levels can be compared with the background noise seen during dry air tests. The ability of an analyte to enter into the polymer matrix governs the nature and level of response that will be observed. Solvent based molecules effect an initial swelling based interaction which is then enhanced by some of the secondary mechanisms listed (see Fig. 6.1), while larger molecules are unable to interact to this extent and the response is based upon surface interactions rather than those occurring within the film bulk.

The levels of response varied, with the most important factors seeming to be analyte volatility, molecular size and shape, the nature of the incorporated anion and the film structure. The number of charges positioned on the counter-ion appears to have a significant effect also in that the number of sulphonate groups present on a counter-ion increases the level of response observed. This may be related to slight changes in the

morphology of a chemiresistor the increase in charge present leading to a slightly more porous structure and allowing slightly deeper penetration by the organic analyte.

Statistical analysis performed on the data obtained from each run was used to form the tabulated template data, each analyte having three sets of data associated with it. Multiple discriminate analysis underlines the effectiveness of the NOSE to discriminate between analytes of low molecular weight and high volatility. The clusters observed for the reference analyte, methanol, ethanol, and acetone are clearly visible. The grouping of analytes with increased molecular weight, higher boiling points and reduced volatility, are less well defined and clustered, within a small area. Expansion of this cluster group shows that despite being closely clustered the three individual runs associated with each template are within close proximity in most cases.

Table 6.3 Responses and standard deviations to organic analytes for polypyrrole chemoresistors incorporating aromatic dopants

	283	513	304	301	300	305	299	522	520	518	519	521
PG/Water	1.50	0.77	1.88	0.01	0.04	1.89	1.10	0.74	4.37	1.60	0.25	0.97
σ	0.07	0.08	0.13	0.03	0.01	0.13	0.06	0.03	0.41	0.12	0.03	0.10
Methanol	0.14	-0.21	-0.55	0.40	-0.08	-0.47	4.61	0.81	9.94	1.94	5.83	4.52
σ	0.22	0.17	0.18	0.27	0.11	0.14	4.91	0.82	6.31	1.15	6.49	3.39
Ethanol	-0.24	-0.13	-0.21	-0.02	-0.05	-0.19	-0.12	-0.10	-0.05	-0.27	-0.08	-0.13
σ	0.13	0.11	0.28	0.03	0.05	0.21	0.09	0.05	0.17	0.34	0.08	0.10
Acetone	-0.77	-0.46	-0.53	-0.05	-0.18	-0.50	-0.56	-0.37	-1.23	-0.12	-0.46	-0.67
σ	0.24	0.05	0.07	0.05	0.03	0.08	0.51	0.23	0.67	0.44	0.26	0.67
Diacetyl	0.00	-0.03	-0.05	-0.07	-0.05	-0.06	0.08	0.02	0.15	0.00	-0.03	-
σ	0.00	0.06	0.06	0.03	0.00	0.06	0.03	0.03	0.04	0.04	0.03	-
Propanaldehyde	-0.16	-0.12	-0.20	0.00	-0.06	-0.18	-0.03	-0.09	-0.04	0.33	-0.04	-0.08
σ	0.05	0.03	0.05	0.05	0.01	0.05	0.08	0.03	0.08	0.35	0.06	0.05
n-Butyl acetate	0.08	-0.01	-0.02	-0.03	-0.03	-0.05	0.15	0.06	0.27	0.06	-0.05	-
σ	0.03	0.03	0.08	0.06	0.06	0.06	0.06	0.03	0.11	0.03	0.05	-
Ethyl acetate	0.03	0.05	0.10	0.01	0.02	0.10	-0.15	-0.05	-0.79	-0.03	-0.01	-0.07
σ	0.14	0.14	0.18	0.05	0.06	0.17	0.10	0.05	0.76	0.22	0.09	0.03

	283	513	304	301	300	305	299	522	520	518	519
Diethyl ether	0.10	0.03	0.05	0.02	-0.02	0.01	0.15	0.10	0.28	0.12	0.03
σ	0.00	0.03	0.00	0.03	0.03	0.03	0.04	0.00	0.02	0.03	0.06
THF	-0.17	-0.09	-0.17	-0.08	-0.06	-0.12	-0.08	-0.11	-0.20	-0.19	-0.11
σ	0.06	0.08	0.12	0.06	0.08	0.08	0.03	0.01	0.05	0.05	0.04
Toluene	0.13	0.11	0.15	-0.02	0.04	0.11	0.05	0.06	0.00	-0.04	0.04
σ	0.18	0.17	0.20	0.03	0.09	0.20	0.13	0.08	0.17	0.06	0.09
Pyridine	-0.05	-0.03	-0.07	-0.05	-0.05	-0.03	0.00	-0.02	0.02	0.12	-0.03
σ	0.00	0.03	0.03	0.00	0.00	0.03	0.04	0.03	0.03	0.03	0.06
Chloroform	-0.05	-0.05	-0.10	-0.06	-0.03	-0.07	-0.04	-0.02	-0.03	-0.02	-0.07
σ	0.00	0.00	0.00	0.03	0.03	0.04	0.01	0.02	0.08	0.06	0.03
Acetonitrile	-0.10	-0.04	-0.10	-0.01	-0.02	-0.09	-0.02	-0.02	-0.24	-0.07	-0.07
σ	0.05	0.01	0.06	0.01	0.03	0.03	0.10	0.06	0.20	0.06	0.03
Camphor	-0.02	-0.04	-0.10	-0.06	-0.05	-0.05	0.15	0.08	0.30	0.12	-0.05
σ	0.03	0.01	0.00	0.03	0.00	0.04	0.05	0.03	0.07	0.03	0.05
DMSO	-0.07	-0.05	-0.05	-0.03	-0.02	-0.05	-0.08	-0.08	-0.20	-0.12	-0.06
σ	0.03	0.05	0.00	0.03	0.03	0.03	0.03	0.06	0.05	0.03	0.01

Fig 6.3 MDA plot of polypyrrole chemiresistor responses

162
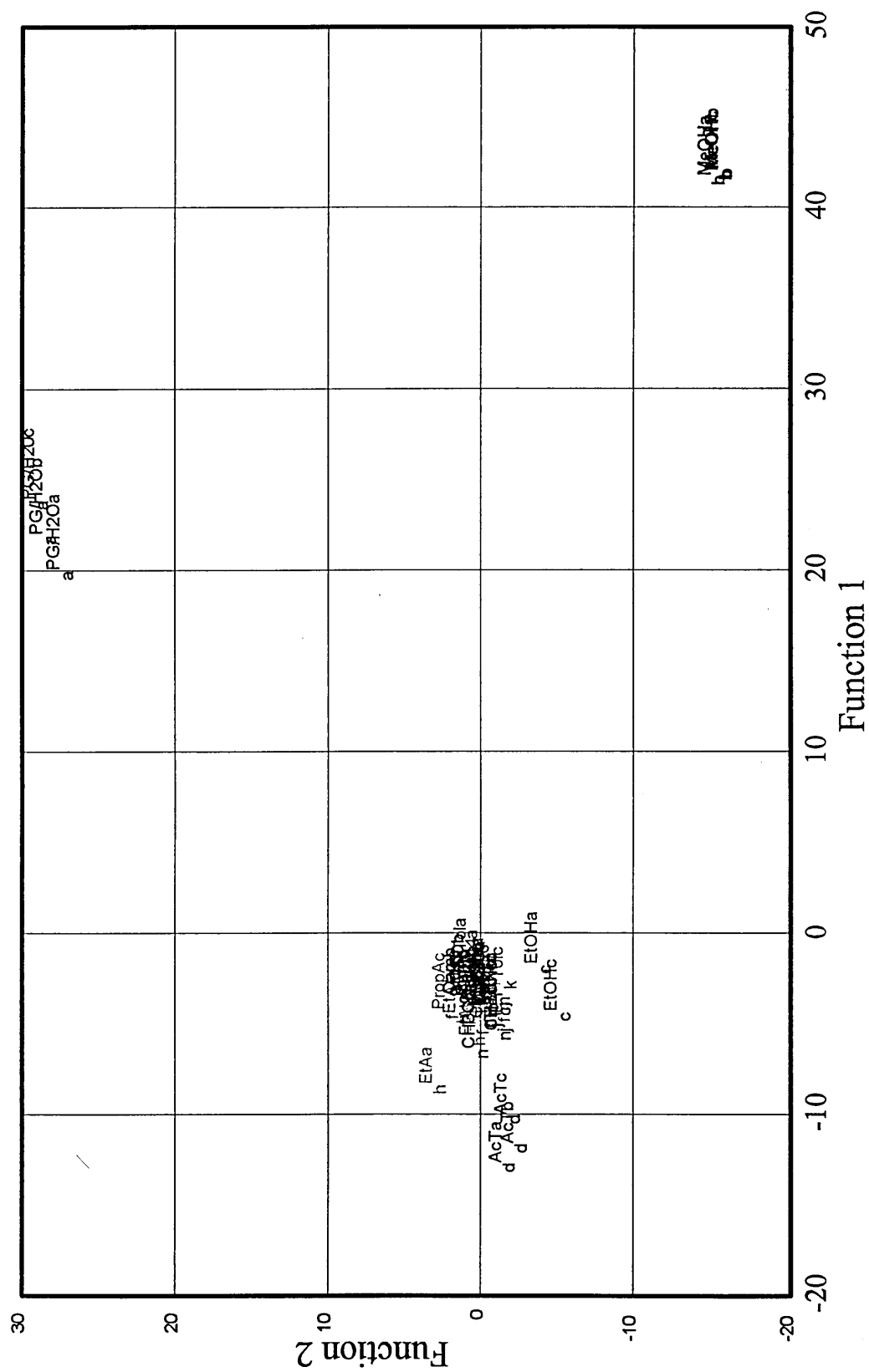
Fig. 6.3a Enhanced MDA plot of polypyrrole chemiresistor responses

Function 1

Function 2

163
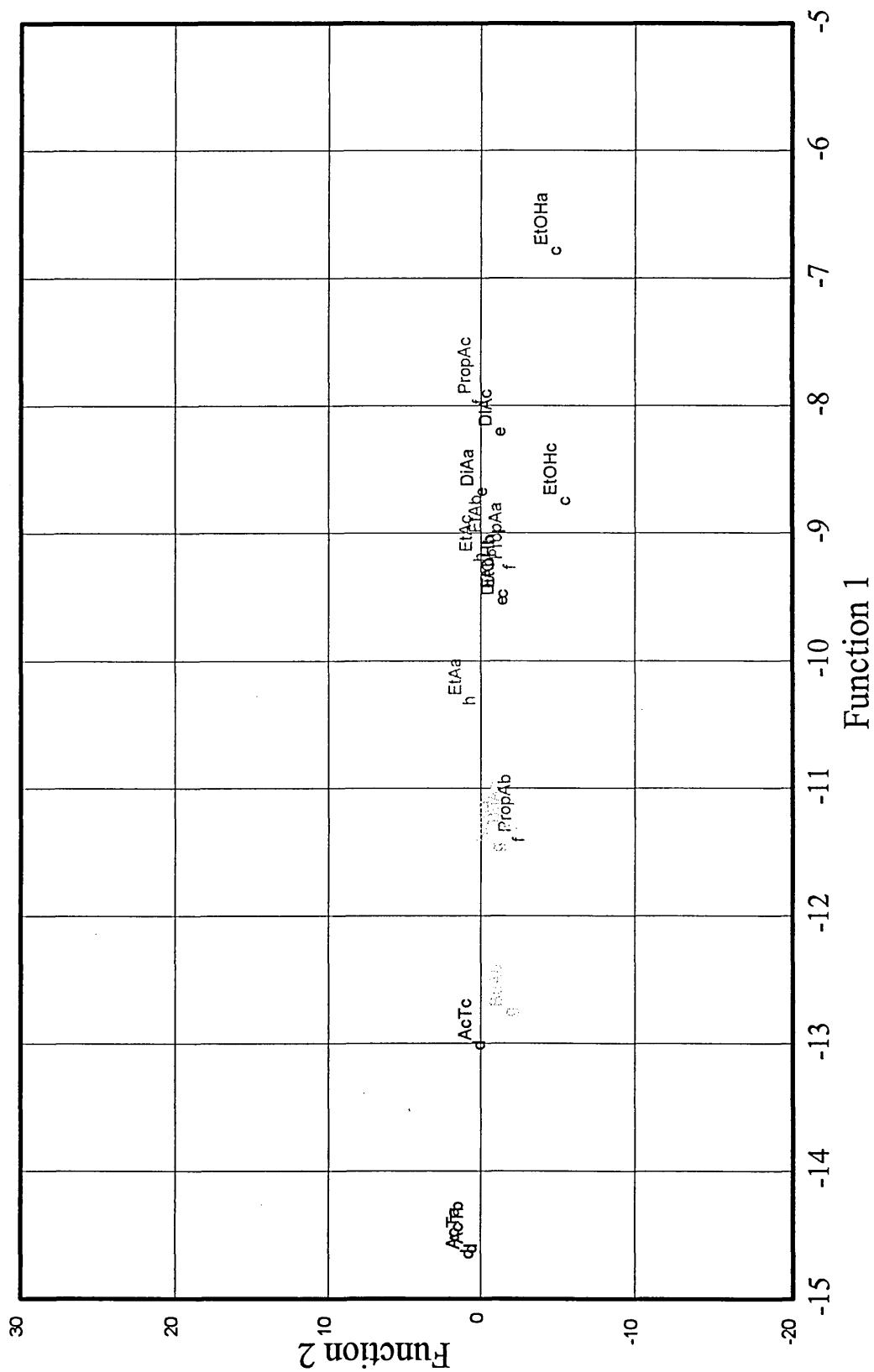
Fig 6.3b Enhanced MDA plot of polypyrrole chemiresistor responses

164
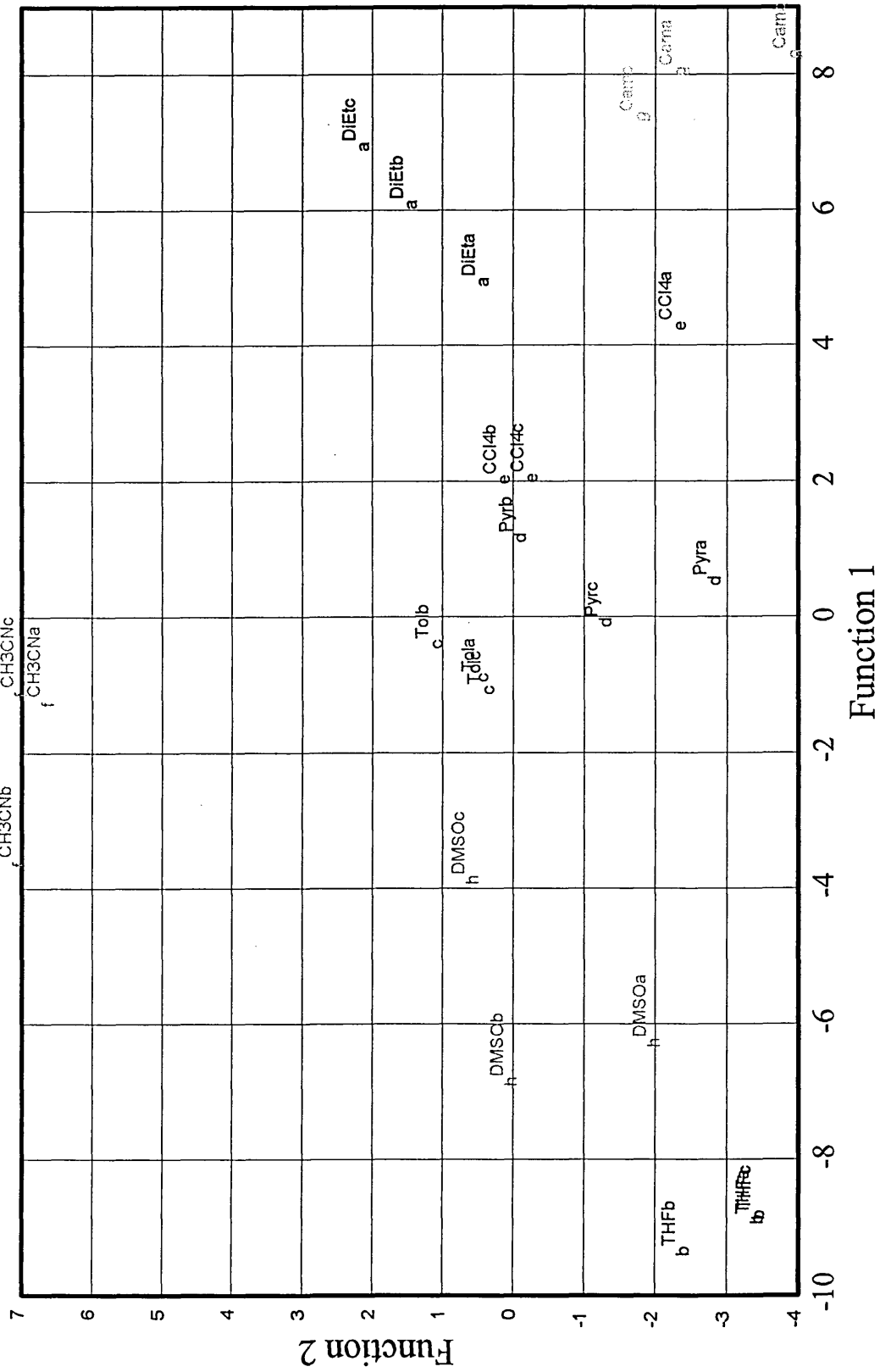
6.3 Determination of the effectiveness of chemiresistors deposited in aqueous conditions.

Further to the initial series of chemiresistors which were tested another set of twelve sensors was combined to produce a multisensor array (Table. 6.4). The common factor in this group is the method of electrochemical deposition, all the systems being deposited in aqueous conditions. Together with the information obtained from the first array this data was to provide information about the overall effectiveness of certain sensor types and the effect of the counter-ion on response.

Table 6.4 Composition of multisensor array including resistance data

Head Number	Index number	Sensor	Initial resistance / Ω	Six month resistance / Ω
1	540	PPy/3-SuBzA(Na)/H$_2$O	4.15	5.10
2	541	PPy/5-SuIA(Na)/H$_2$O	7.24	8.62
3	542	PPy/DM-5-SuI(Na)/H$_2$O	7.06	7.96
4	543	PPy/n-B-SuPM(Na)/H$_2$O	30.28	42.35
5	545	PPy/DOSS(Na)/H$_2$O	3.76	5.47
6	546	PPy/4-OcBzSA(Na)/H$_2$O	6.06	6.82
7	547	PPy/2-M-2PSA(Na)/H$_2$O	55.35	92.34
8	257	PPy/BuSA(Na)/H$_2$O	19.88	23.26
9	302	PPy/DDS(Na)/H$_2$O	3.88	4.35
10	514	PPy/3-NBzSA(Na)/H$_2$O	8.04	8.57
11	265	PPy/TEATS/H$_2$O	5.39	6.44
12	263	PPy/pTSA(Na)/H$_2$O	20.46	24.41

A series of organic analytes was tested using the same sampling procedures adopted in the initial study. The number of analytes was reduced, extensive testing of higher molecular weight, low volatility analytes was not felt necessary due to the responses obtained in Section 6.1.

The results again showed that the NOSE produced the most significant response to the samples with low molecular weight and high volatility. The instruments ability to discriminate between water and methanol was clear when using MDA (Table 6.5). As the molecular weights increased the outputs observed were again reduced and respective template responses were grouped together. With the expansion of this group it can be observed that the data manipulation techniques had succeeded in sub-grouping the individual analytes (Fig. 6.4 and 6.4a).

The responses observed in the tabulated results (Table 6.5) show that the discrimination between sample analytes was being performed by certain sensor types (i.e. 257, 263, 264, 543 and 547). From combined analysis of the individual sensors used in the organic analyte analysis certain trends emerged. Sensor systems incorporating counter-ions with electron donating properties, or containing electron donating groups effected larger outputs and were more effective discriminators. Films containing counter-ions with electron with-drawing groups showed less significant outputs and were poor discriminators (i.e. 540, 541 and 542). Systems which possessed a porous, disordered structure also allowed deeper penetration of the sample analyte to effect more significant responses than those films with tightly packed, more ordered structures (i.e. 300, 301).

Table 6.5 Responses and standard deviations to organic analytes for a series of polypyrrole chemoresistors

	257	263	264	302	540	541	542	543	545	546	547
PG/Water	2.77	0.96	1.30	0.16	0.22	0.28	0.73	3.54	0.00	0.25	3.34
σ	0.08	0.08	0.08	0.03	0.06	0.03	0.05	0.10	0.04	0.03	0.09
Methanol	3.36	0.50	0.56	2.01	0.02	0.00	0.17	1.64	3.22	1.04	6.78
σ	0.80	0.21	0.19	1.60	0.03	0.00	0.06	0.51	2.05	0.46	2.90
Ethanol	0.25	-0.02	0.01	0.03	-0.01	0.00	-0.02	0.12	0.03	0.00	0.20
σ	0.05	0.03	0.03	0.03	0.01	0.00	0.03	0.03	0.03	0.05	0.05
Acetone	0.12	-0.01	0.00	0.02	-0.02	-0.02	0.00	0.07	0.14	0.03	0.09
σ	0.03	0.03	0.00	0.03	0.0	0.03	0.00	0.03	0.05	0.03	0.01
Propanaldehyde	0.97	0.01	0.14	0.02	-0.10	0.00	-0.01	0.91	0.19	0.02	0.91
σ	0.03	0.03	0.06	0.10	0.03	0.00	0.01	0.03	0.13	0.03	0.06
Ethyl acetate	0.16	-0.01	-0.02	-0.03	0.00	-0.01	-0.03	0.09	0.04	0.00	0.10
σ	0.03	0.01	0.03	0.03	0.00	0.03	0.03	0.01	0.05	0.00	0.00
Diethyl ether	0.34	0.00	0.03	0.00	0.00	0.05	-0.02	0.27	0.03	-0.02	0.30
σ	0.15	0.00	0.03	0.24	0.00	0.05	0.03	0.13	0.03	0.03	0.11
Toluene	0.66	0.03	0.11	-0.09	0.01	-0.01	0.02	0.59	0.00	-0.02	0.58
σ	0.34	0.06	0.14	0.05	0.03	0.03	0.03	0.28	0.06	0.03	0.38

Fig 6.4 MDA plot of polypyrrole chemiresistor responses

168

Fig. 6.4a Enhanced MDA plot of polypyrrole chemiresistor responses

169
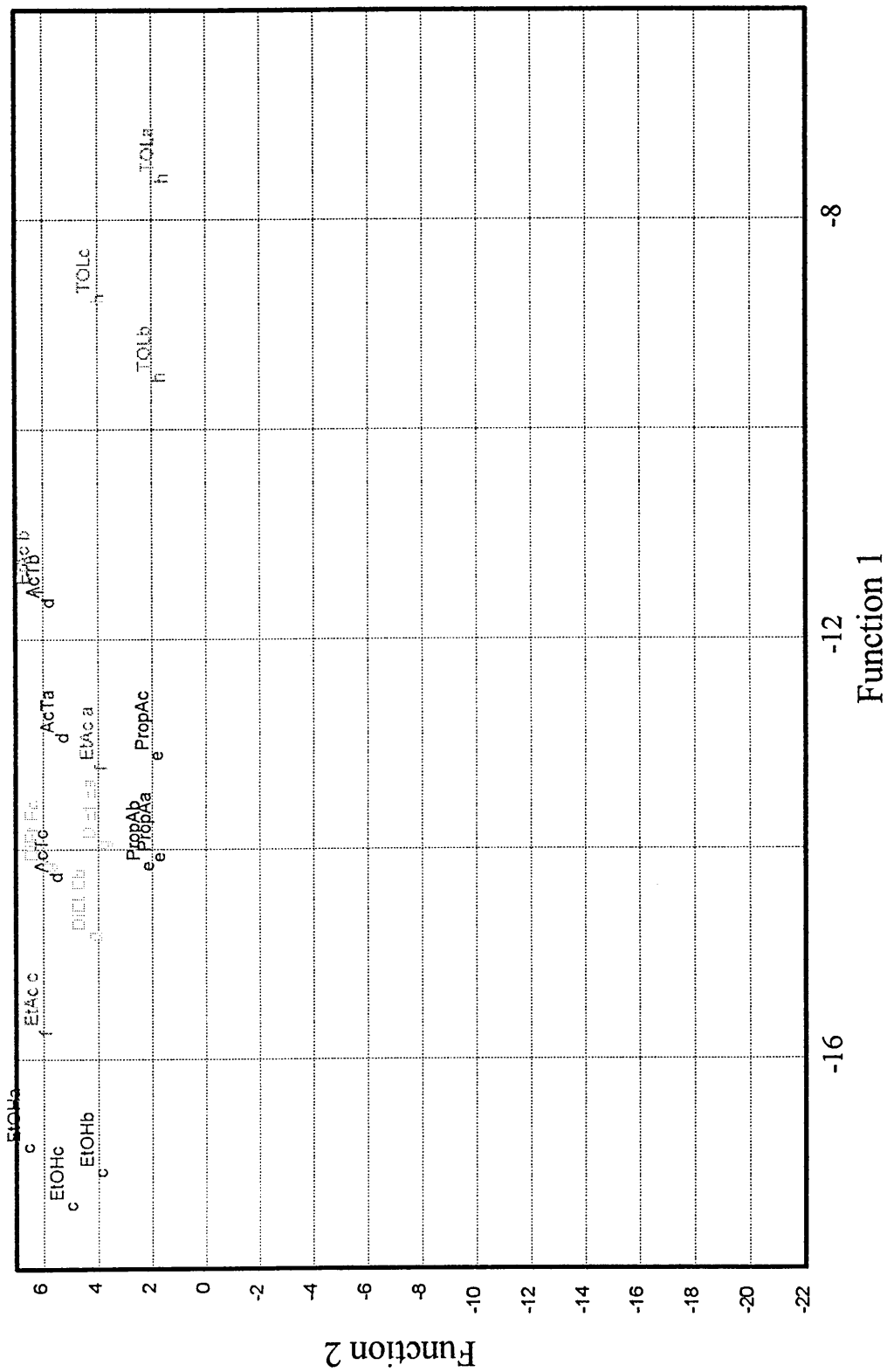
6.4 Summary of analysis results

The effects observed during the routine exposure of organic analytes to the sensors developed during the project are based on a variety of chemical and physical effects. The predominant process which is thought to occur is the physical effect of film swelling which in turn alters the films' conduction pathways (via modulation of the molecular electronics) thus effecting a response. The level of swelling which occurs is primarily dependent on the film's structure i.e. the level of porosity, the film thickness. The molecular size and structure and the volatility of the sample analyte also contribute to the level of response observed. The ease with which a sample analyte can alter the bulk film conductivity will determine the nature and level of the output observed. Analytes which are only able to effect a surface interaction with the chemiresistor, due to their size or structure, will only exhibit limited outputs in terms of response.

The optimisation of chemiresistors, as outlined in Chapter 5, will enable significant improvements to be made in the overall sensing properties of chemiresistors. Output levels and increased discriminatory ability may be improved via the optimisation of properties such as film thickness, porosity, dopant levels, minimisation of polymer chain irregularities, resistance level, increasing charge to volume ratio (of counter-ion units within the polymer matrix) and controlled deposition conditions. The translation of the improvements shown in Chapter 5 to the chemiresistors used in these multisensor arrays should improve their ability to differentiate between individual sample analytes. Reduction in film thickness and mass of deposited polymer will also reduce sampling time, as the films will return to equilibrium more rapidly.

The analysis work has highlighted trends in the response patterns observed for certain categories of chemiresistor From these emerging patterns the formation of more effective sensing devices will become a reality. The analysis study also showed that the multisensor arrays were not as effective at differentiating between individual sample analytes as had been expected. As analyte molecular weights increased and volatility

decreased the instrument became less able to distinguish between the analytes that it was exposed to. Combined with the minimal responses which were obtained for non-polar analytes the instrument's effectiveness is at present limited. Tight control of the environmental conditions in which the instrument operates, predominantly temperature and humidity, are essential This is shown clearly by the significant outputs obtained from the analysis of the reference analyte. It was demonstrated that the conducting polymer based devices are particularly sensitive to the presence of water, hence the use of dry air in the purging system of the NOSE. The analysis of aqueous sample analytes is hindered by the apparent masking effect of water in the sample upon the conducting polymers. This further problem limits the instrument's sampling potential, but industrially based trials have shown it to be effective in certain types of analysis. Improvements in the processing of resistance changes from the chemiresistors in arrays have been achieved by enhancement using signal processing techniques (operational amplifiers) and mathematical algorithms in the latest model. This has been effective in providing better discrimination of sample analytes.

Chapter 7 Conclusions and further work

7.0 Introduction

The research areas investigated during this PhD have been developed and applied directly to industrial production of the current Neotronics e-NOSE 4000. The further development of sensor types having broad ranging sensitivities and improved stability has led to a greater variety of chemiresistors available for the fabrication of multisensor arrays. The understanding of fundamental characteristics which affect the sensing properties of conducting polymer chemiresistors has led to the optimisation of the sensors enclosed within this document to considerably improve their overall performance. The project had a variety of initial aims (Section 1.9) which have been researched and have enabled useful conclusions to be draw. A comprehensive study was performed on the development of chemiresistors based upon polypyrrole; a wide variety of parameters were investigated providing information on the characteristics that an ideal conducting polymer chemiresistor should have (Section 4.0). Polypyrrole films were deposited in a variety of media and the sensing properties of aqueous/non-aqueous polymer system were compared. The formation conducting polymer films using other monomers was investigated although this did not prove as successful as first envisaged. The brief analytical study into the effectiveness of the electronic nose as a sensing device raised some series questions and also highlighted some instrumental limitations. The following discussion highlights some of the more significant positive and negative aspects of the results obtained during the course of this research.

172

7.1 Developments for the improvement of conducting polymer based multisensor arrays

The technology regarding the use of conducting polymers as sensing materials is still in its comparative infancy, although advances and developments have been significant during the past decade. As a result of our own experimental work the following progress (and enhanced understanding) has been made regarding the formation of microelectronic conducting polymer chemiresistors for inclusion in multisensor arrays.

1. The range of chemiresistor devices has been increased significantly (see Chapter 4) from the initial study by *Bartlett et al*[49]. These have included sensor types based upon the inclusion of alkyl and aryl sulphonates, (including aromatic dyes) as the dopant species within the polymer films. These sensors have exhibited the properties expected of devices which are suitable for array type sensing. The research has been effective in identifying systems which are less compatible with the technology (predominantly due to poor environmental stability).

2. The implications of both physical and chemical parameters which affect sensor performance and response have been investigated. The advances made have led to the optimisation of the sensor types (see Chapter 5) produced within the experimental section, considerably improving their outputs and stability. The work also led to the realisation that an individual sensor type could produce more than one form of chemiresistor as the nature of the response output can be varied dramatically by variation in the electrodeposition protocols. The physical parameters which proved most significant were the morphology, structural order, porosity, electrochemical deposition technique, film thickness, oxidation level, level of structural disorder, environmental stability and baseline resistance.

3. The nature of the counter ions incorporated into polymer films during the electrochemical deposition process affected the properties and response characteristics observed (see Chapter 6). From the data obtained it was apparent that there were underlying trends with certain types of counter-ion providing different

levels of response. The nature of the counter-ion was also found to be closely related to the environmental stability exhibited by the films as follows.

a. The presence of electron donating groups (-CH$_3$, -OCH$_3$)on aromatic ring systems enhances the response observed. It is also noted that alkyl and aromatic systems (i.e. benzene and naphthalene containing one or more sulphonic acid functionalities to confer solubility, but containing no further functional groups) also help provide effective chemiresistors. The delocalised nature of the aromatic system contributes to the conduction process. The formation of a chemiresistor containing an amine group on a benzene ring was attempted, but no film was formed. This may have been due to the electron donating effects of the amine stabilising the radical cation formed during the polymerisation process.

b. The reverse is true for the presence of electron withdrawing groups (-COOR, - COOH, -NO$_2$) present on aromatic ring systems. These tend to inhibit the response observed with the presence of multiple numbers of electron withdrawing groups leading to a negligible response.

c. The use of surfactant based molecules such as dodecylbezene sulphonate leads to the formation of chemiresistors with dense, ordered morphologies, the porosity of the film being greatly reduced. Therefore the ability of the analyte to penetrate the film and effect a response is limited. The result of this is a reduced response although in optimisation processes it was noted that films of this nature benefit from a reduction in thickness and increased current density/potential during electrochemical deposition hence increasing porosity.

d. The final category are the inorganic/organic, univalent anions. These species lead to films with a highly disordered, nodular structure which is highly porous. The films have proved to be highly ineffective as chemiresistors due to their lack of environmental stability (i.e. greatly affected by ambient humidity) and drift during

174

use as sensors. The films formed have also been less reproducible and prone to sporadic failure during sensing.

4. The use of other monomers was investigated, but the use of alkylthiophenes and anilines appeared to be particularly sensitive to fluctuations in the relative humidity. Their overall environmental stability was considerably poorer that those systems developed using polypyrrole.

5. The investigation of films prepared from two or more monomers is an area which received some investigation. The possibility of incorporating two polymer sequences with potentially different properties is of interest. The formation of composite films containing both the heterocyclic monomer pyrrole and the bicyclic hydrocarbon monomer azulene showed that this type of approach was potentially feasible. The initial results on environmental stability are promising but as yet no initial studies have been performed to investigate response characteristics.

Conducting polymers have many characteristics which can be exploited in the development of multisensor array devices although, at present, they do have certain technical limitations, as do the many other technology types highlighted in the introduction (see Chapter 1 Section 1.4). Continued development of conducting polymer chemiresistors may overcome these limitations so that a really effective instrument can be developed using this technology base. At the present time the technology could benefit from the inclusion of other technology types within the array format, thus exploiting some of the benefits of other technologies. The main limitations of conducting polymer technology and its incorporation into the e-NOSE 4000 are as indicated below.

1. Although significant developments have been made in conducting polymer chemiresistors, sensor drift is still an important issue requiring research. The level of sensor drift has been greatly reduced by sensor optimisation and the

incorporation of certain counter-ions. The main factors responsible for the gradual deterioration in sensor conductivity are thought to be both environmental exposure to humidity, and repeated sensor exposure to sample analytes. Although the sensors exhibited drift, the level and nature of the responses observed did not vary over a four month period when tested.

2. With some sensor types the issue of sensor adhesion to the substrate design has arisen. This area could be addressed by changing the nature of the substrate material or the surface roughness of the binding surface. It is reported in the literature[162] that conductivity is increased by decreasing the surface roughness, and that adhesion in turn is increased with increasing surface roughness. The constraints of the instrument make the decision to sacrifice conductivity for adhesion a difficult one.

3. Sensor response to non-polar compounds has been poor, and this issue needs to be rectified if the instrument is to remain a multi-purpose detection system for aromas.

4. The instrument provides its own limitations, the formation of chemiresistors is limited to the area of highly conducting polymers predominately films of PPy, P3MT and PA, and also copolymer systems.

5. Conducting polymer chemiresistors are sensitive to temperature changes and therefore careful monitoring of the instrumental operating temperature is required. As with many other sensing technologies this problem is not uncommon. The development of devices which can be exposed to temperature changes without variation in their baseline resistances would enable sampling at enhanced temperatures. This would create a higher concentration of volatile components from the sample, perhaps increasing sensor output due to the nature and level of volatile components reaching the polymer interface.

6. Sensor response to aqueous analytes provides significant problems for the existing conducting polymer based technology. Sample analysis has shown that the ability to realistically distinguish differences between aqueous analytes is hampered by the response of conducting polymers to water vapour itself.

7.2 Further work.

The continued development of successful multisensor array devices using conducting polymers depends primarily on overcoming some of their limitations. The problems which need to be resolved require further extensive research. The discriminatory ability of the sensors so far developed is broad ranging but there are classes of organic compounds (predominately non-polar) which the sensors are unable to detect effectively and to distinguish between; their effectiveness in discriminating single organic analytes is also questionable. The sensitivity of the conducting polymers to water vapour affects both their drift, environmental stability and their response to aqueous analytes. The formation of chemiresistors based upon polypyrrole has been investigated and improvements made but the feasibility of considering a range of other polymeric materials is reduced due to instrumental limitations especially the restrictive operational limit for chemiresistor conductivities. Therefore, to achieve developments within this area it may be necessary to produce a highly conducting polymer composite containing two or more materials. Although a range of fairly simple classical and non-classical dopants has been investigated, further research in the area of more complex dopants (e.g. organometallic systems) may radically alter the nature of the responses obtained. These factors may enable a reduction in sensor drift, improve long-term stability and increase the operating temperature at which the devices can perform useful analysis. The following proposals highlight areas of research which may benefit the further development of multisensor array devices which use conducting polymers.

1. Electrodeposition of devices from mixtures of monomers to form composite based conducting polymer films. The main factor requiring attention is the relative anodic deposition potentials of the monomers involved. It is important that the two monomers have comparable electrodeposition potentials so that a composite material is obtained. The feasibility of this has already been investigated using pyrrole and azulene to form conducting polymer films. Other candidates for inclusion into composite systems are 5-substituted indoles, pyrene and azulene.

2. The continued research and development of complex counter-ions to produce films with increased stability and porosity. An electrolyte solution containing both a univalent spherical anion and a surfactant based dopant may produce a chemiresistor with enhanced stability compared to films containing only small, spherical counter-ions. Films incorporating small anions generally have increased porosity compared to films containing only surfactant based counter-ions which are structurally more ordered and less porous. The combination of these two characteristics by inclusion of both counter-ion types within an electrolyte solution may produce chemiresistors with reformed sensing characteristics.

3. Further development of stable films could be achieved using cyclic voltammetry techniques. A film with a porous structure could be electrochemically deposited using small spherical counter ions; cyclic voltametry could then be used to remove the initial anion and replace it with an alkyl or aryl sulphonate based counter-ion. This would confer long-term environmental stability on the chemiresistor with the advantage of a porous less ordered structure allowing rapid adsorption-desorption of sample analytes.

4. The development of chemiresistors incorporating metallic based counterions, predominately transition metal salts. Recent research has highlighted that there are an ever increasing number of potential counterions which could be exploited. These include ethylenediaminetetraacetate derivatives[196] ($M^{III}EDTA^-$ where $M = Co$, Cr or Fe. The conductivites of these materials have been found to be dependent on the nature of the metal ion), M^{II} tetra dentate counterions ($M = Cu$ or Ni and tetra dentate $= N,N'$-alkylene or (aylene) bis-(5-sulfosalicylaldehydeimine) or N,N'-alkylenebis(oxamido) chelating groups) and films containing $Ni(mnt)_2^-$ and $Pd(mnt)_2^-$ (where mnt represents the S-donor chelate 1,2-dicyanoethylene-1,2-dithiolene)[197]. The current research into these systems has been completed on PPy films with some of these systems showing reasonable environmental stability. The major problem that could be envisaged with this particular class of counter ions when forming chemiresistors is film adhesion. Such problems were encountered with metal tetrasulphophthalocyanines and with polymeric counter-ions which may

require the investigation of other substrate materials to produce effective and robust chemiresistors.

5. The accepted resistance range for chemiresistors that are to be incorporated into the e-NOSE 4000 is presently 1-100 ohms but this may be over restrictive. Any broadening of this criterion could conceivably provide an expansion in the number of conducting polymers which could be acceptable for use with the instrument. Films which could then be investigated might conceivably have sensing and discriminatory characteristics not previously observed.

6. The substrate design could be improved significantly by the inclusion of interdigitation and reduction in the insulating gap width from 10µm down to 2µm. This would enable a reduction in the mass and film thickness of the polymeric material required to form an effective chemiresistor. These changes could decrease the response period and also the sampling time, and such changes could make the instrument capable of real-time analytical measurement.

The research project was successful in the development and expansion of knowledge surrounding conducting polymer multisensor array technology. It also allowed the continued development of a commercial instrument for a variety of industrial applications. The resulting conclusions have highlighted the strengths and weaknesses of the NOSE technology in its present format, and have provided ideas to advance the formation of useful chemiresistors from conducting polymers.

References

1. J. W. Gardner, P.N. Bartlett, G. H. Dodd and H.V. Shurmer. *The design of an artifical olfactory system* in D. Schilid (ed), Chemosensory information Processing, NATO ASI Series H: Cell Biology, Springer, Berlin, 1990, **39** 131-173.

2. P. N. Bartlett, N. Blair and J. W. Gardner. *Electronic Noses, Principles, Applications and Outlook.*, ASCI, Monpellies, 1993, 16-625

3. A. Coghlan, *New Scientist*, 1994, 5th February 20

4. A. Coghlan, V. Kiernan and J. Mullins, *New Scientist* supplement, 1995, 4th November, 1-7

5. G. H. Dodd, P. N. Bartlett and J.W.Gardner. *Odours-The stimulus for an electronic nose* J.W. Gardener and P.N.Bartlett (eds) Sensors and sensory systems for an electronic nose, Kluwer Academic Pub., 1992, 1-11

6. G. H. Dodd and K. Persaud., *Biochemical mechanisms in vertabrate primary olfactory neurons.*, Biochemistry of taste and olafaction, Academic Press Inc. 1981, 333-357.

7. R. L. Doty, *Toxicology and Industrial health* ,1994, **10**, 4/5, 359-367.

8. J. E. Amoore, *Chemical Sensors and Flavour,* 1977, **2**, 267-281.

9. The olfactory apparatus in *Grays Anatomy*, 1995, **37**, 1171-1180, Churchill Livingstone.

10. J. E. Amoore, J. W. Johnston and M. Rubin., *Scientific American*, 1964, **210**, 42-49.

11. J. W. Gardner and P.N. Bartlett, *Sensors and Actuators* B, 1994, **18-19**, 211-220.

12. Smell is the least understood of the special senses. *Human Physiology-From cells to systems.* Laurence Sherwood (2nd ed.) West Publishing Company, New York, 1993, 192-193.

13. K. C. Persaud, J. Bartlett and P. Pelosi. *Robots and Biological systems*, NATO ASI series Springer-Verlag, 1994, 579-602

14. S. G. Shirley and K. C. Persaud, *The Neurosciences*, 1990, **2**, 59-68.

15. J. S. Kauer, *Trends in Neuroscience*, 1991, **14**, 79-85.

16. H. A. Schultens and D. Schild., Biophysical properties of olfactory receptor neurones, J.W. Gardner and P.N. Bartlett (eds.), *Sensors and Sensory Systems for an electronic Nose*, Kluwer Academic Pub., 1992, 13-24.

17. K. C. Persaud, Olfactory measurements and modelling in P.Payne (ed) *Concise Encyclopedia of Biological and Biomedical Measurment Systems*, Perg. Press, 1990, 291-296

18. G. H. Dodd, P. N. Bartlett and J. W. Gardner, *Biochemical Society Transactions*, 1990, **19**, 36-39.

19. S. Actander, Perfume and flavour chemicals, Pub. S. Actander, USA, !969.

20. J. E. Amoore, Molecular basis of odour ed C. Thomas, Springfield, Illinios, 1970.

21. R. E. Moncrieff, *J. Applied Physiol.*, 1961, **16**, 742.

22. W. F. Wilkens and A.D. Hataman, *Ann. NY ACAD. Sci.*, 1964, **116**, 608.

23. T. M. Buck, F.G. Allen and M. Dalton, Detection of chemical species by surface effects on metals and semiconductors, in T. Bregman and A. Dravnieks (eds.), *Surface effects in Detection*, Spartan Books Inc., USA, 1965.

24. A. Dravnieks and P.J. Trotter, *J. Sci. Instrum.*, 1965, **42**, 624.

25. S. Deutsch, *Models of the Nervous System*, The instinctive recognition of chemical patterns, John Wiley and Sons, U.K Ch 10. 1967.

26. K. C. Persaud and G. H. Dodd, *Nature*, 1982, **299**, 352-355.

27. A. Ikegami and M. Kaneyasu, Olfactory detection using integrated sensors Proc. 3rd Int Conf. Solid-State *Sensors and Actuators (Transducers'85)*, Philadelphia, PA, USA, June 7-11, 1985, 136-139

28. M. Kaneyasu, A. Ilekgami, H.Arima and S. Iwanga, *IEEE Trans. Components, Hybrids Manufact. Technol.*, CHMT-10, 1987, 267-273.

29. J. W. Gardner, Pattern recognition in the Warwick electronic nose, *8th Int. Congress of European Chemoreception Research Organisation*, University of Warwick, UK, July, 1987.

30. J. W. Gardner and P. N.Bartlett, Pattern Recognition in gas sensing, in P.J. Moseley, J. Norris and D. Williams (eds.), *Techniques and mechanisms in Gas Sensing*, Adam Heilger, Bristol, 1991, 347-380.

31. T. Moriizumi, T. Nakamoto and Y. Sakuraba Pattern recognition in electronic noses by artificial neural network models in J.W. Gardener and P.N.Bartlett (eds.), *Sensors and sensory systems for an electronic nose*, Kluwer Academic Pub., 1992, 217-235.

32. H. V. Shurmer, *I.E.E. Review* 1990, March, 95-98

33. H. V. Shurmer and J. W. Gardner, *Sensors and Actuators* B, 1992, **8**, 1-11

34. H. V. Shurmer, *Analytical Proceedings*, 1994, **31**, 39-40

35. H. V.Shurmer, J. W.Gardner and P. Corcoran, *Sensors and Actuators* B, 1990, **1**, 256-260.

36. J. W. Gardner, H. V.Shurmer and P. Corcoran, *Sensors and Actuators* B, 1991, **4**, 117-121

37. J. W. Gardner, E. L.Hines and M.Wilkinson, *Meas. Sci. Technol.* 1990, **1**, 446-451

38. H. V. Shurmer, Basic limitations for an electronic nose, *Sensors and Actuators* B, 1990, **1**, 48-53.

39 H. V. Shurmer, *I.E.E. Proceedings*, 1990, **137**, 3.

40. J. W.Gardner, *Sensors and Actuators* B, 1991, **4**, 109-115.

41. P. Cororan and H. V.Shurmer, An intelligent gas sensor, *Sensors and Actuators*, A, 1994, **41-42**, 192-197.

42. H. V.Shurmer, J.W. Gardner and H. T. Chan, *Sensors and Actuators*, 1989, **18**, 361-371.

43. H.V. Shurmer, P.Cororan and M.K. James, *Sensors and Actuators* B, 1993, **15-16**, 256-259.

44. P. Cororan, H. V.Shurmer and J. W. Gardner, *Sensors and Actuators* B, 1993, **15-16**, 32-37.

45. P. Bartlett, P Archer and S. Ling-Chung, *Sensors and Actuators* B, 1989, **19**, 125-140.

46. P. Bartlett and S.Ling-Chung, *Sensors and Actuators* B, 1989, **19**, 141-150.

47. P. Bartlett and S. Ling-Chung, *Sensors and Actuators* B, 1989, **20**, 287-292.

48. H. V. Shurmer, P.Corcoran and J.W. Gardner, *Sensors and Actuators* B, 1991, **4**, 29-33.

49. T. C. Pearce, J. W. Gardner, S. Freil, P. N. Bartlett and N. Blair, *Analyst*, 1993,. **118**, 371-377.

50. J. W. Gardner, T.C. Pearce S. Friel, P. N. Bartlett and N. Blair, *Sensors and Actuators*, B, 1994, **18-19**, 240-243.

51. H. Shurmer, Identifying or measuring components of a mixture UK patent application GB 2 203 249 A, 1988

52. J. W. Gardner and P.N.Bartlett Device for sensing volatile materials Int Patent WO93/03355

53. D. Hodgins, *Sensor review*, 1994, **14**, 1, 29-35

54. Neotronics Olfactory Sensing Equipment, Neotronics Scientific Ltd. 2, Cambridge Rd., Stanstead Mountfitchet, Essex, U.K., *Publicity material*, 1994

55. D. J. Simmonds and D. Hodgins, *J. of Auto.Chem.*, 1995, **17**, 5, 179-185.

56. K. Persaud and P.Pelosi Sensor arrays using conducting polymers for an electronic nose in J. W. Gardner and P. N. Bartlett (eds.), *Sensors and sensory systems for an electronic nose*, Kluwer Academic Pub., 1992, 237-256

57. K. C. Persaud, *Analytical Proceedings*, October 1991, **28**, 339-341.

58. J. V. Hatfield, P. Neaves, P. J. Hicks, K. C. Persuad and P. Travers, *Sensors and Actuators* B, 1994, **18-19**, 221-228.

59. M. E. Hassan Amrani, P. A. Payne and K. C. Persaud, *Transducers* Eurosensors IX, Sweden, 1995, 811-813.

60. F. Musio, M. E. H. Amrani and K. C. Persaud, *Sensors and Actuators* B, 1995, **23**, 223-226.

61. E. Moy, *LC-GC INT.* 1995, **8**, 4, 221-225

62. Nose wars, *Chemistry and Industry*, 1994, 710.

63. G. H. Dodd, *The impact of the electronic nose in the Food and Drink Industry*, First Annual Symposium, 1995.

64. A. R. Newman, *Analytical Chemistry*, 1991, **63**, 10, 585-588

65. J. D. Wright, *Chem. Brit.* 1995, **31**, 374-377.

66. D. H. Shurmer, A. Fard, J. Barker, P. N. Bartlett and G. Dodd *Phys. Technol.*, 1987, **18**, 170-176.

67. K. Ema, M. Yokoyama, T. Nakamoto and T. Moriizumi, *Sensors and Actuators*, 1989, **18**, 291-296.

68. B. Hivert, M. Hoummady, J. M. Henriod and D. Hauden, *Sensors and Actuators*, B, 1994, **18-19**, 645-648.

69. M. Holmberg, F. Winquist, I. Lundstrom, J. W. Gardner, E. L. Hines, *Sensors and Actuators* B, 1995, **26-27**, 246-249.

70. I. Lundstrom, E. Hedborg, A. Spetz, H. Sundgren and F. Winquist, Electronic Noses based on field effect structures in J. W. Gardener and P. N. Bartlett (eds), *Sensors and Sensory Systems for an electronic nose*, Kluwer Academic Pub., 1992, 303-319.

71. N. Taguchi, *G.B. Patent*, 1971, 1 257 155

72. J. F. McAleer, P. T. Moseley, J. O. W. Norris and D. E. Williams, *J. Chem. Soc., Faraday Trans.* 1, 1987, **83**, 1323-1346.

73. J. W. Gardner, *Sensors and Actuators*, 1989, **18**, 373-387.

74. P. T. Moseley, A. M. Stoneham and D. E. Williams Oxide semiconductors: Patterns of response behaviour according to material type in P.T. Moseley, J. Norris and D. E. Williams(eds.), *Techniques and mechanisms in gas sensing*, Hilger, 1991, 108-137.

75. J. Watson, *Sensors and Actuators*, 1984, **5**, 29-42.

76. R. Olafsson, E. Martinsdotter, G. Olafsdottir, P. I. Sigfusson and J. W. Gardner, Monitoring of fish freshness using tin oxide gas sensors in J. W. Gardner and P.N. Bartlett (eds), *Sensors and Sensory systems for an electronic nose*, Kluwer Academic Pub., 1992, 257-272

77. C. M. A. Brett and A. M. O. Brett, *Electrochemistry Principles, Methods, and Applications*, Oxford Sciencs Pub. (UK), 1992, 276-277.

78. T. Nakamoto, A. Fukuda and T. Moriizumi, *Sensors and Actuators* B, 1991, **3**, 221-226.

79. J. Idle, T. Nakamoto and T. Moriizumi, *Sensors and Actuators* B, 1993, **13-14**, 351-354.

80. J. M. Slater, E. J. Watt, N. J. Freeman, I. P. May and D. J. Weir, *Analyst*, 1992, **117**, 1265-1270.

81. T. Nakamoto, A. Fukuda and T. Moriizumi, *Sensors and actuators* B, 1993, **10**, 85-90.

82. G. Kraus, A. Hierlemann, G. Gauglitz and W. Gopel, *Transducers '95 Eurosensors IX*, 1995, **170-D1**, 675-678

83. Y. Okahata and H. Ebato, *Tr. Ana. Chem.*, 1992, **11**, 9, 344-354

84. A. Venema, E. Nieuwkoop, M. J. Vellekoop, M. S. Nieuwenhuizen and A. W. Barendsz, *Sensors and Actuators*, 1986, **10**, 47-64.

85. C. G. Fox and J. F. Alder, Surface Acoustic Wave sensors for Atmospheric Gas monitoring in P. T. Moseley J. Norris and D. E. Williams(eds), *Techniques and Mechanisms in Gas sensing*, Hilger, UK, 1991, 324-345

86. J. Janata, *Principles of chemical sensors*, Mass sensors, Plenum Pub. UK 1987, 54-80

87. A. D'Amico and E. Verona, *Sensors and Actuators*, 1989, **17**, 55-56

88. S. J. Patrash and E. T. Zellers, *Analytical Chimica Acta* , 1994, **288**, 167-177.

89. E. T. Zellers, S. A. Batterman, M. Han, and S. J. Patrash, *Anal. Chem.* 1995, **67**, 1092-1106.

90. C. S. I. Lai, G. J. Moody, J. D. Ronald Thomas, D. C. Mulligan, J. F. Stoddart and R. Zarzycki, *J. Chem. Soc. Perkin Trans. II,* 1988, 319-324.

91. J. M. Slater and E. J. Watt, *Analyst*, 1991, **116**, 1125-1130.

    Z. Deng, D.C. Stone and M. Thompson, *Analyst*, 1996, **121**, 671-679

92. H. Wang, *Biotech Adv.*, 1993, **11**, 701-710.

93. M. Ohnishi, *Sensors and Materials*, 1992, **4**, 1, 53-60

94. Y. Okahata, G. En-na and H. Ebato, *Anal. Chem.* 1990, **62**, 1431-1438.

95. T. Bein and K. Brown, *J. Am. Chem. Soc.,* 1989, **111**, 7640-7641.

96. A. Crocker, Metal-Oxide-Semiconducting gas sensors in P. J. Moseley, J. Norris and D. Williams (eds), *Techniques and Mechanisms in gas sensing*, Blackie, 1987, 281-323.

97. MOSFET Devices in T. Edmonds (ed), *Chemical Sensors*, Blackie, UK, 1987, 225-235.

98. M. Fryder, M. Holmberg, F. Winquist and I. Lundstrom, *Transducers '95. Eurosensors IX*, 1995, 683-686.

99. G. G. Roberts, P. S. Vincett and W. A. Barlow, *Phys. Technol.*, 1981, **12**, 69-76.

100. T. Moriizumi, *Thin Solid Films*, 1988, **160**, 413-429

101. M. Imanpour, Development of processing conditions for the production of Langmuir-Blodgett films for and electronic nose, *MSc Dissertation*, University of Warwick, 1986.

102. S. Baker, G. G. Roberts and M. C. Petty, *Proc. IEE*, 1985, **130** I, 260-263

103. R. H. Tredgold, M. C. J. Young, P. Hodge and A. Hoorfar, *Proc. IEE*, 1985, **132** I 151-156

104. M. Wouhltjen, W. Barger, A. Snow and N. J. Jarvis, *IEEE Trans.*, 1985, **32**, 1170-1174.

105. J. J. Miasik, A. Hooper and B. C. Tofield, *J. Chem. Soc., Faraday Trans. 1*, 1986, **82**, 1117-1126.

106. J .J Miasik, A. Hooper, P.T. Moseley and B. C. Tofield, Electronically Conducting Polymer Gas Sensors in L. Alcacer (ed), *Conducting Polymers*, D. Reidel Publishing Company, 1987, 189-198.

107. T. Hanawa, S. Kuwabata and H. Yoneyama, *J. Chem. Soc., Faraday Trans. 1*, 1988, **84,** (5), 1587-1592.

108. A. G. Angeli, Gazz. *Chem. Ital.*, 1916, **46** II, 279

109. A. F. Diaz, K. K. Kanazawa, G. P. J. Gardini, *J. Chem. Soc., Chem Commun,.* 1979, 635-636.

110. A. F. Diaz J. Crowley, J. Bargon, G. P. Gardini and J. B. Torrance, *J. Electroanal. Chem.*, 1981, **121**, 355.

111. G. K. Chandler and D. Pletcher, *The Electochemistry of Conducting Polymers,* *'Electrochemistry', (Specialist periodical Reports),* Royal Society of Chemistry, 1985, **10**, 117-150.

112. J. W. Gardner, *Sensors and Actuators* B, 1991, **4**, 109-115

113. C. D. Natale, F. A. M. Fabrizio, A. D'Amico, P. Nelli, S. Groppelli and G. Sberveglieri, *Transducers '95, Eurosensors* IX, 1995, 711-714.

114. F. Winquest, E. G. Hornesten and I. Lundstrom, *Mass. Sci.technol.,* 1993, **4**, 1493-1500.

115. A. M. Pisanelli, A. A. Qutob, P. Travers, S. Szyszko and K. P. Persaud, *Life Chemistry Reports,* Harwood Academic Pub. Malaysia, 1994. **11**, 303-308.

116. P. N. Bartlett and J. W. Gardner, *Physics World,* 1990, 19-20.

117. e-NOSE™ 4000 Electronic Nose System, *Publicity material,* Neotronics Scientific Ltd, 2, Cambridge Rd., Stanstead Mountfitchet, Essex, UK. 1995.

118. W. H. Smyrl and M. Lien, Electrical and electrochemical properties of electronically conducting polymers in B. Scrosati, *Applications of Electroactive Polymers,* Chapman and Hall, 1993, 29-74.

119. A. F. Diaz and J. Bargon, Electrochemical Synthesis of Conducting Polymers in T. A. Skotheim (ed) *Handbook of Conducting Polymers.* 1986, **1**, 1-115, Marcel Dekker Inc. New York

120. J. Lei, C. R. Martin, *Synthetic Metals,* 1992, **48**, 331

121. G. B. Street, Polypyrrole- from powders to plastics in T. A. Skotheim (ed) *Handbook of Conducting polymers,* **1986, 1,** 265-291, Marcel Dekker Inc. New York.

122. G. B. Street, T. C. Clarke, R. H. Geiss, V. Y. Lee, A. Pfluger and J. C. Scott, *J. Phys (Paris),* 1983, **C3,** 599

123. B. R. Saunders, R. J. Fleming and K. S. Murray, *Chem. Mater.,* 1995, **7,** 6, 1082-1094.

124. E. Hall, *Biosensors,* Open University Press, 1990,. Ch. 4, Semiconductor Electrodes, 74-96.

125. A. Watanabe, M. Tanaka, A. Tanaka, *J. Bull. Chem. Soc., Jpn.,* 1981, **54,** 2278

126. J. C. Scott, J. L. Bredas, K. Yakaushi, P. Pfluger and G. B. Street, *Synthetic Metals*, 1984, **9**, 165-172

127. J. C. Scott, J. L. Bredas, J. H. Kaufman, P. Pfluger, G. B. Street and K. Yakushi, *Mol. Cryst. Liq. Cryst.* 1985, **118**, 163-170.

J. H. Kaufman, N. Colaner, J. C. Scott, K. K. Kanazawa and G. B. Street, *Mol. Cryst. Liq. Cryst.*, 1985, **118**, 171-177

128. J. R. Ferraro and J. W. Williams, *Introduction to Synthetic Electrical Conductors*, Academic Press Inc., (London) 1990, 263-285.

129. J. L. Bredas, B. Themans, J. M. Andre, R. R. Chance, R. Sibley, *Synthetic Metals*, 1984, **9**, 265-271.

130. J. L. Bredas, J. C. Scott, K. Yakushi, G. B. Street, *Phys. Rev. B*, 1984, **30**, 1023.

131. P. R. Edwards, Manufacturing Technology in the Electronics Industry, Chapman & Hall, *Semiconductor Device Manufacture*, 1991, Ch 4, 91-109.

132. S. M. Sze, *Semiconductor Devices*: Physics & Technology, John Wiley & Sons, 1990, Ch. 11, 428-467.

133. H. A. Strobel, *Chemical Instrumention*, 1977, Addison-Wesley Press.

134. W. Grimm, *Spectrochemica Acta*, 1968, **23B**, 443.

135. M. Ives, *PhD thesis*, 1994, Sheffield Hallam University, United Kingdom.

136. Interdigitated Microsensor Electrodes (IME's), ABTECH Laboratory Products Group, P.O. Box 376, Yardley, Pennsylvania 19067, U.S.A, *Publicity Material*, 1994.

137. D. J. Walton, C. E. Hall and A. Chyda, *Analyst*, 1992, **117**, 1305-1311

138. C. E. Hall, *PhD thesis*, CNAA Coventry Poly., 1992.

139. V. Weinmayr, *J. Am. Chem. Soc.,* 1955, **77**, 3009-3014

140. B. L. Bray, P. H. Mathies, R. Naef, D. R. Solas, T. T. Tidwell, D. R. Artis and J. M. Muchowski, *J. Org. Chem.,* 1990, **55**, 6317-6328.

141. J.Rokach, P.Hamel and M. Kakushima, *Tetra. Let.*, **22**, 49, 4901-4904

142. M. Kakushima, P.Hamel, R. Frenette and J. Rokach, *J. Org. Chem.*, 1983, **48**, 3241-3219.

143. D. Delabouglise and F. Garnier, *Synthetic Metals*, 1990, **39**, 117-120

144. J. Henize and M. Dietrich, *Materials Science Forum*, 1989, **42**, 63-78.

145. G. G. Wallace, Dynamic Conduct, *Chem. Brit.* 1993, **29**, 967-970.

146. P.T. Kissinger and W. R. Heinman, *Laboratory Techniques in Electroanalytical Chemistry*, Marcel Dekker Inc., 1984, Ch. 13, 367-380.

147. C. M. A. Brett and A. M. O. Brett, *Electrochemistry, Principles, Methods and Applications*, Oxford Sciences Pub., (UK), 1992, 174-198.

148. A. R. Gabriel, *SEM-A Users Manual for Materials Science*, 1972, North-Holland Press.

149. D. K. Bowen and C. R. Hall, *Microscope of Materials*, 1975, Macmillam Press.

150. L. Donahue, *PhD thesis*, 1995, Sheffield Hallam University, United Kingdom.

151. D. C. Harris, *Quantitative Chemical Analysis*, W. H. Freeman and Company, 1982, 553-563.

152. Vibrational Spectra and Structure, Vol. 18, *Applications of FT-IR Spectroscopy* in J. R. During (ed), Elsevier, 1990.

153. The NOSE-Neotronics Olfactory Sensing Equipment, *User Manual*, Neotronics Scientific Ltd., 2, Cambridge Rd.,Stanstead Mountfitchet, Essex, U.K. May 1994.

154. A. F. Diaz and K. K. Kanazawa, in *Extended Linear Chain Compounds* J. S. Miller (ed), Plenum, New York, 1982, 417.

155. A. F. Diaz, J. Castillo, K. K. Kanazawa, J. A. Logan, M. Salmon and O. Fajardo, *J. Electroanal. Chem.* Interfacial Electrochem., 1982, **133**, 233.

156. R. J. Waltman, J. Bargon and A. F. Diaz, Electrochemical studies of some conducting polythiophene films, *J. Phys. Chem.* 1983, **87**, 1459-1463.

157. G. Tourillon and F. Gardiner, *J. Electroanal. Chem.*, 1982, **135**, 173.

158. A. F. Diaz, *Cheimica Scripta.* 1981, **17**, 145-148.

159. J. Bargon, S. Mohmand and R. J. Waltman, *IBM J. Res. Dev.*, 1983, **27**, 330.

160. S. Asavapiryanont, G. K. Chandler, G. A. Gunawardena and P. Pletcher, *J. Electroanal. Chem.,* 1984, **117**, 229-244.

161. W. Wernet, M. Monkenbusch and G. Wegner, *Mol. Cryst. Liq. Cryst.,* 1985, **118**, 193-197.

162. B. K. Moss, R. P. Burford and M. Skyallas-Kazacos, *Materials Forum*, 1989, **13**, 35-42.

163. B. F. Cvetko, M. P. Brungs, R. P. Burford and M. Skyallas-Kazacos, *J. Mater. Sci.*, 1988, **23**, 2102-2106.

164. A. Dall'Olio, Y. Dascola, V. Varacca and V. Bocchi, *Comptes Rendus*, 1968, **C267**, 433.

165. M. Salmon, A. F. Diaz A. J. Logan, M. Karounbi and J. Bargon, *Mol. Cryst. Liq. Cryst.*, 1982, **83**, 265-276.

166. G. R. Mitchell, F. J. Davis and C. H. Legge, *Synthetic Metals*, 1988, **26**, 247-257

167. L. F. Warren, J. A. Walker, D. P. Anderson, C. G. Rhodes and L. C. Buckley, *J. Electrochem. Soc.*, 1989, **136**, 2286-2291.

168. S. Kuwabata, K. Okamoto and H. Yoneyama, *J. Chem. Soc., Faraday Trans. 1*, 1988, **84**, (7), 2317-2326.

169. A. Kassim, F. J. Davis and G. R. Mitchell, *Synthetic Metals*, 1994, **62**, 41-47

170. D. J. Walton, C. E. Hall and A. Chyla, *Synthetic Metals*, 1991, **45**, 363-371.

171. A. F. Diaz and B. Hall, *IBM J. Res. Dev.* 1983, **27**, 4, 342-347.

172. B. Yan, J. Yang, Y. Li and R. Qian, *Synthetic Metals*, 1993, **58**, 17-27.

173. G. L. Duffit and P. G. Pickup, *J. Phys. Chem.*, 1991, **95**, 9634-9635.

174. F. W. Fifield and D. Kealey, *Principles and Practice of Analytical Chemistry*, Blackie Academic and Professional, 1995, 184-222.

175. M. Sato,S. Tanaka and K. Kaeriyama, *J. Che. Soc.,Chem. Commun.*, 1985, 713-714.

176. J. Roncali, A. Yassar and F. Garnier, *J. Chem. Soc., Chem. Commun.*, 1988, 581-582.

177. G. Tourillon, Polythiophene and its derivatives in T. Skotheim (ed), *Handbook of Conducting Polymers*, Marcel Dekker Inc., 1986, **1**, 293-350

178. T. Osaka K. Naoi and T. Hirabayashi, *J. Electrochem. Soc.*, 1987, 2645-2649.

179. J. Bargon, S. Mohamand and R. J. Waltman, *Mol. Cryst. Liq. Cryst.*, **1983**, 93, 279.

180. R. Zahradnik in *Nonbenzenoid Aromatic Compounds* J. P. Snyder (ed), Academic, New York, 1971.

181. K. Naoi, K. Ueyama and T. Osaka, *J. Electrochem. Soc.*, 1990, **137**, 2, 494-499.

182. R. Burzyniski, P. N. Prasad, S. Bruckenstein and J. W. Sharkey, *J. Electrochem. Soc.*, 1985, **11**, 293-301.

183. N. C. Billingham, P. D. Calvert, P. J. S. Foot and F. Mohammad, *Polymer Degradation and Stability*, 1987, **19**, 323-341.

184. *Molecular Electronics*, G. J. Ashwell, Research Studies Press Ltd, Taunton, UK, 1992, 87-89.

185. J. C. Thieblemont, A. Brun, J. Marty and M. F. Planche, *Polymer*, 1995, **36**, 8, 1605-1610.

186. B. K. Moss and R. P. Burford, *Polymer* 1992, **33**, 9, 1902-1908.

187. T. L. Tansley and D. S. Maddison, *J. Appl. Phys.*, 1991, **69**, (11), 7711-7713.

188. Y. Li and R. Qian, *Synthetic Metals*, 1993, **53**, 149-154.

189. L. W. Warren and D.D. Anderson, *J. Electrochem. Soc.*, 1987, **134**, 101-105

190. J. M. Slater, J. Paynter and E. J. Watt, *Analyst*, 1993, **118**, 379-384.

191. P.R. Teasdale and G. G. Wallace, *Analyst*, 1993, **118**, 329-334.

192. J. M. Charlesworth, A. C. Partidge and N. Garrard, *J. Phys. Chem.*, 1993, **97**, 5418-5423.

193. P. Topart and M. Josowicz, *J. Phys. Chem.*, 1992, **96**, 7824-7830.

194. D. Blackwood and M. Josowicz, *J. Phys. Chem.*, 1991, **95**, 495-502.

195. R. Erlandsson , O. Ingans, I. Lundstrom and W. R. Salanock, *Synthetic Metals*, 1985, **10**, 303-318.

196. B. R. Saunders, K. S. Murray, R. J. Fleming D. G. McCulloch, L. J. Brown and J. D. Cashion, *Chem. Mater.*, 1994, **6**, 697-706.

197. B. Kaye and A. E. Underhill, *Synthetic Metals,* 1989, **28**, C97.

Acknowledgments

Appendix 1 List of counter-ion abbreviations

Abbreviation	Chemical name
$LiClO_4$	Lithium perchlorate
$LiNO_3$	Lithium nitrate
TEATFA	Tetraethylammonium trifluoroacetate
$LiPF_6$	Lithium hexafluorophosphate
$TEABF_4$	Tetraethylammonium tetrafluoroborate
LiTFMS	Lithium trifluoromethanesulphonate
2M-2PSA(Na)	2-methyl-2-propanesulphonic acid (sodium salt)
BuSA(Na)	Butane sulphonic acid (sodium salt)
p-TSA(Na)	p-toluenesulphonic acid (sodium salt)
TEATS	Tetraethylammonium sulphonate
BzSA(Na)	Benzene sulphonic acid (sodium salt)
2-NapSA(Na)	2-Naphthalene sulphonic acid (sodium salt)
DDBzSA(Na)	Dodecylbenzene sulphonic acid
4-ABzSA(Na)	4-Acetylbenzene sulphonic acid (sodium salt)
NBzSA(Na)	Nitrobenzene sulphonic acid (sodium salt)
1,3-BzDSA(2Na)	1,3-Benzene disulphonic acid (disodium salt)
1,5-NapDSA(2Na)	1,5-Naphthalene disulphonic acid (disodium salt)
4-OcBzSA(Na)	4-Octylbenzene sulphonic acid (sodium salt)
3-SuBz(Na)	3-Sulphobenzoic acid (sodium salt)
5-SuIA(Na)	5-Sulphoisohthalic acid (sodium salt)
DM-5-SuI(Na)	Dimethyl 5-isophthalate (sodium salt)
1,3,5-BzSA(3Na)	1,3,5-Benzenetrisulphonic acid (trisodium salt)
(1R)-(-)10CSA	(1R)-(-)10Camphorsulphonic acid
FDSA(2Na)	Ferrocenedisulphonic acid (disodium salt)
DDS(Na)	Dodecylsulphonate (sodium salt)
n-t-(2SP)N(Na)	n-tert-Butyl-α-(2sulphophenyl)nitrone (sodium salt)

DOSS(Na)	Dioctyl sulphosuccinate (sodium salt)
OcS(Na)	Octane sulphonate
Cu(II)PTSA(4Na)	Copper(II)phthalocyanine tetrasulphonic acid (tetrasodium salt)
P(St-4-NaS)	Poly(styrene-4-sodium sulphonate)
Bu_4NBzS	Tetrabutylammonium benzene sulphonate
$Bu_4NDDBzS$	Tetrabutylammonium dodecylbezenesulphonate
Bu_4N-2-NapS	Tetrabutylammonium-2-naphthalenesulphonate
$(Bu_4N)_2$-1,3-BzDS	Ditetrabutylammonium 1,3-benzenedisulphonate
$(Bu_4N)_2$-1,5-NapDS	Ditetrabutylammonium 1,5-Naphthalenedisulphonate
Bu_4N-4-ABzS	Tetrabutylammonium-4-acetylbenzenesulphonate
Bu_4N-(±)-10CS	Tetrabutylammonium (±)-10Camphor sulphonate

195

Stability data for PPy/LiClO$_4$/H$_2$O films

Stability data for PPy/LiNO$_3$/H$_2$O films

Stability data for PPy/TEATS/ H$_2$0 films

Stability data for PPy/p-TSA(Na)/H$_2$0 films

Stability data for PPy/BzSA(Na)/H$_2$O films

Stability data for PPy/1,3-BzDSA(2Na)/H$_2$0 films

199

Stability data for PPy/(1R)-(-)10CSA/H$_2$O films

Stablility data for PPy/(1S)-(+)10CSA/H$_2$0 films

Stability data on PPy/DDS(Na)/H$_2$O films

Stability data for PPy/DDBzSA(Na)/H$_2$0 films

201

Stability data for PPy/2-NSA(Na)/H$_2$O films

Stability data for PPy/1,5-NapDSA(2Na)/H$_2$O films

202

Stability data for PPy/BuSA(Na)/H$_2$O films

Stability data for PPy/FDSA(2Na)/H$_2$0 films

Stability data for PPy/4-ABzSA(Na)/H_2O films

Stability data for PPy/3-NBzSA(Na)/H_2O films

204

Stability data for PPy/TEATS/CH$_3$CN films

Stability data for PPy/Bu$_4$BzS/CH$_3$CN films

Stability data for PPy/Bu$_4$N 2-NapS/CH$_3$CN films

Resistance / ohms vs Time / weeks

- Film 1
- Film 2
- Film 3

Stability data for PPy/Bu$_4$N DDBzS/CH$_3$CN films

Resistance / ohms vs Time / weeks

- Film 1
- Film 2
- Film 3

Stability data for PPy/(Bu₄N)₂ 1,3-BzDS/CH₃CN films

Stability data for PPy/(Bu₄N)₂ 1,5-NapDS/CH₃CN films

207

Stability data for PPy/Bu₄N 4-ABzS/CH₃CN films

Stability data for PPy/TEATS/PC films

208

Stability data for P3MT/LiClO$_4$/CH$_3$CN films

Stability data for P3MT/Bu$_4$NBF$_4$/CH$_3$CN films

Stability data for P3MT/Bu$_4$NCF$_3$SO$_3$H/CH$_3$CN films

Stability data for P3MT/LiPF$_6$/CH$_3$CN films

Stability data for PPy/Methyl Orange/H$_2$O films

Resistance / ohms vs *Time /weeks*

Film 1
Film 2
Film 3

Stability data for PPy/Nitrazine Yellow/H$_2$O films

Resistance / ohms vs *Time / weeks*

Film 1
Film 2
Film 3

211

Stability data for PPy/Naphthol Yellow S/H$_2$O films

Stability data for PPy/Orange G/H$_2$0 films

212